

1st Year Ph.D. Report
2002/2003

Vapour Sensing Properties,
and Computer Simulation,
of Peratech's
Quantum Tunnelling Composite

E. J. Williams

St. Cuthbert's Society, University of Durham

Supervisors: Dr. G. H. Cross
Professor D. Bloor



University of Durham
Department of Physics



CONTENTS

<u>1. INTRODUCTION</u>	<u>2</u>
<u>1.1 What is an electrically conductive conductor-insulator composite?</u>	<u>2</u>
<u>1.2 What is a Quantum Tunnelling Composite (QTC)?</u>	<u>4</u>
<u>1.3 Tunnelling mechanisms</u>	<u>5</u>
<u>1.4 Conductive sphere in electric field</u>	<u>8</u>
<u>1.5 Field enhancement due to spikes</u>	<u>10</u>
<u>1.6 Theory of polymer swelling</u>	<u>11</u>
<u>1.7 Concept of “electronic nose” using metal-polymer composite</u>	<u>12</u>
<u>1.8 Applications and current standard of composite vapour sensors</u>	<u>14</u>
<u>1.9 Measuring solvent vapour concentration</u>	<u>15</u>
<u>2. EXPERIMENTAL MATERIALS, METHODS, RESULTS, AND DISCUSSION</u>	<u>17</u>
<u>2.1 Computer simulation of QTC</u>	<u>17</u>
2.1.1 How the program works	17
2.1.2 Results and discussion	21
<u>2.2 Vapour-sensing properties of QTC</u>	<u>24</u>
2.2.1 The multi-sensor array experimental set-up	24
2.2.2 Results and discussion	30
<u>2.3 Orientation-measuring device utilising QTC</u>	<u>36</u>
<u>3. FUTURE WORK PLANNED</u>	<u>38</u>
<u>4. ACKNOWLEDGEMENTS</u>	<u>41</u>
<u>5. REFERENCES</u>	<u>41</u>
<u>APPENDICES</u>	<u>44</u>

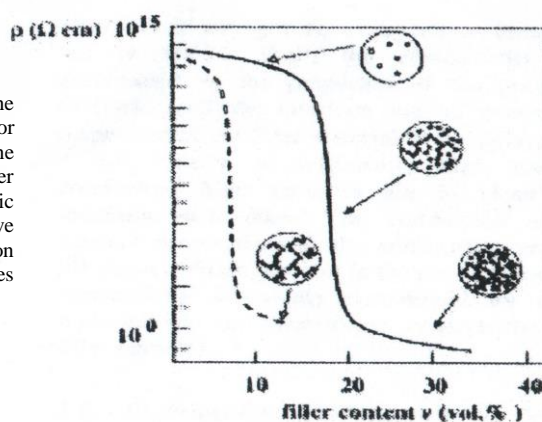
1. INTRODUCTION

1.1 What is an electrically conductive conductor-insulator composite?

Electrically conductive conductor-insulator composites have enjoyed a long and distinguished history, being researched experimentally now for more than 40 years.¹ Their considerable technological utility, finding applications as diverse as sensitive pressure sensors, EMI shielding, electrostatic dissipation, conductive adhesives, reusable fuses,² and transducer elements in “electronic nose” artificial olfactory systems,³ provides the driving force for this relentless and fervent investigation. By blending together a conductor (typically in the guise of micron-sized metallic particles) and an insulator (invariably a polymer), in a random dispersion, the resulting material benefits from the flexible qualities of the rubber, whilst allowing the electrical properties of the conductor to be retained. The degree of this retention is a sensitive function of the concentration of the conductive filler particles (also known as the volume filler fraction, loading ratio, or vol. %) within the host polymer, in addition to their size, shape, and orientation.

The mean distance between filler particles for very low filler fractions will be large, hence the composite will have the d.c. electrical properties of the host polymer, typically yielding a resistivity of the order of 10^{12} to 10^{13} Ωm . Upon increasing the loading ratio, the particle separation will decrease to a point where electrical contact is established between neighbouring particles, resulting in conductive chains. At a certain filler fraction, the extent of linkages will be such that a conductive pathway spans from one end of the material to the other – this filler fraction is termed the *percolation threshold*.⁴ A slight increase in the loading ratio now causes a dramatic decrease in resistivity to close to that of the conductive filler, which may be as low as 10^{-7} to 10^{-8} Ωm for metals such as nickel, aluminium, copper and silver, or 10^{-1} to 10^{-3} Ωm for an organic material such as carbon black;² further increase in the filler fraction will lead to eventual complete realization of the filler’s resistivity. This can be seen in **Fig.1**,² where it is also apparent that the morphology of the filler has an impact on the value of the percolation threshold, with anisotropic carbon black particles being conducive to a strikingly lower value than for isotropic particles.

Fig.1: Scheme showing how the resistivity of a conductor-insulator composite is a strong function of the filler fraction, as well as the filler particle morphology. Anisotropic particles (dashed line) tend to have significantly lower percolation thresholds than isotropic particles (solid line)



Furthermore, the type of polymer also has a profound bearing on this critical filler concentration, which has been shown to vary from 10 to 50 vol. %.⁵ Though this

effect may be entirely attributed to the density of the polymer, there is the suggestion that the ability of the polymer to wet the particular filler has a major role to play. Conventional composites, which contain filler particles with a smooth surface, rely upon incomplete wetting of the filler material, since fully coated particles will be prevented from forming electrical contacts with each other. Exclusively in the case of a composite with an infinitely high polymer resistivity, or an infinitesimally small filler resistivity, the following relation applies well to the DC conductivity, σ_{DC} , for filler fractions, f , above the percolation threshold, f_c .⁶

$$\sigma_{DC} \propto (f - f_c)^n \quad (1)$$

with a value of n between 1.6 and 2, in the case of 3-D composites. In an effective medium theory of a composite, the inhomogenous two-component replaced with a homogeneous mixture of one component that has the same macroscopic properties. There exist two distinct cases – the symmetric case is where the actual medium consists of a random mixture of spherical or ellipsoidal particles, of which there are at least 2 components. If one component has a high conductivity, and the other low, the effective medium conductivity will undergo a sudden transition at a certain filler fraction. The antisymmetric case is where one component in the actual medium is invariably completely coated with the other component, in which case a transition in the effective medium conductivity does not occur.² Metal-polymer composites will contain both symmetric and anti-symmetric cases, hence Bruggeman's two effective medium theory equations were combined by McLachlan to give rise to the generalized effective medium (GEM) equation:⁷

$$\frac{(1-f) \left(\sigma_l^{\frac{1}{t}} - \sigma_m^{\frac{1}{t}} \right)}{\sigma_l^{\frac{1}{t}} + \left[\frac{(1-f_c)}{f_c} \right] \sigma_m^{\frac{1}{t}}} + \frac{f \left(\sigma_h^{\frac{1}{t}} - \sigma_m^{\frac{1}{t}} \right)}{\sigma_h^{\frac{1}{t}} + \left[\frac{(1-f_c)}{f_c} \right] \sigma_m^{\frac{1}{t}}} = 0 \quad (2)$$

where σ_l , σ_m , and σ_h are the conductivities of the low, medium, and high conductivity components, respectively, and t is dependent upon the shape of the particles and the percolation threshold, and expressions for it exist for certain scenarios.⁵ With knowledge of t , the percolation threshold, and the conductivities of the polymer and conductive filler, the conductivity of the composite can be deduced from (2) for any particular filler fraction; the fit to experimental data has been shown to be very good.⁵ It can be shown that (2) reduces to an expression of the form of (1) for an infinite conductivity ratio between the high and low conductivity components, as would be expected.

Subjecting a composite to mechanical deformation, either through compression or extension, is effectively equivalent to modifying the loading ratio. Hence, if a composite is fabricated with a filler fraction in the vicinity of the percolation threshold (just above is optimum), it can function as a pressure sensor with changes in resistivity of up to nine orders of magnitude in large applied pressures of 10^6 to 10^7 Pa.² Stretching a conventional composite will progressively ostracize conductive pathways, resulting in a gradual increase in resistivity of typically 10^3 Ωm ; however,

if the sample is stretched to a point where it almost fractures, the change in resistivity has been shown to be as large as $10^{10} \Omega\text{m}$.² The volume coefficient of thermal expansion of a polymer is about three orders of magnitude larger than that of a metal,^{8,9} hence heating a composite gives rise to an expansion of the polymer that is much more pronounced than that for the metal; to all intents and purposes, other than the change in resistivity of the metal during heating, this is equivalent to decreasing the filler fraction. Then, since the resistivity of the composite will increase with temperature, it can be said that a composite has a PTCR effect.

Poisson's ratio for a rubber is very nearly 0.5 (the theoretical maximum, meaning that the volume remains constant upon mechanical deformation), while for a metal it is typically 0.3.¹⁰ The metal in a metal-polymer composite will undergo negligible deformation upon subjecting the composite to stress, however its presence is likely to significantly constrain decreases in dimension orthogonal to the direction of applied stress, hence a Poisson's ratio of closer to zero can be expected.

1.2 What is a Quantum Tunnelling Composite (QTC)?

Accidentally discovered in 1996, a Quantum Tunnelling Composite is a unique brand of metal-polymer composite, patented to Peratech. Traditionally, it is composed of a polydimethylsiloxane (silicone rubber, predominantly Silastic Silicone T4) binder with spiky, spherical nickel filler particles (typically Inco 123, with particles of diameter 3 to 7 microns). The spikiness of the particles, giving rise to electric field enhancement, is essential in promoting quantum tunnelling of electrons between particles – the composite's main conduction mechanism. It is this special combination of materials that permits a complete wetting of the filler with polymer, which is clearly visible in SEM pictures.^{11,12} Since no direct physical contact can be established between the nickel particles, it is not unreasonable to assume that there will be no percolation threshold; experiment confirms this hypothesis - at low compression, resistivity has been found to drop sharply from 82 to 85 w/w % (33 to 38 vol. %), then starts to slowly increase for 87 and 88% loading (42 to 44 vol. %), with Inco 123.¹¹ This strongly implies a smoothing of the spiky nickel surface, due to increased mixing energy required at higher loadings to mix the nickel, polymer and curing agent together to form a macroscopically homogeneous sample. 83 w/w % (35 vol. %) is now regarded as being the optimum filler fraction to create the most sensitive QTC. In the case of spherical particles, for most conductor- polymer combinations, this will be far above the percolation threshold. For the same volume filler fraction, the number density of spiky particles will be substantially larger than that for spherical particles with the same characteristic size, hence the average particle separation will be much smaller with spiky particles. The fact that QTC remains a perfect insulator in an unstrained state (i.e. it is intrinsically non-conductive) illustrates perfectly again the complete wetting of the conductive particles. The material displays an unprecedented sensitivity to pressure, with its resistivity changing by more than twelve orders of magnitude, down to close to the resistivity of the nickel itself, using merely finger pressure. An undesired property is that of the current drifting upwards when a constant voltage is applied for a compliantly compressed sample; this is thought to be due to particle charging effects, as well as defects and impurities in the polymer, at which electrons of a certain energy can become pinned – as more traps become filled, a greater number of electrons entering

the composite are then able to contribute to conduction, accounting for the rise in current. Percolating composites are not prone to this affliction, but all metal-polymer composites suffer from the viscoelastic nature of polymer giving rise to creep, where an applied uncompliant force continues to deform the material over time, due to a relaxation of the polymer in order to maintain the same reaction force. Bulk QTC under compliant compression or extension has unique, non-ohmic I-V characteristics,¹³⁻¹⁵ where on the upwards voltage sweep, at a certain voltage, the current begins to decrease with increasing voltage – evidence of Coulomb blockade behaviour, due to excessive charge on dead-end conductive pathways prohibiting current flow through other pathways. On the downwards voltage sweep, a negative differential resistance regime gives further credence to the “pinching off” hypothesis, since below a certain voltage, the excessive charge will be able to backtrack to find alternative routes through the sample. A property unique to QTC is that under increasing extension, the resistivity is seen to undergo a dramatic reduction – this is diametrically opposed to the trend observed for conventional composites. This can be explained by considering that the decreases in dimension orthogonal to the direction of stretching are sufficient to cause new “zig-zagging” conductive pathways to be created; however, since the act of stretching will have electrically isolated all the conductive particles, the classical conduction mechanism of percolation renders these new pathways inaccessible, even though the mean distance between particles will actually be decreasing with increasing extension, for small extensions. The reason these new conductive networks are utilized within QTC must be by virtue of some quantum mechanical tunnelling mechanism.

1.3 Tunnelling mechanisms

The problem of considering an energy barrier consisting of a metal-polymer interface is complicated by the thin oxide layer, several Angstroms thick, that is likely to exist on the surface of the metal. Contrary to a recent report,¹³ the oxide layer on the nickel particles of QTC *has* been shown to have a significant effect.¹⁶ However, its presence will be neglected in the following treatment, for simplicity.

Fig.2: Diagram showing the energy barrier at a metal – polymer interface. An electron at the Fermi level in the metal requires an energy of the work function of the metal to escape into the vacuum; to escape into a polymer, this required energy is reduced by the electron affinity of the polymer. The Schottky effect modifies the work function in the presence of an electric field, by lowering the image force potential energy, leading to a reduced barrier of height, y , and width, x .

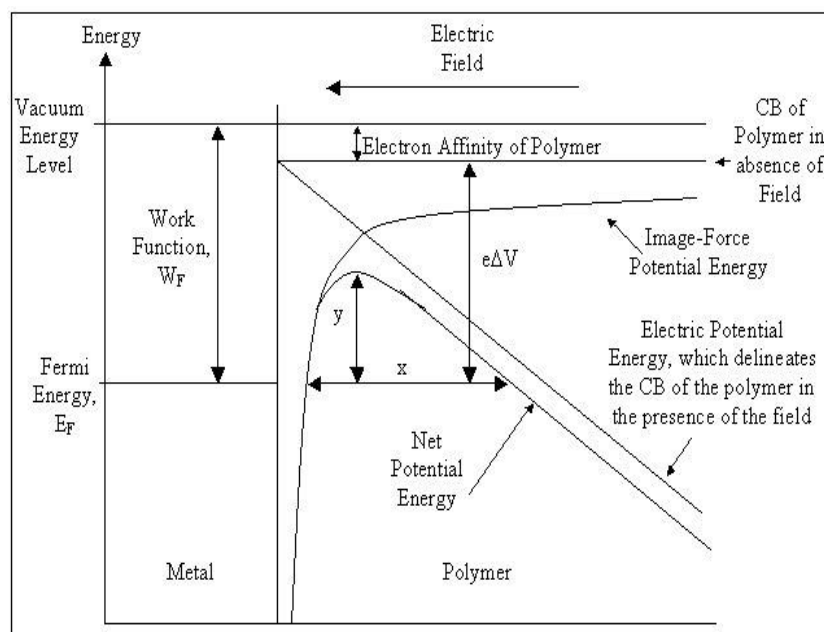


Fig.2 shows the energy barrier that exists at a metal–polymer interface; the situation is very similar to that of a metal–vacuum boundary. In the absence of an electric field, an electron at the Fermi level, E_F , in the metal requires an energy of the work function, W_F , of the metal to escape into the vacuum; to escape into a polymer, this required energy is reduced by the electron affinity of the polymer, though this energy is likely to be very small – hence, it will be neglected in all subsequent theory. The work function stems from the fact that when an electron attempts to leave the surface of a metal, it is attracted back by an image force, which the electron must overcome if it is to escape. At finite temperature, “hot” electrons in the tail-end of the electron energy density of states function may possess an energy greater than $E_F + W_F$, in which case they can escape the confines of the metal completely, in a process known as thermionic emission; however, most electrons have an energy within $k_B T$ of the Fermi energy, and are thus permanently bound. The Schottky effect modifies the work function of the metal in the presence of a sufficiently large electric field, by lowering the image force potential energy, leading to a reduced barrier of height, y , and width, x . Hence, an electron at the Fermi level now has a finite probability of tunnelling through this barrier; into a vacuum, this is termed *Schottky emission*; into a polymer, it is known as Fowler-Nordheim emission,¹⁷ where the electron tunnels through the barrier, directly into the conduction band of the polymer, after which it can conduct essentially as a free electron, which will be carried by the field into another metal particle, if one exists.

The problem of an electron of known energy impinging on a square energy barrier of known height is easily solved using Schrodinger’s equation, yielding exact analytical solutions. However, when the height of the barrier varies with position in a complicated way, an approximation must be used. One such simplification is the *Wentzel-Kramer-Brillouin (WKB) approximation*, which expresses the potential energy as a Taylor expansion about the Fermi level, and is only valid for smoothly varying potential profiles.¹⁸ Using this, an expression for the tunnelling probability, T , of an electron, at the Fermi level, incident on a barrier of height, W_F , in the presence of a uniform electric field, E , can be derived:¹⁹

$$T = \exp \left[-\frac{4}{3} \left(\frac{2m}{\hbar^2} \right)^{\frac{1}{2}} \frac{W_F^{\frac{3}{2}}}{eE} v(y) \right] \quad (3)$$

where m is the electron mass, \hbar is Planck’s constant divided by 2π , e is the electronic charge, and $v(y)$ is a slowly-varying function of E and W_F , and is approximately equal to one for the large fields required for finite tunnelling probability. $v(y)$ models the curvature of the potential energy, due to the Schottky effect, so neglecting it leads to a triangular barrier approximation; in this case, T simplifies to a form:

$$T = \exp \left(-\frac{B}{E} \right) \quad (4)$$

where $B=8 \times 10^{10}$ V/m, using $W_F=5.15$ eV for nickel. Hence, in order to ascertain a reasonable tunnelling probability of, say, one in a thousand, an electric field of the order of 10^{10} V/m is required. However, the dielectric strength of silicone rubber is 16×10^6 V/m,⁸ hence Fowler-Nordheim tunnelling can be deduced to have no effect in a composite if only the effects of a uniform electric field are considered.

Fig.3: Diagram showing how charge on the surface of two metallic particles, separated by a polymer layer, affects the profile of the electric potential energy between them. The gradient of the potential energy, divided by the electronic charge, gives the electric field, which varies as an inverse square law with distance. Hence, the electric field will be infinite (i.e. infinite potential energy) at the surface of the metal, and will fall off quickly with distance, leading to a much smaller field near the centre of the particles, helping to avoid dielectric breakdown of the polymer. The surface charge results from polarisation of the metallic particles in the external field; for particles that are close together, the applied field will contribute little to the field between the particles. Any net charge on a particle may detract from, or enhance, the field

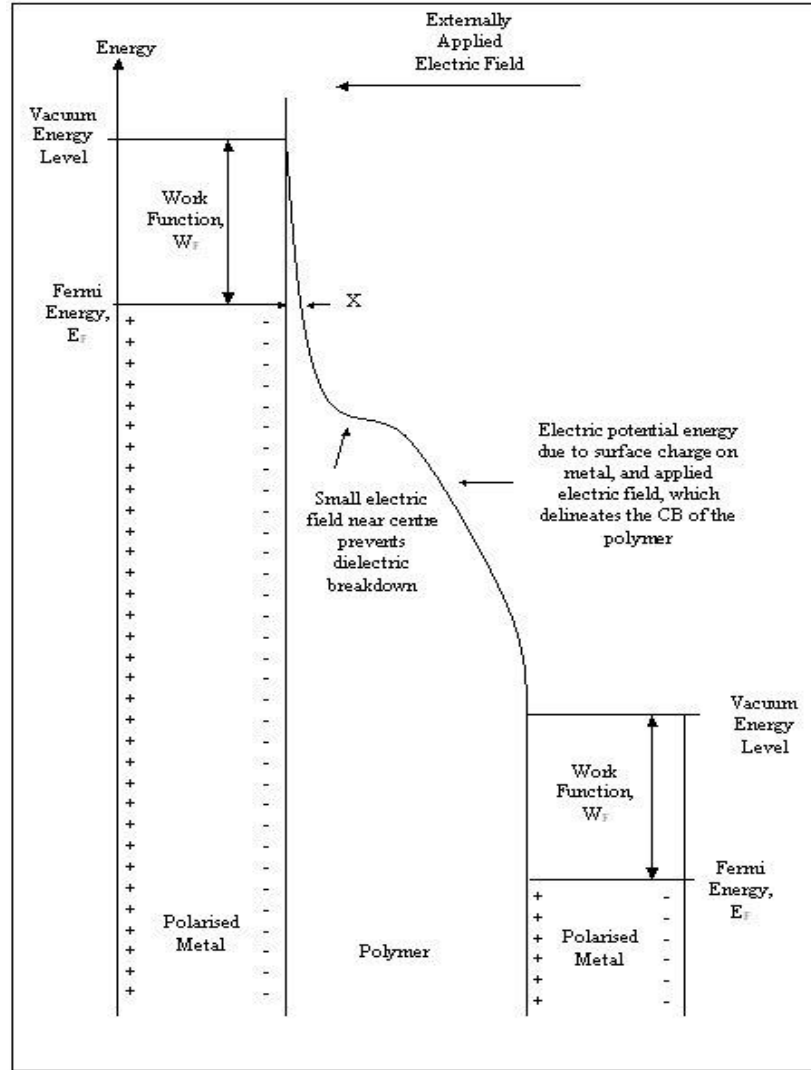


Fig.3 shows how, in the presence of an externally applied electric field, charge in conductive particles migrates to the surface to maintain the condition that the field inside is zero; this results in polarised particles, with positive charge at one end, and negative charge at the other. Thus, a considerable electric field is generated between the particles, within the polymer, which can be much larger than that due to the applied field, especially if the particles are in close proximity to each other. Any net charge, which may be present due to previous electron tunnelling to/from the particle, will uniformly distribute itself around the particle, which may mar or enhance the field between adjacent particles, depending upon polarity. The gradient of the potential energy, divided by the electronic charge, gives the electric field, which varies as an inverse square law with distance from the particle. Hence, the electric field will be infinite (i.e. there is infinite potential energy) at the surface of the metal, and will fall off quickly with distance, leading to a much smaller field near the centre

of the particles; this is imperative to prevent dielectric breakdown of the polymer, which would lead to permanent degradation. The barrier in **Fig.3** may be modelled as being triangular, with a height, W_F , and a width, x . The barrier width can be seen to have been reduced to a size that is remarkably smaller than the thickness of the polymer. To remove the divergent electric field at the surface of the metal, a model incorporating the Schottky effect is ideal. The applicability of (3) is dubious, since the field in **Fig.3** may not be smoothly varying, but a reasonable approximation of tunnelling probability may be ascertained by calculating the average electric field across the insulating gap, then substituting this value into (3) as E . However, a tunnelling probability equation that is derived by considering the exact shape of the electric potential energy is desired.

Numerous other conduction mechanisms have been proposed for metal-polymer composites; these include *fluctuation-induced tunnelling* (involving thermally activated fluctuations in the shape and size of the energy barrier),²⁰ *hopping* (which involves electrons that have become pinned in traps “hopping” between adjacent traps in the polymer, which is always thermally assisted to some extent, but may involve tunnelling at lower temperatures),²¹ and *resonant tunnelling* (exploiting a phenomenon used by resonant tunnelling diodes, whereby multiple adjacent energy barriers, separated by a very narrow gap such that only a few electron energy levels are permissible within the gap – resonant energy levels – may allow electrons to tunnel through all barriers with minimal attenuation if a common energy level exists between them; the presence of oxide layers on the nickel particles may allow such an event).²² However, the predominant conduction mechanism in QTC is thought to be Fowler-Hordheim tunnelling.

1.4 Conductive sphere in electric field

In conventional composites, the conductive particles can often be considered as being spheres. As previously discussed, in the presence of an electric field, a conductive particle will become polarised.

Fig.4: Polarised sphere in an external electric field directed in the negative z-direction. Free electrons in the conductor will migrate to the surface of the sphere, in order to oppose the field. Just inside the sphere, the negative surface charge will produce an electric field vector directed outwards. In order to oppose the external field, the magnitude of this field must equal $E_z \cos \theta$. Just outside the sphere, the negative surface charge will produce an electric field directed radially inwards. Positive surface charges will produce oppositely directed electric field vectors

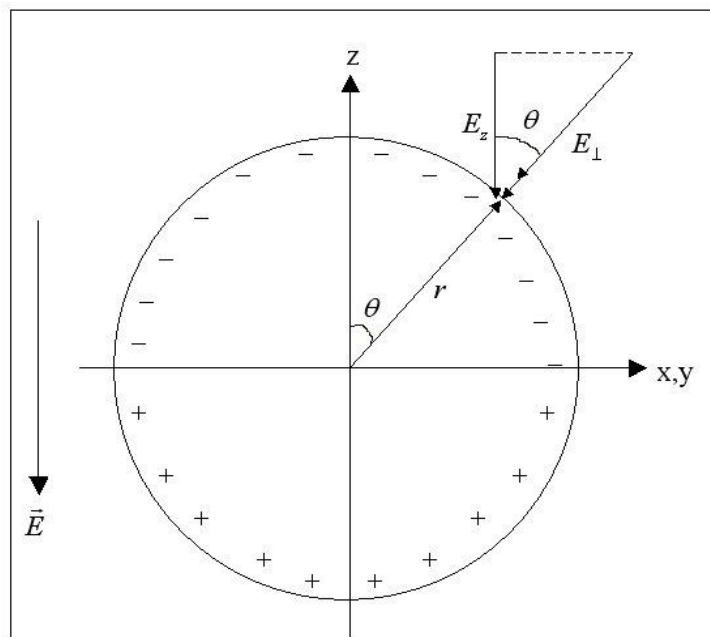


Fig.4 shows a polarised conductive sphere in a uniform, external electric field, \vec{E} , directed in the negative z-direction. Nickel contains 2 free electrons per atom, so for spheres of diameters from 3 to 7 micrometers (i.e. the range of diameters in Inco nickel 123, the most common QTC filler), there will be of the order of 10^{12} to 10^{13} free electrons. Some of these electrons will migrate to the surface of the sphere, in order to oppose the field, leaving an excess of positive charge on the other side of the particle. Just inside the sphere, the negative surface charge will produce an electric field vector directed outwards, E_{\perp} , which has the following form, by Gauss's law:²³

$$E_{\perp} = \frac{\sigma}{\epsilon_0 \epsilon_p} \quad (5)$$

where σ is the surface charge density on the sphere, ϵ_0 is the permittivity of free space, and ϵ_p is the dielectric constant of the surrounding medium, which in this case will be polymer. The surface charge density is a function of the azimuthal angle, θ , as shown in **Fig.4**. In order to oppose the external field, E_z , the magnitude of this field must equal $E_z \cos \theta$. Hence:

$$E_z = |\vec{E}| = E_{\perp} \cos \theta = \frac{\sigma}{\epsilon_0 \epsilon_p} \cos \theta \quad (6)$$

$$\Rightarrow \sigma = \frac{\epsilon_0 \epsilon_p E}{\cos \theta} = \frac{dq}{dA} \quad (7)$$

where dq is an infinitesimal charge on infinitesimal area, dA . In spherical polar coordinates:

$$dA = r^2 \sin \theta d\theta d\phi \quad (8)$$

$$\Rightarrow dq = \epsilon_0 \epsilon_p E r^2 \tan \theta d\theta d\phi \quad (9)$$

$$\Rightarrow Q = \int_0^Q dq = \epsilon_0 \epsilon_p E r^2 \int_0^{\frac{\pi}{2}} \tan \theta d\theta \int_0^{2\pi} d\phi \quad (10)$$

where Q is the total negative charge on the upper hemisphere of **Fig.4**; this is also the total positive charge on the lower hemisphere. The integral over θ is a standard integral:

$$\int \tan \theta d\theta = \ln |\sec \theta| + c \quad (11)$$

where c is a constant of integration. Unfortunately, the integral diverges to infinity at the limit $\pi/2$, implying infinite charge there. However, no lines of electric flux will penetrate this part of the sphere, hence the charge will be zero there. To remove this divergence, the integral must be calculated from zero to as close as $\pi/2$ as possible. Hence:

$$\lim x \rightarrow \frac{\pi}{2} \int_0^x \tan \theta d\theta = 37.3318892262 \quad (12)$$

This was calculated using Fortran with double precision numbers. Thus, the total charge on the surface of a hemisphere of radius, r , is:

$$Q = \frac{2\pi\epsilon_0 V r^2}{d} (37.3318892262) \quad (13)$$

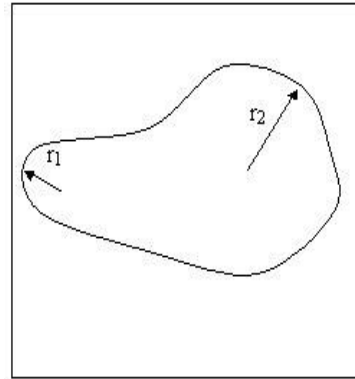
where V is the voltage applied across the sample, and d is the effective thickness of the polymer; knowledge of the volume filler fraction can be used to yield the fraction of polymer in the sample, hence multiplying this by the volume of the composite yields the volume occupied by polymer; dividing this by the cross-sectional area gives the value of d . (13) was derived using:

$$E = \frac{V}{d\epsilon_p} \quad (14)$$

The electric field within the polymer is reduced by a factor of ϵ_p , which is the dielectric constant of the polymer, since the polymer itself becomes partially polarised, attenuating the applied field. Electric potential only drops across the polymer regions because, as has just been shown, there can be no electric field within the conductive spheres. Just outside the sphere, the negative surface charge will produce an electric field, E_\perp , directed radially inwards, depending only upon θ . Positive surface charges will produce oppositely directed electric field vectors. Any net charge will uniformly distribute itself around the sphere, giving its own contribution to E_\perp .

1.5 Field enhancement due to spikes

Fig.5: An arbitrarily shaped object may be considered as having different radii of curvature at different points upon the surface. If the object is a conductor with charge on its surface, the surface charge density can be shown to be larger where the radius is small, as with r_1 , to be contrasted with r_2



An arbitrarily shaped conductor is depicted in **Fig.5**. If charge is placed on the conductor, it will distribute itself over the surface so that it becomes an equipotential surface. The potential of a sphere, V , of radius, r , in air, carrying a charge, Q , is given by:⁹

$$V = \frac{Q}{4\pi\epsilon_0 r} = \frac{4\pi r^2 \sigma}{4\pi\epsilon_0 r} = \frac{r\sigma}{\epsilon_0} \quad (15)$$

$$\Rightarrow \sigma = \frac{\epsilon_0 V}{r} \quad (16)$$

Since V is constant all around the surface, the surface charge density can be seen to be inversely proportional to the radius of curvature of the surface at a particular point. Hence, a spiky morphology would be conducive to a very large surface charge density (and thus, outward electric field vector, from (5)) at its tip. It has been reported²⁴ that a simple theoretical expression exists for the field enhancement factor (i.e. the factor by which an electric field from a surface is increased), β , of a surface irregularity with a smooth surface, of height, h , and radius of curvature, r , is given by:

$$\beta \approx 1 + \frac{h}{r} \quad (17)$$

where emission is from the tip, and:

$$\beta \approx \left(1 + \frac{h}{r}\right)^{\frac{1}{2}} \quad (18)$$

where emission is from the edge. Should this surface irregularity feature itself much smaller surface irregularities, the field enhancement factors of these extra irregularities multiply with the enhancement factor of the original irregularity to form an overall enhancement factor. Hence, long, sharp spikes with a dendritic structure, on the surface of a sphere, would be expected to give rise to considerable Fowler-Nordheim tunnelling in a metal-polymer composite; this is the case in QTC with nickel 123 filler particles.

1.6 Theory of polymer swelling

A sample of cross-linked elastomer may be thought of as a three-dimensional network of elastic bands (representing the molecules) of uneven length, with a highly non-crystalline structure. In the unstrained state, there will exist volume between the polymer molecules that is occupied by whatever inert gas the sample is in the presence of; this can be termed *actual free volume* within the polymer. Assuming a Poisson's ratio of 0.5, any compression or extension of the sample in one dimension would be expected to leave the actual free volume intact. Compressing the sample in three dimensions would decrease the actual free volume; conversely, extending the sample in three dimensions will increase the actual free volume, realising *potential free volume*.

When placed in the presence of a solvent vapour, a concentration gradient (in terms of vol. % of solvent) will exist across the boundary of the polymer, promoting diffusion of solvent molecules inwards. However, the probability of a solvent molecule spontaneously mixing with the polymer increases substantially when the diffusion process is associated with a larger decrease in the Gibb's free energy of the system, ΔG_{mix} , which has the following dependence at constant pressure and temperature:²⁵

$$\Delta G_{mix} = \Delta H_{mix} - T\Delta S_{mix} \quad (19)$$

where ΔH_{mix} is the *enthalpy of mixing*, T is the temperature of the system, and ΔS_{mix} is the *entropy of mixing*. Most processes involving the mixing of gases and solids will be endothermic (i.e. $\Delta H_{mix} > 0$), opposing solution; the following relation is generally true:²⁶

$$\Delta H_{mix} \propto (\delta_1 - \delta_2)^2 \quad (20)$$

where δ_1 and δ_2 are the *solubility parameters* of the solvent and the polymer:²⁶

$$\delta = \left(\frac{\Delta H_V}{V_M} \right)^{\frac{1}{2}} \quad (21)$$

where ΔH_V is the enthalpy of vaporisation at zero pressure, and V_M is the molar volume. Thus, commensurate solubility parameters between polymer and solvent are conducive to a greater tendency of formation of solution. The entropy of a solution of polymer and composite is very difficult to calculate, having rotational, vibrational, translational and combinatorial components, but it is always true to say that a positive change of entropy is associated with the process of a solvent molecule diffusing into the polymer, and the magnitude of this change will be larger for a bigger solvent concentration mismatch between inside and outside the polymer. From (19), it can be seen that events yielding the largest change in entropy of the system are the most probable, and that diffusion is likelier the higher the system temperature is. Hence, actual free volume at the surface of the sample will begin to fill with solvent molecules; once the solvent concentration in this free volume is locally the same as that outside the polymer, a large entropy change can still be associated with further diffusion events into this free volume – this extra packing of molecules into the actual free volume, realising potential free volume, is the origin of polymer swelling. Diffusion will continue further on into the sample, liberating more potential free volume in its wake. To accommodate the solvent molecules, there will be an accompanying diffusion outwards of the original gas molecules in the sample, again with the proviso that a diffusion event is more likely when it is associated with a greater reduction in the Gibb's free energy of the system. The extent of swelling is limited by the degree of cross-linking in the polymer, with a material of higher bulk modulus offering enhanced resistance to expansion. Consequently, even if the Gibb's free energy of the system can be decreased with a certain diffusion event, the event can only occur if the change in energy is sufficient to overcome the elastic energy. As the solvent concentration inside the sample approaches that outside, the change in entropy of the system invoked by a diffusion event becomes lessened, eventually to the extent that further inwards diffusion is halted at the point where the free energy of the system can no longer be reduced; *saturation* of the polymer by the solvent is said to have occurred.

1.7 Concept of “electronic nose” using metal-polymer composite

If a conventional metal-polymer composite, with filler fraction just above percolation threshold, is exposed to solvent vapour, the swelling of the polymer will effectively decrease the loading ratio of the material, progressively ostracising conductive pathways, giving rise to an increase in resistivity of several orders of magnitude [ref], at a rate proportional to the swelling. In the case of QTC, the material must first be

mechanically deformed into a conductive state, constraining polymer expansion in the direction of deformation; however, any potential free volume liberated would be expected to produce a much more drastic change in resistivity. (19) and (20) state that solvent saturation will occur at a higher concentration of solvent within the polymer (i.e. more potential free volume is liberated) for greater matching of the solubility parameters, and higher system temperatures, in addition to a higher solvent concentration outside the polymer (from entropy considerations). This culminates in the fact that the change in resistivity of a metal-polymer composite under exposure to a solvent vapour will depend upon the polymer-solvent combination and the solvent concentration – this gives rise to the possibility that a composite may be used as a vapour sensor that permits *quantitative*, in tandem with *qualitative*, information about vapours it is placed in the presence of. The standard diffusion equation:

$$\frac{\partial C}{\partial t} = D \nabla^2 C \quad (22)$$

may be used to roughly model the time dependence of the diffusion, given appropriate boundary conditions. Here, C is the concentration of the solvent (i.e. number density of molecules) in the polymer, so it can immediately be seen that a higher solvent concentration at the periphery of the composite will result in a faster rate of diffusion. In order for this concentration to be maintained, the vapour must be flowed past the composite to replenish that which has diffused into the polymer – this leads to the condition that a slow or non-existent flow rate will impair the rate of diffusion. From entropic considerations, a higher pressure of solvent vapour may be expected to catalyse diffusion, and also give rise to enhanced polymer swelling, however the reduction of the actual free volume of the polymer, in the presence of a higher pressure of air, may cause the opposite effect. The diffusion coefficient, D , will be related to the magnitude of the Gibb's free energy of mixing, becoming zero for non-negative values of ΔG_{mix} . Complex mathematical treatments of the kinetics of swelling have been published.²⁷

When the composite containing solvent molecules is placed in the presence of an inert gas (e.g. nitrogen, of which 78% of normal air is composed), a concentration gradient of solvent will exist across the wall of the sample in the reverse direction, hence diffusion of solvent molecules out of the composite is promoted. Initially, the rate of flushing of the molecules out of the sample will be considerably faster than the rate at which they were diffusing inwards, since now polymer relaxation assists in expelling molecules, whereas before it was inhibiting diffusing. Once the actual free volume of the polymer returns to its original value, the resistivity of the composite will also be expected to have almost resumed its initial magnitude; this may not be true if any chemical interactions have occurred between the solvent and the polymer or conductive filler, or if a reordering of molecules has taken place, which is likely to occur for samples that have had no previous chemical or mechanical history. A faster flow rate of this purging gas, to maintain the highest possible solvent concentration mismatch across the polymer wall, will be conducive to swifter purging. A higher pressure of surrounding gas, in this instance, will also promote solvent expulsion. Re-exposing the sample to solvent before complete purging has taken place would be expected to result in much faster saturation. Breaking a sample up, to increase its surface area in contact with the vapour, will also expedite the onset of saturation; faster purging, when placed in the presence of an inert gas, will also result, by the

same reasoning – this will be fortuitous for a vapour sensor which detects and identifies a gas by examination of the fractional change in resistance between purge and exposure, for many purge and exposure cycles. Hence, granules of metal-polymer composites may out-perform equivalent bulk samples in the vapour sensing application. In the case of QTC, a larger loading ratio of around 90 w/w % (49 vol. %) is found to be optimum, due to a different fabrication process being deployed for granules compared to bulk samples. The I-V characteristics of granules have been found to be comparable to those of bulk QTC.²⁸

Other than the act of polymer swelling, there are other phenomena that can alter the electrical characteristics of a composite. *Physisorption* or *physical adsorption* arises due to non-specific van der Waal's forces between solvent molecules and the surface of the polymer (and conductive particles, if any may be protruding from the sample); even though several layers of adsorbed solvent may result, the fact that the interaction is very weak and temporary, with desorption occurring readily upon purging, the process of physisorption can be deemed to have negligible effect upon a composite's sensing properties.²⁹ In contrast, *chemisorption* or *chemical adsorption* stems from much stronger binding forces, leading to actual chemical bonding between the solvent and polymer/conductor molecules; desorption in this instance is not always possible, and when it is, often the desorbed molecule is chemically different to that adsorbed, leading to a permanently altered composite. In the case of granules, this may have a profound impact on the quality of electrical contact that is established between them, giving rise to unrepeatable responses to solvent exposure; furthermore, subsequent exposure to different solvents may yield a response that is dependent upon all previous chemical history, which will have detrimental consequences with regard to the exceptionally important issue of reproducibility. However, chemisorption ceases once a single monolayer has been adsorbed, hence, if permanent, phenomenon will no longer pose a problem for subsequent exposures to different solvents.²⁹

In the interests of optimising sensor sensitivity to the presence of a vapour (i.e. enhancing minimum detection levels), the degree of cross-linking of the polymer should be sufficiently low such that there is as little resistance to swelling as possible, whilst being high enough to prevent polymer degradation due to the solvent dissolving the polymer.

1.8 Applications and current standard of composite vapour sensors

Array-based vapour sensors eschew the “lock and key” approach whereby a sensor is tailor made to respond strongly and highly selectively to a particular analyte;³⁰ this renders them less useful for applications where a specific target compound is to be monitored in the presence of background interference. Instead, array-based sensors exploit the simultaneous use of a wide range of sensors, each of which responds broadly and cross-reactively to a wide range of analytes; some specificity is introduced by selecting sensors with as wide a chemical diversity as possible.³¹ A distinct pattern of responses can then be associated with a certain analyte; a form of multi-variate data analysis, *principal component analysis (PCA)*, is then often used³⁰⁻³⁵ to reduce the data set down to a minimum number of dimensions, after which a 3-D graph can be plotted where a certain point on the graph is associated with a particular analyte and a particular concentration of that analyte; other discriminant

algorithms are sometimes used.³⁶ In order to optimise the technique of PCA, data is often denoised and pre-processed by use of the wavelet transform.^{32,34} It has been shown³³ that a particular metal-polymer composite array, utilising just ten sensors, can outperform even the human olfactory system with regard to discriminating power. A big advantage to the use of a sensor array is that it can allow recognition of new odours that the array was not originally designed to detect.³¹

Electronic noses find applications in many industries, including the detection of leakages in chemical plants (petrochemical), the sensing of chemical warfare (military),³⁵ and the evaluation of the quality of products such as wine, beer and cheese (food industry). Perhaps the ultimate vapour sensor comes in the guise of a mass-spectrometer, but such a device is extremely expensive and bulky. An American company, Cyrano Sciences Inc.,³⁷ have made commercially available a relatively cheap, handheld electronic nose that incorporates a chip on which there are fabricated 32 intrinsically conducting composites, with carbon-black filler particles. The device, called the “Cyrano 320”, can qualitatively identify 100 programmed smells within 10 seconds, and may be “trained” to recognise new smells. The reason for this remarkably fast response time is that the 320 doesn’t always allow saturation to occur, but simply measures the fractional change in resistance a few seconds after exposure; hence the rate of polymer swelling is of just as much relevance as its ultimate extent. Accurate quantitative information takes longer to ascertain, and this can only be done reliably for the 100 pre-programmed smells. The unit also has a wide operating temperature range of 0 to 40 degC. Cyrano have been successful in fabricating hundreds of sensors on a chip measuring just 0.04 cm²,³⁵ hence their dominance in the market looks set to continue.

1.9 Measuring solvent vapour concentration

A liquefied solvent, when placed in an evacuated chamber, will evaporate to fill the chamber, until the air pressure reaches a value known as the equilibrium *vapour pressure*, P , of the solvent. In a vacuum, this parameter is a function of the solvent temperature, T , only, and is described well by the *Clausius-Clapeyron* equation:³⁸

$$\ln P = -\frac{\Delta H_V}{RT} + c \quad (23)$$

where ΔH_V is the enthalpy of vaporisation at the solvent temperature, R is the molar gas constant, and c is the *Clausius-Clapeyron constant* for the particular solvent, which can be calculated from (23) if the vapour pressure for a particular temperature is known. (23) has been derived by assuming that ΔH_V is a constant, yet it has a slight temperature dependence. It also assumes that the molar volume of the vapour is considerably less than that of the liquid, which is a very good assumption at around room temperature and below. Also assumed is that the vapour is an ideal gas, which is also a reasonable assumption for pressures around atmospheric and lower; making use of the van der Waals corrected form would introduce considerably greater complexity into the form of (23). If an inert gas is present in the chamber, at a pressure, P_g , the vapour pressure becomes a partial pressure, and is modified to a new equilibrium vapour pressure, P^* , given by the following equation:²⁵

$$P_* = P \exp \left[\frac{V_m (P_g - P)}{RT_g} \right] \quad (24)$$

where V_m is the molar volume of the solvent, and T_g is the temperature of the gas, which will very nearly equal the solvent temperature if the chamber is thermally insulated. (24) is also derived by making use of the assumption that the overall gas is ideal. If the volume of the chamber is known (discounting the volume occupied by the liquefied solvent), substitution of it into the ideal gas equation, along with P_* and T_g , can yield a value for the number of moles of vaporised solvent in the chamber. For a chamber that is large in extent above the surface of the liquefied solvent, this number will remain nearly constant if a small aperture is placed in the top of the chamber that allows the air inside to slowly flow out to the atmosphere, since any molecules that leave the vessel will be replenished by the vaporisation of new solvent molecules at the surface of the liquefied solvent. If an inert gas was allowed to enter the vessel by passing a reasonable distance (e.g. 10 cm) through the solvent in the form of very small bubbles, by the time a bubble has reached the surface it will contain the same concentration of solvent as the air already in the chamber, provided that air is allowed to exit the vessel at the same rate as it enters. Hence, if the volume flow rate, \dot{V} , of air entering the chamber is known, the number of moles per unit time, \dot{n} , leaving the vessel can be deduced from the ideal gas equation:

$$\frac{\dot{n}}{\dot{V}} = \frac{P_*}{RT_g} \quad (25)$$

where the quantity on the left-hand side of the brackets is the number of moles of solvent per unit volume of carrier gas. With units of milligrams of solvent per litre of carrier gas, this quantity is said to be the parts per million (ppm) of the solvent; Cyrano use this definition of ppm to describe their solvent concentrations [refs], which works when the “part” describes a unit of mass, and the reference volume is liquefied water. (25) is only valid for finite flow rates; when $\dot{V} = 0$, \dot{n} will still have a non-zero component that will become negligible for large volume flow rates.

The mass flow rate, \dot{M} , of a gas through a system with a pressure gradient, ΔP , across it is related to the resistance to gas flow, R_{flow} , within the system by the following equation:

$$\dot{M} = \frac{\Delta P}{R_{flow}} \quad (26)$$

which is analogous to Ohm’s Law for the flow of electrical current through a system with a potential difference across it. Thus, the mass flow rate can be considered to be constant throughout the system. It is related to the volume flow rate and the density of the gas, ρ , by the following equation:

$$\dot{M} = \rho \dot{V} \quad (27)$$

Hence, as the density of the gas increases, the volume flow rate decreases, and vice versa. The density of a gas increases with temperature and pressure; since the pressure will drop as the gas passes through the system, the volume flow rate will increase. A mass flow controller works by regulating the air pressure at the start of a system such that the volume flow rate leaving the system is that specified by the user, usually expressed in standard ml/min (i.e. the volume is at s.t.p.). Hence, if there is a source of flow restriction to the gas leaving the chamber, the air pressure inside will be higher, leading to a higher density and thus a lower volume flow rate. It should be stressed that “mass flow rate” and “volume flow rate” here refer exclusively to the carrier gas; the addition of solvent molecules to the gas flow will complicate matters still further. A lower temperature of gas in the chamber (which will essentially be equal to the solvent temperature) will also be conducive to a lower volume flow rate. From (25), since the right-hand side is constant, this will lead to a lower rate of solvent molecules leaving the system. Since the mass flow rate of the carrier gas remains constant, the rate of carrier gas molecules leaving the system is constant. This implies that the ppm value depends upon the air pressure in the chamber – also, the temperature of the solvent appears to affect the ppm value in a different way than simply affecting the vapour pressure of the solvent.

Another means of expressing the concentration of a solvent vapour is by writing the vapour pressure as a fraction of the saturated vapour pressure at a standard solvent temperature (usually 25 degC). It has been shown³⁹ that in this form, the minimum detection level of a sensor (i.e. the smallest concentration of solvent that creates a sensor signal that can just be discerned above the noise) is approximately independent of the analyte being tested. Thus, once the minimum fraction of vapour pressure has been found for one solvent, the minimum ppm values for all other solvents to “just” cause a response from a particular sensor can be ascertained.

2. EXPERIMENTAL MATERIALS, METHODS, RESULTS, AND DISCUSSION

2.1 Computer simulation of QTC

2.1.1 How the program works

A computer simulation, to model the movement and distribution of charge through QTC, has been written in Fortran; the code is shown in **Appendix A**. Considering the complexity that is inherent in a system consisting of spiky spherical particles, as a starting point, it was decided to model the filler particles as perfect spheres; while this will not accurately simulate the motion of charge in a QTC, it should provide a good simulation of a conventional composite, which will be useful as a point of comparison once spiky particles have been somehow incorporated, replacing the spheres.

The program begins by creating a virtual QTC by randomly placing spheres, of size within a specified range, within a volume of QTC as chosen by the user, in the form of x, y, and z Cartesian coordinates; this defines a provisional volume of the QTC. The electric field is to be applied in the negative z-direction. The loading ratio of filler particles is specified by the user in terms of a w/w %. When QTC is manufactured,

the mass of the silicone rubber is measured before curing; the process of curing will lead to a mass loss of the rubber, leading to a lower than stated volume fraction of polymer. Fortunately, a 30 g sample of uncured silicone rubber plus curing agent has been shown to suffer a mere 0.15 % loss in mass upon curing, which will have a negligible effect regarding the volume fraction of polymer. The density of cured silicone rubber is 0.97 g/cm^3 ,⁸ and this value is substituted into the equation given in **Appendix D**, to convert from the w/w filler fraction to the total volume occupied by the filler within the composite. Assuming a uniform size distribution of particles, this volume is then converted into the number of spheres, N , within the specified sizes, that are required to fill the QTC to the stated filler fraction. The QTC volume is then divided up into N cubes, which may be regarded as unit cells. Each of the three QTC dimensions are then divided by the length of this unit cell, to yield the number of unit cells in the x-, y-, and z-directions. The composite then has new dimensions, given by the product of the number of cells along the particular dimension and the unit cell dimension; this then defines a new volume of QTC. An $N \times 6$ matrix is then initialised, so that every element is zero, except all elements in the 6th column, which are given the initial value “-1” – once the QTC particles have been generated, each one is given a net electron, hence the 6th column represents the number of net unit charges on a particular particle. The first 3 columns are to represent the coordinates of the centre of a particle, in Cartesian x-, y-, and z-coordinates, the 4th column is the particle diameter, and the 5th column will be the number of polarised electrons on the upper hemisphere (i.e. pointing in the positive z-direction), and the number of equivalent positive charges on the lower hemisphere, calculated from (13). 4 random numbers are generated, where the first three represent provisional Cartesian coordinates for the centre of a particle within a cubic cell, and the 4th is used to generate a particle diameter between the stated range. The first unit cell is at the origin of the Cartesian system; since there are no filler particles in the QTC yet, the first particle goes straight into this unit cell, so that the global Cartesian coordinates of its centre are the coordinates within the unit cell multiplied by the cell dimension. This data is stored in the first row of the matrix. The next unit cell to be considered is right next to the first, in the positive x-direction. 4 random numbers are generated, as before, and the particle can then be placed in the second unit cell. If the particle is found to overlap with the first, new particle coordinates must be generated for this 2nd particle. If the user requested a uniform particle size distribution, the original particle diameter is retained, otherwise a new particle diameter is randomly generated. The new coordinates are used to place the particle in the second cell again; if it is found to overlap with the first, the process is repeated again. 100,000 attempts are made to randomly place the particle in the unit cell without overlapping with adjacent particles. After 100,000 attempts, the unit cell remains empty, and the next unit cell is considered, which is the next one up in the positive x-direction. If the user does not stipulate a uniform particle size distribution, the fact that the particle size is randomly generated for each attempt makes it more likely for a smaller particle to be successfully placed in a cell without overlap, leading to a non-uniform particle size distribution. Even if requested, the fact that a cell is more likely to be left empty for a larger particle always leads to a non-uniform particle size distribution. Cells are filled up in this fashion until all cells in the x-direction (and first y- and z-planes) have been considered. All the cells in the x-direction of the second y-plane (still in the first z-plane) are now considered, where extra checks are now required to ensure particles are not overlapping; the particle coordinates, in microns, have 10 significant figures, hence particles may be as close as 0.1 fm to each other. This process is repeated until

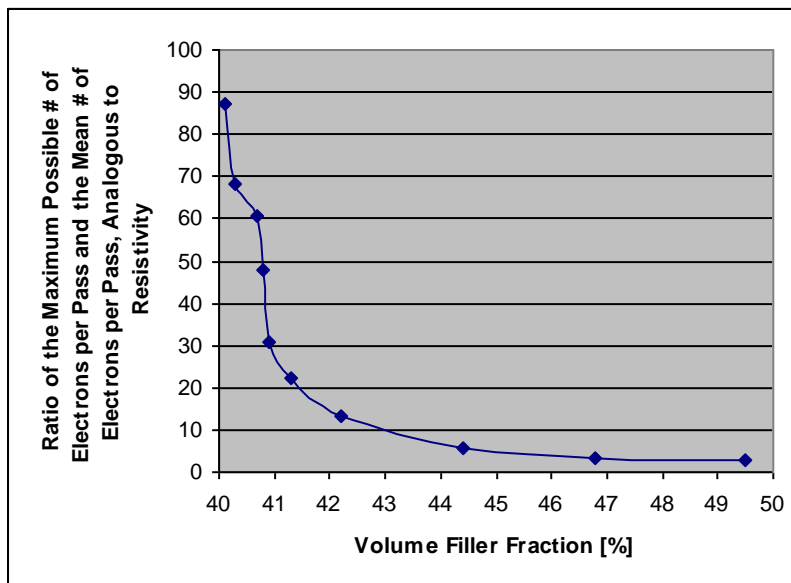
all the cells in the first z-plane are filled, after which all cells in the next z-plane are filled in exactly the same way, and so on, until all unit cells in the QTC have been considered. The actual volume occupied by these spheres is then calculated, yielding an actual volume filler fraction; this is then converted back to a w/w %. The number of polarised electrons on each particle is then calculated, and stored in column 5. The data can then be stored as a text file (e.g. “1” is stored as “1.txt”) using the option in the main menu; previously-stored data can be retrieved in the same way. The QTC can be stretched and compressed; when stretched, this automatically assumes constant volume, hence the factor by which the z-dimension is increased results in the x- and y- dimensions decreasing by the square root of the same factor. The coordinates of the centres of the particles are scaled by the same respective factors (e.g. a “110%” extension means that all z-coordinates are multiplied by 1.1; this means that particles are now able to overlap with one another. Under compression, a choice is given as to whether a constant volume is maintained; if so, the particle coordinates are scaled in the same way as for extension; if not, only the z-coordinates are scaled. Once a QTC has been deformed, it remains deformed, hence further deformation is in addition to previous deformation; the QTC data can be stored in this deformed state. An option in the main menu allows the number of overlapping particles to be calculated, where a particular instance of overlapping is only counted once. The maximum, minimum, and average distances between neighbouring particles can also be ascertained. In addition, the particle size distribution can be displayed.

Once the QTC data has been satisfactorily generated, an electric field is then ready to be applied. A voltage is specified by the user, as well as the number of “passes” through the material. The voltage is converted to an electric field by using (14), where the DC dielectric constant of silicone rubber may be considered to be very nearly equal to the low frequency case, which is found to be 2.8.⁸ In one pass, each particle is considered in the same order that was used to fill the QTC, where the single net electron that is placed on each particle is given the opportunity to propagate. To begin with, percolation is considered to the next z-plane, first to the particle in the same x- and y-planes. If the distance between the surfaces of the particles is less than 1nm, the particles are considered to be touching; this is a good assumption, since quantum tunnelling across such a small insulating gap would be very likely. If touching, or overlapping, all net electrons will propagate between particles, leaving the receiver with all of these extra net negative charges, and the supplier with no net charges; this is with the proviso that the supplier has net negative charges to give, and that the receiver does not have more net negative charges than the supplier – if these conditions are not fulfilled, no propagation occurs, and an attempt is made to propagate to another neighbouring particle in the next z-plane. Once all neighbouring particles in the next z-plane have been considered, quantum mechanical tunnelling is considered between all particles in the next z-plane, if the user has selected that such effects be considered. As soon as any electrons propagate, the next particle is given a chance to propagate charge. The calculation of the electric field within the polymer layer between the particles is extremely complicated. It involves finding the midpoint of the polymer layer, then considering how much of the surface areas of the giver and receiver particles is visible from this midpoint. This area is then divided up into 20 patches on each particle, and (10) is used to calculate how much charge exists on each patch, using appropriate limits of integration for θ and ϕ (see **Appendix E**). This charge includes contributions from the polarised electrons and polarised “positive electrons”, as well as the net charge on a particle, which will give rise to a uniform

charge distribution, as described in **Appendix C**. The centre of each patch is at a known distance from the midpoint, hence the electric field vector at the midpoint due to each patch of charge on the two particles can be ascertained, yielding an overall electric field vector at the midpoint, which includes the contribution from the externally applied field in the negative z -direction. The component of this vector in the direction of the line joining the centres of the two particles (i.e. in the direction of tunnelling, reducing the problem to a 1-D energy barrier) can then be calculated by taking the dot product of the electric field vector with the unit vector in the direction of propagation. The resulting component of the electric field is the value of E used in (4). However, tunnelling is only considered if the electric field vector at the midpoint has a component in the direction of the supplier particle, otherwise electrons there will be repulsed, and electrons at the receiver particle will be attracted; at some point in the future, the program may be adapted to allow for the possibility of backwards-propagation of electrons, caused by this misdirected electric field. A random number is generated, and if less than the tunnelling probability from (4), the electrons are transferred between particles, in exactly the same way as for percolating particles, where the same provisos are in operation. If no tunnelling can occur to all neighbouring particles in the next z -plane, percolation is considered to all adjacent particles in the same z -plane. If unsuccessful, quantum tunnelling is then considered to all neighbouring particles in the same z -plane. After all this, if no electron propagation has occurred, the supplier particle retains its electrons for this particular pass, and the next particle is given the opportunity to propagate electrons. Once all particles have been given this opportunity, this is the end of one pass, and the next pass is begun, until the stated number of passes has been carried out. When propagation is being considered to the final z -plane, if successful, the electrons propagated immediately pass to the particle in the first z -plane, in the same x - and y -planes as the receiver particle. The number of electrons that return back to the start of the QTC in this way are counted for each pass; this value forms the basis of very crude estimations of the current, resistance, resistivity and conductivity. If the number of electrons emerging from the QTC in one pass is equal to the number of particles in the composite, then the composite can be considered as conducting like a metal (in this case, pure nickel) with the same dimensions as the QTC; this will only yield reasonable values for a very large number of filler particles. The equations used to calculate these values are shown in **Appendix B**. The composite now has an electrical history, and can be saved in this form, so that the charge distribution can be observed, for instance, in any z -plane by plotting column 6 in the text file against the corresponding x - and y -coordinates.

2.1.2 Results and discussion

Fig.6: Computer simulation data showing how the number of electrons emerging from a QTC per pass decreases sharply as the volume filler fraction reduces, with a percolation threshold at about 40 vol. %. These composites were 0.1 mm in all 3 dimensions, with filler particles of diameter 3 microns; to elicit a conductive state, they were all compressed to 80% in the z-direction, and quantum effects were ignored. All composites had no electrical history prior to this data acquisition



Some data generated by the computer simulation is shown in **Fig.6**, where samples of different volume filler fraction (converted from w/w % by using the equation in **Appendix D**) were each compressed to 80 %, and under application of 1 V (though any voltage will give the same result, when quantum effects are neglected), the mean number of electrons per pass was measured; the number of electrons per pass was found to converge, within a few passes, to one or, interestingly, two alternating values (that were similar in magnitude, the average of which was calculated, yielding negligible error). The maximum number of emerging electrons permissible per pass is equal to the number of particles in the composite, since the QTC is initialised with one electron per particle. Thus, the normalised reciprocal of the mean number of electrons emerging per pass is a measure of the resistivity of the composite, where a ratio of unity corresponds with the resistivity of the filler. Decreasing the volume filler fraction below that shown in **Fig.6** would rapidly lead to an infinite resistivity (i.e. no electrons emerging), whereas in reality there would be convergence to the resistivity of the polymer. However, other than this, the data in **Fig.6** can be seen to be very realistic when comparison is made with data from real conventional composites, as depicted in **Fig.1**; a percolation threshold of approximately 40 vol. % is certainly possible for a real composite. The simulation would yield lower values for the percolation threshold if the spheres were not allowed to overlap during compression, so such a feature is planned to be incorporated at some point. These composites were all 0.1 mm in all 3 dimensions, with filler particles of diameter 3 microns; to elicit a conductive state, all were compressed to 80% in the z-direction, and quantum effects were ignored. All composites had no electrical history prior to this data acquisition.

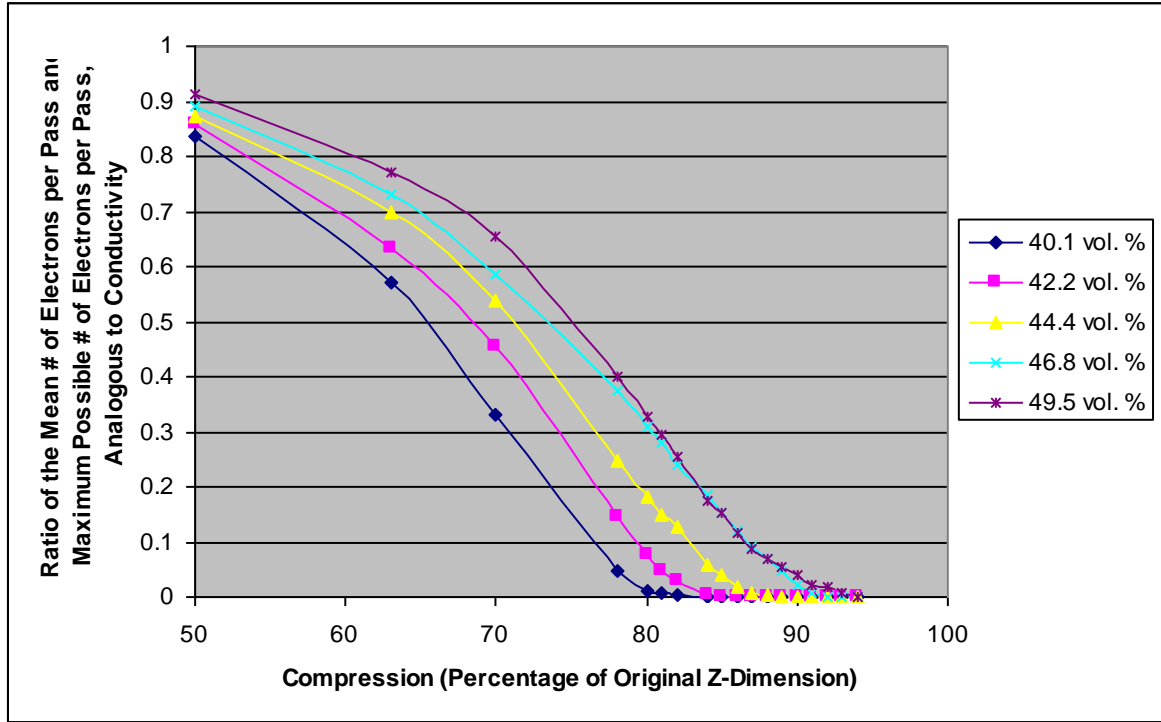


Fig.7: Computer simulation data showing how the number of electrons emerging from a QTC per pass increases under compression in the z-direction. As the volume filler fraction is increased, less compression is required to cause a conductive state, though minimal difference in sensitivity (the gradient of the line) can be observed between composites with different filler fractions. The quantity on the y-axis is analogous to conductivity, where a value of unity corresponds with the conductivity of the filler material. These composites were 0.1 mm in all 3 dimensions, with filler particles of diameter 3 microns, and quantum effects were ignored. All composites had no electrical history prior to this data acquisition

It can be seen in **Fig.7** how the number of electrons emerging from a QTC per pass increases under compression in the z-direction, showing how composites may be used as pressure sensors. As the volume filler fraction is increased, less compression is required to cause a conductive state, though minimal difference in sensitivity (the gradient of the line) can be observed between composites with different filler fractions. The quantity on the y-axis is analogous to conductivity, where a value of unity corresponds with the conductivity of the filler material. At 50% compression, all samples can be seen to be converging to the same conductivity, though this level of compression is not realistic, since the filler particles will have overlapped considerably by this stage. Hence, a larger filler fraction is associated with a bigger range of conductivities, which is realistic. If the particles were not allowed to overlap, the amount of compression possible would become constrained, and less compression would be required to elicit a conductive state. The volume was not assumed to be constant during compression, so that no change in dimension was created in the x- and y-directions; this will not be the case in reality, where some separation of particles will be occurring orthogonal to the direction of compression, inhibiting conduction. These composites were 0.1 mm in all 3 dimensions, with filler particles of diameter 3 microns, and quantum effects were ignored. Composites have been shown not to enter a conductive state under extension, even at high filler fractions, and even though a constant volume is assumed; this is observed in reality for composites below their percolation thresholds. All composites had no electrical history prior to this data acquisition.

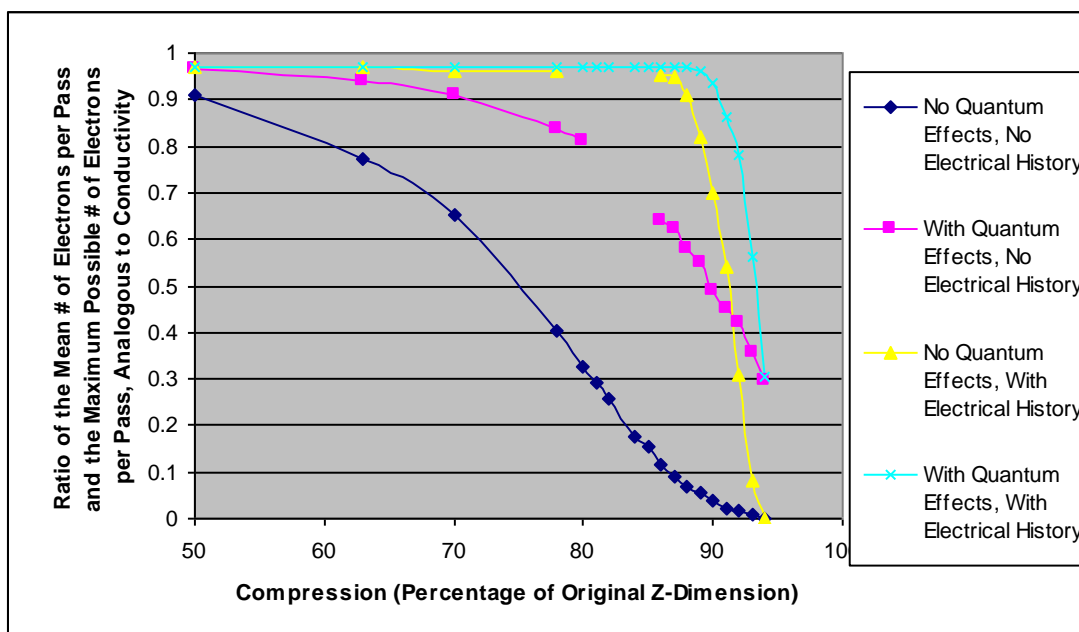


Fig.7: Computer simulation data showing how the number of electrons emerging from a QTC per pass is highly dependent upon electrical history, as well as quantum effects. By successively compressing a sample and applying a voltage, without allowing relaxation between measurements, a considerably more sensitive composite results than for the case where a fresh composite is used for each measurement, which is compressed directly to the stated value. These composites had a volume filler fraction of 49.5%, and were 0.1 mm in all 3 dimensions, with filler particles of diameter 3 microns. For these dimensions of sample, quantum effects only occur when a voltage of the order of 1,000,000 V is applied, and they can be seen not to increase the sensitivity of a composite, but allow a current to flow even in the absence of compression (albeit not shown on the graph). 100 passes were used per data point, yielding a negligibly small error on the mean

There is considerable evidence of an electrical history effect in **Fig.8**, where quantum effects have also been considered. By successively compressing and applying a voltage, without allowing relaxation between measurements, a strikingly more sensitive composite results, compared to the case where a fresh sample is used for each measurement, so that it is compressed immediately to the stated value before a voltage is applied, so there is no electrical history, as has been the case for all previous data. The justification for this surprising effect is obscure – it may be a defect of the program (though this is highly improbable), or it might be that conduction to dead-end pathways is less likely if new pathways are introduced in small stages, rather than abruptly. Quantum effects only occur when a voltage of the order of 1,000,000 V is applied (a million volts used here), for these dimensions of sample, and they can be seen not to increase the sensitivity of a composite, but allow a current to flow even in the absence of compression (though this is not shown on the graph). The field generated between the particles by the polarised spheres is of the order of the applied field, unless the particles are in very close proximity to each other. This gives credence to the idea that tunnelling effects are negligible in conventional composites, although the use of the electric field half way across the polymer layer, in the probability equation, is somewhat of a simplification. These composites had a volume filler fraction of 49.5 %, and were 0.1 mm in all 3 dimensions, with filler particles of diameter 3 microns. Many suggestions for improvements to the simulation are discussed in §3.

2.2 Vapour-sensing properties of QTC

2.2.1 The multi-sensor array experimental set-up

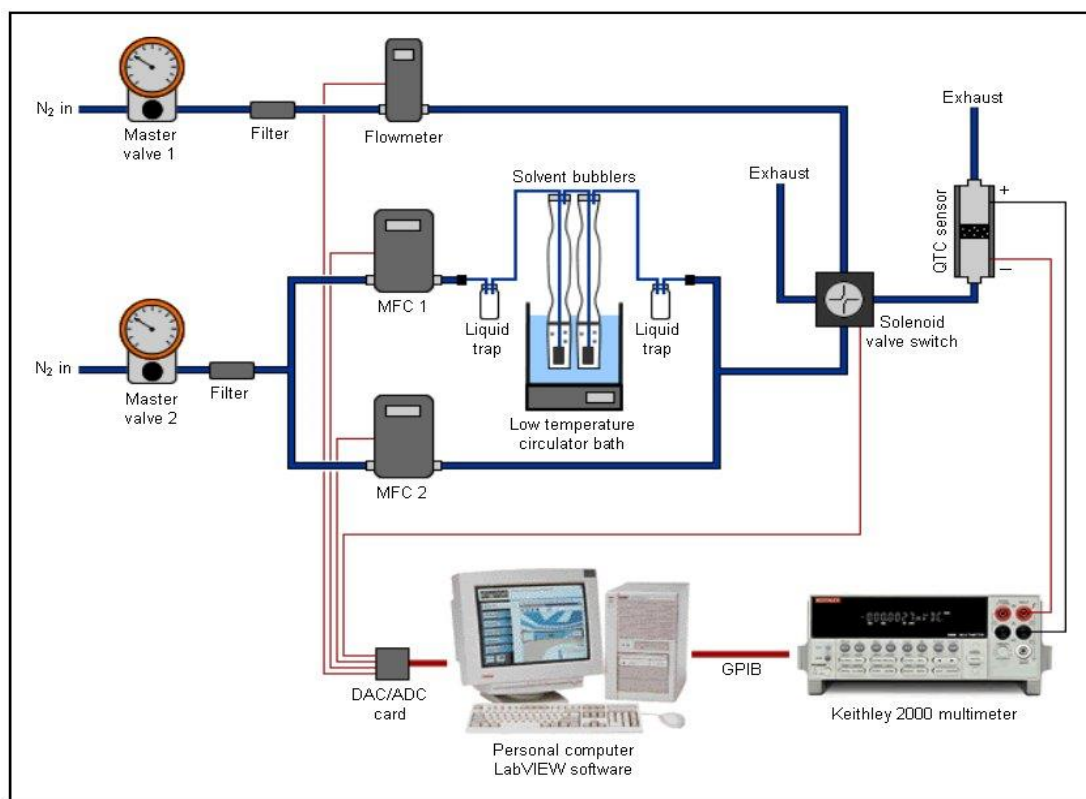
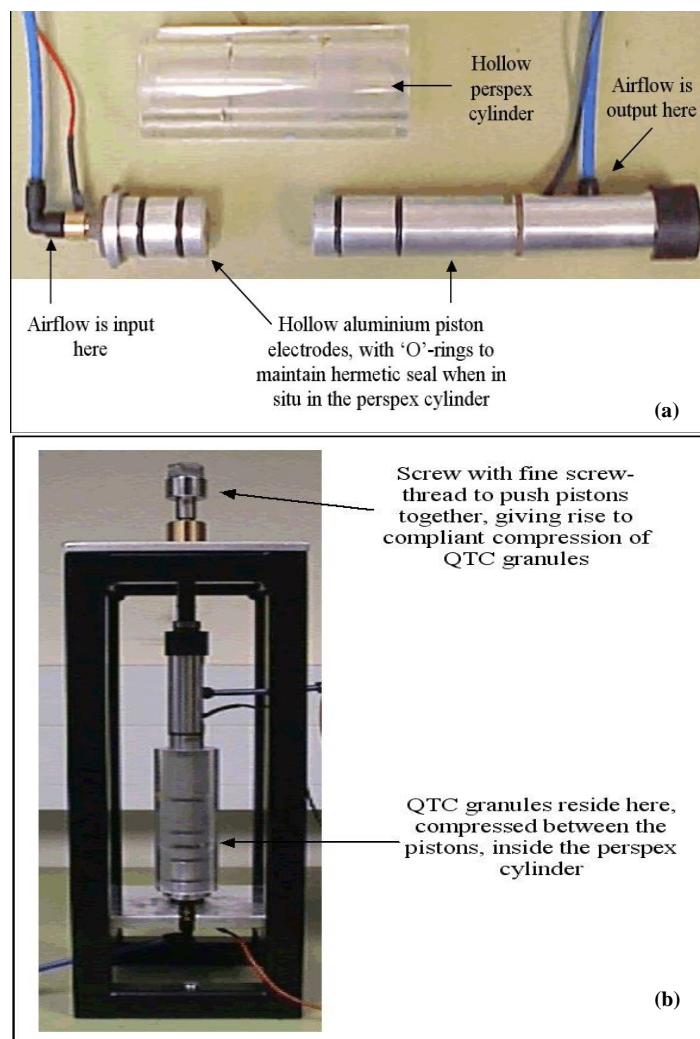


Fig.9: Scheme of the original vapour-sensing experimental set-up, for a single sensor. The system is fully automated, where a PC running a LabVIEW program controls a solenoid valve that allows the airflow to the sensor to be switched from purging with nitrogen, to exposing with solvent-saturated nitrogen flowing from the bubblers, which are at a temperature controlled by a circulator bath. Two mass flow controllers, MFC1 and MFC2, respectively control the volume flow rates of nitrogen through the bubblers and through a dilutant line, and a flowmeter is used to gauge the volume flow rate in the purge line. A Keithley 2000 multimeter is used to measure electrical resistance of the sensor, and these readings are sent to be stored on the PC at a set rate. This figure is reproduced by kind permission of Phil Hands

A scheme of the original vapour-sensing experimental set-up, for a single sensor, is depicted in **Fig.9**; this was inherited from a previous Ph.D. student.¹² The system is fully automated, where a PC running a LabVIEW program controls a solenoid valve that allows the airflow to the sensor to be switched from purging with nitrogen, to exposing with solvent-saturated nitrogen flowing from the bubblers, which are at a temperature controlled by the circulator bath (or “fridge”); when air is not flowing through the sensor, it is passed through the solenoid exhaust line, out of the laboratory’s window. Nitrogen is flowed through two solvent-containing bubblers, connected in series, in order to ensure complete saturation of the carrier gas with solvent at the set temperature; porous metal frits, at the end of the tubing submerged in the liquefied solvent, disperse the nitrogen flow into bubbles of diameter of less than 0.1 mm. Two mass flow controllers, MFC1 and MFC2, respectively control the volume flow rates of nitrogen through the bubblers (solvent line) and through a dilutant line, and a flowmeter is used to gauge the volume flow rate in the purge line; these have a range of up to 50 ml/min (with a $\pm 1.5\%$ error across the range, corresponding with a ± 0.75 ml/min error on any reading), and are protected by 10 μm filters. Hence, solvent concentration can be controlled by the fridge temperature, in addition to the ratio of flow rates between the solvent and dilutant lines; these rates are set and monitored by the PC, via a DAC/ADC card. A Keithley 2000 multimeter

is used to measure electrical resistance of the sensor, and these readings are sent to be stored on the PC at a set rate, by virtue of a GPIB connection.

Fig.10: (a) Photo of the original sensor assembly, showing the aluminium piston electrodes with a pair of 'O'-rings each, to enable a gas-tight seal once the pistons are placed in the cylinder, and (b) is a photo of the compression rig, used to apply compliant compression to QTC granules between the pistons. These photos are reproduced by kind permission of Phil Hands



The original vapour sensor structure is illustrated in **Fig.10(a)**, showing the aluminium piston electrodes with a pair of 'O'-rings each, enabling a gas-tight seal once the pistons are placed in the cylinder. A thin sheet of nickel gauze secured at the end of each piston, under which there is a coarse wire "sieve" mesh, to provide greater rigidity. The pistons are 24 mm in diameter, which means that a 3 g sample of granules has a thickness of 2 or 3 mm between the pistons - this is necessary to adequately separate the electrodes, preventing a short circuit. **Fig.10(b)** depicts the rig used to apply compliant compression to the QTC granules residing between the pistons. Using this equipment, a variety of QTC granules (with polymers silicone rubber, polyurethane and PVA) have been exposed to a range of organic solvent vapours (THF, hexane, ethanol, methanol, acetone, toluene, chloroform, ethyl-acetate, nitromethane and - to test the effects of humidity – water),^{12,28} and fractional changes in resistance of more than 7 orders of magnitude (beyond the range of measurement of the Keithley) are commonplace when samples are exposed to vapours from solvents at room temperatures; conventional composites only appear capable of producing a fractional change in resistance of the order of 10^5 for similar concentrations of vapours.⁴⁰ Also, a certain shape and size of response can often be attributed to a

certain polymer-solvent combination, boding well for the qualitative and quantitative discrimination abilities of a possible sensor array. However, for such an array to be incorporated into a handheld device, considerable miniaturisation of the sensors is a prerequisite. At the request of Peratech, electrode assemblies that allowed samples of 3 mm diameter to be compressed were designed and fabricated; ten sensors were deemed sufficient as a starting point for the multi-sensor array.

Fig.11: (a) Photo of the new, miniaturised sensor assembly, showing the brass piston electrodes with a pair of nitrile 'O'-rings each, again enabling a gas-tight seal when placed in the perspex cylinder. The QTC granules reside in the chamber between the electrodes. (b) is a photo of the new compression rig, accommodating ten sensors. The cylinders here are made from PEEK, since perspex was shown to be prone to cracking after repeated exposure to solvent vapours

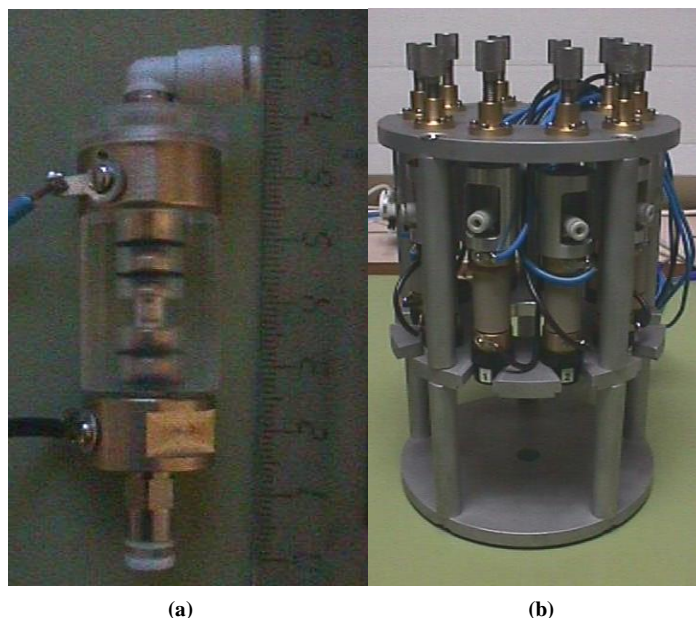
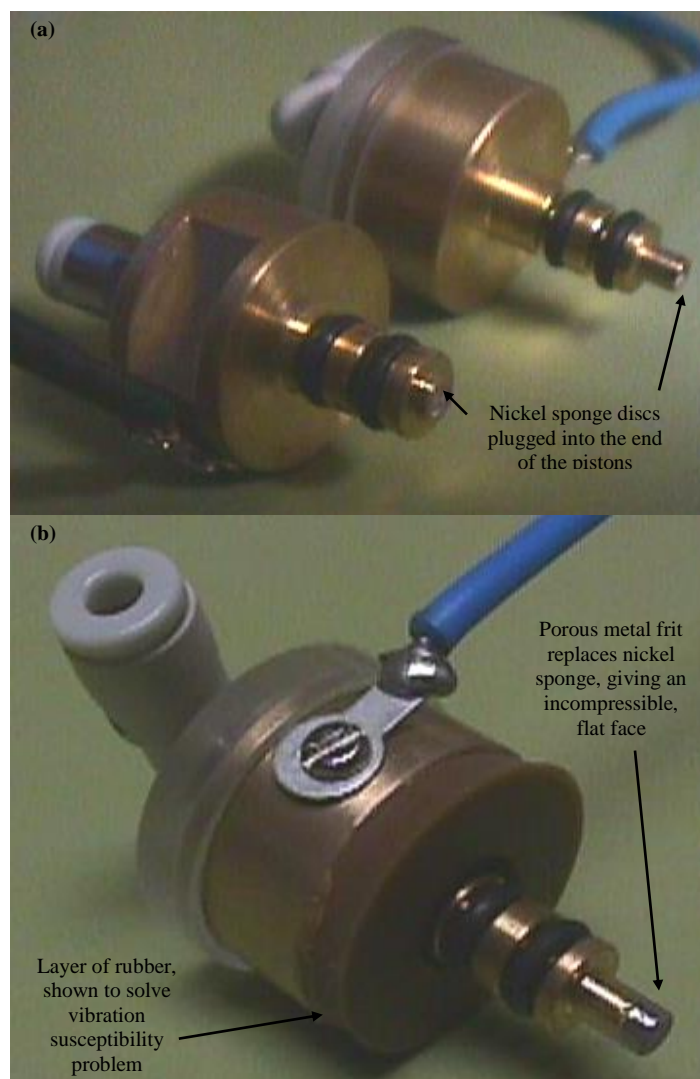


Fig.11(a) shows the new, miniaturised sensor assembly design, with brass piston electrodes fitted with a pair of nitrile (chosen because of its relatively good solvent resistance) 'O'-rings each, again enabling a gas-tight seal when placed in the perspex cylinder. After repeated exposure to solvent vapours, hairline fractures were beginning to appear in the perspex, at the point between the pistons; eventually, these would deepen into appreciable cracks, allowing vapour to bypass the granules altogether; thus, it was deemed necessary to remake the cylinders out of PEEK (poly ether ether ketone), which is second only to PTFE (polytetrafluoroethylene) in terms of chemical resistance, but is far less susceptible to mechanical wear. These are shown in **Fig.11(b)**, which displays the new compression rig, offering compliant compression to ten sensors simultaneously.

Fig.12: (a) A 2 mm deep, 2 mm diameter mouth was made in the end of each piston. Initially, this hole was plugged with 2 mm diameter discs of nickel sponge, followed finally by a 2 mm diameter piece of fine nickel gauze, in an attempt to prevent granules escaping from the sensor. The nickel sponge was compressible, and did not allow for a flat face at the end of the piston – not ideal for compressing granules with. (b) shows a solution to this problem, by instead plugging the hole with a porous metal frit, which is incompressible and provides a flat face with which to compress granules, as well as fulfilling the necessary criteria of being conductive and allowing gas to pass through. A layer of rubber, sandwiched between the underside of the top piston and the top of the PEEK cylinder, was found to completely remedy a previously huge problem with vibration susceptibility



The fundamental problem associated with shrinkage of the sensors to such small dimensions was that of compressing the granules with something that was electrically conductive and incompressible, yet still allowed gas to pass through; it was entirely impractical to port over from the original, big sensor the technique of using coarse gauze covered with a layer of thin nickel gauze. **Fig.12(a)** shows how the quandary was initially solved by plugging the 2 mm deep, 2 mm diameter mouth, that existed in the end of each piston, with several 2 mm diameter discs of nickel sponge, followed finally by a 2 mm diameter piece of fine nickel gauze, in an attempt to prevent granules escaping from the sensor. However, there were several major faults associated with this method, namely that the nickel sponge was compressible (likely to cause repeatability problems), and it did not allow for flat, parallel faces with which to compress granules (meaning that all sensors would compress the QTC differently, yielding detrimental consequences to the major issue of reproducibility). Also, the non-uniformity of the faces allows for the possibility of granules at the periphery of the electrodes being compressed by the brass pistons into a conductive state, whilst leaving those in contact with the nickel sponge in an insulating state; granules in contact with the brass portions of the electrodes will not be fully exposed to the vapour passing through the sensor, hence the response to solvent exposure may be significantly impaired. A problem also exists with the thin nickel gauze, in that the hole size was found to be 50 μm – testing of granules of less than 45 μm was desired.

A solution presented itself in the form of a sintered stainless steel, porous metal frit, which could be plugged securely into the hole at the end of the piston (with the aid of PTFE tape), so that granules could be compressed with flat, parallel, incompressible electrodes that allow all granules in the sensor to be exposed to vapour, since now the whole of the face is able to pass gas. Mottcorp, of America, displayed astonishing generosity by supplying 55 frits free of charge; these came in the form of cylinders that were 1/8" (3.17 mm) in diameter, 1/8" in length, and were machined down to 3 mm diameter for half their length, and 2 mm diameter for the remainder – the process of machining rendered the outside surface of the frit non-porous, though this was fortuitous from the perspective of forcing gas through the frit, rather than allowing it to flow around the outside, where it could perhaps bypass the majority of granules. A frit is shown, in situ, in **Fig.12(b)**. Other than the difficulty with machining such a small object, the main problem posed by the introduction of frits has been the restriction to gas flow that they present. To pass 50 ml/min of nitrogen through a sensor complete with nickel sponge, a negligible pressure gradient was required across the assembly (i.e. less than 0.01 bar) – the average sensor complete with frits requires about 0.3 bar of pressure difference to pass the same flow rate. The first problem is in matching this resistance to vapour flow between all the sensors, since mass flow rate will split up unevenly, analogous to electrical current through non-equal resistors in parallel, if they each present a different degree of flow restriction, tending to take the path of least resistance; the mismatch of the corresponding volume flow rates will affect the speed of response of all the sensors. The higher pressure in the bubblers may also affect the ppm of solvent flowing to the samples. The resistance to gas flow of a frit would be expected to increase with decreasing pore size, so a larger pore size may be one way of lowering the flow restriction; however, it is inevitable that granules of all sizes will contain some bare nickel particles, and almost invariably these will be nickel 123, which has particles as small as 3 μm – hence, the current pore size of 2 μm in the frits is as large as can be used, without allowing the possibility of the pores becoming blocked with nickel. There is already a question mark over the longevity of the frits, since the porous face may become worn over time, leading to an increase in flow restriction. When sensors with frits are incorporated into the experimental set-up as depicted in **Fig.9**, there is a very long time delay between exposing a sensor to vapour from the bubblers, and achieving the stated flow rate through the sensor, since the required air pressure must first build up in the first liquid trap, then the two bubblers, then the second liquid trap, before finally the pressure before the sensor is such that the pressure gradient across it is sufficient to flow gas through to the stated flow rate; placement of a “solvent-resistant” pressure sensor in the line, between the solenoid valve switch and the sensor, reveals that for larger flow rates (e.g. 50 ml/min), the air pressure never reaches its required value. For some time, it was assumed that this must be due to the pressure sensor being, in fact, not solvent-resistant; however, a very recent discovery indicates that the higher pressure in the first liquid trap is exposing a weakness in it, allowing nitrogen to escape from the system. Since the tubing to the trap is always ensured to be very tight, this problem might only be solved by the acquisition of new tubing connectors for the trap. Even once solved, there will still be a long time delay between the start of an exposure and achieving the necessary pressure to produce the required flow rate, and as soon as the solenoid valve switches to purge the sample, this built-up pressure goes straight to atmospheric, since the solenoid exhaust line flows out of the window. Hence, it has been deemed necessary to place an adjustable

flow restrictor in this exhaust line, with another solvent-resistant pressure sensor in the line before it; in conjunction with a pressure sensor between the solenoid valve and the sensor(s), by setting the volume flow rates in the purge line (i.e. the line stemming from “Master valve 1” in **Fig.9**) and the solvent bubbler line as being equal, the flow restrictor can then be set to restrict the flow to the same extent as the vapour sensor(s) by matching the readings on the pressure sensors. Hence, there will be no changes in air pressure between purge and expose, so that the desired flow rate of solvent vapour through the sensor(s) will be achieved immediately. Also, abrupt changes in air pressure between purge and expose result in sudden surges in airflow, shown to cause momentary leaps in the electrical resistance of a sensor, thought to be due to air rushing around granules so vigorously that electrical contact is momentarily broken between them. Since it is clearly of great importance to match the air pressure between purge and expose, the two pressure sensors have been attached to the PC, via the ADC card, so that their readings can be continuously recorded. Also, the use of a mass flow meter in the purge line, as opposed to a mass flow controller, leads to a situation where the air pressure as set by “Master valve 1” is the only way of controlling the volume flow rate, and this air pressure is subject to fluctuations over time, which can again give rise to a mismatched air pressure between purge and expose. To avoid this, the meter was replaced with a mass flow controller; given that the existing flow controllers could only measure up to 50 ml/min, it was deemed appropriate to purchase a controller that could measure up to 100 ml/min, even though this would only be half as accurate as a 50 ml/min version. This was with a view to combining the flow from the solvent and dilutant flow controllers to give a flow rate of 100 ml/min through the bubblers, and matching this with 100 ml/min in the purge line; if the resistance to airflow could be matched between the ten sensors, this would split up into 10 ml/min per sensor, which has been shown to yield just as large a response in sensors as 50 ml/min, just slightly slower. The mass flow meter freed up in the process of incorporating the new mass flow controller has been placed in series with the solvent bubbler mass flow controller, as a check on its accuracy.

In order to monitor the electrical response of the ten sensors “simultaneously”, it has been necessary to attach a scan card to the multimeter (Keithley 2000 SCAN). With the multimeter set to autorange in resistance-measuring mode, it has been found that the time delay between reading each of the ten channels on the scan card depends upon the resistance-mismatch between channels – it is essential to have a constant time delay between channels, and also one that is as small as possible, so the move away from autoranging to manual ranging is mandatory. Further justification stems from the fact that the sudden changes in applied current that occur during autoranging give rise to abrupt changes in resistance, as a result of the non-Ohmic nature of QTC, hence the shape of the resistance profile as a function of time can be very much affected; much worse, the maximum resistance reached can often become limited by such a switch in current, invalidating the very quantity that is trying to be measured. Using manual ranging, the ability to measure up to 100 M Ω means that resistance can only be measured to the nearest 100 Ω ; this is not acceptable if accurate values of fractional change in resistance are to be acquired, especially as 100 Ω or lower is the desired starting resistance; set to measure up to 10 M Ω allows resistance to be measured to the nearest 10 Ω , but this is still not adequate. Hence, it has been decided to use manual ranging to measure up to 1 M Ω (which is unfortunate if the resistance may be increasing up to 10¹² Ω), permitting resistance to be measured to the nearest Ohm; with this setting, it is found that the time delay between channels on the scan

card is 55 ms, hence it will take 0.55 s to read all 10 channels. It is desirable to take one reading of resistance per channel every second, hence this rate of scanning is deemed to be acceptable. When manual ranging is used to measure up to 1 M Ω , a constant current of only 10 μ A is applied - such a low currents will prevent any PTCR effects taking place due to Joule heating of polymer, which can only be described as fortuitous. A modified version of the existing vapour-sensing VI has been written in LabVIEW, to control the running of the scan card, and also to allow real-time plotting of the resistance measurements on ten graphs, so that the response of a particular sensor can be monitored.

Up until a very recent discovery, the sensors suffered from an extreme sensitivity to vibration – this would render any handheld device unusable. Fortunately, the problem has seen a very simple solution in the form of a layer of rubber being sandwiched between the underside of the top piston and the top of the PEEK cylinder; this makes the sensor an extremely rigid structure when under compression in the rig, so that even vigorous shaking of the rig and gas tubing gives rise to a negligible change in signal. Another significant benefit stems from the fact that this inclusion of rubber considerably facilitates setting the starting resistance, since the extra rigidity gives much finer control over the thumbscrews used to compress the sensor.

2.2.2 Results and discussion

Before the acquisition of frits, extensive vapour-sensing data was achieved with the sensors fitted with nickel sponge. It was immediately noticeable with the smaller sensors that the response time had improved over data achieved with the original, big sensor, with the same flow rate – this can be understood by considering that volume flow rate is equal to the product of the speed of the airflow and the cross-sectional area of the tubing through which it is passing; the large sensor has a cross-sectional area that is a factor of 64 larger than that of one of the new sensors, thus the speed of air through the one of the new sensors will be 64 times quicker, for the same volume flow rate. Even with ten sensors used simultaneously, if 100 ml/min is split up equally between them, the speed of the flow will still be nearly 13 times that which was being flowed through the old sensor with 50 ml/min. Hence, miniaturisation of the sensors has given rise to the benefit of a faster response time without having to purchase a whole new set of higher capacity mass flow controllers – a costly proposition. The addition of frits, with the higher air pressure difference required to generate the same mass flow rate, will give rise to lower volume flow rates through the granules, since the air will be more dense, hence a slower response to exposure to solvent vapour may be anticipated than for the small sensors with nickel sponge; however, the increased air pressure may produce a larger degree of polymer swelling – this is still a moot point.

It is instructive to observe the data given in **Table 1**, where it can be seen that the density of granules, in an uncompressed state, increases as the granule size increases, implying that there is much more volume taken up by air with the smaller granules. We are relying on the availability of air between granules to allow them to swell, so it may be expected that smaller granules will yield the largest responses. However, this is the exact opposite of the truth, with smaller granules (i.e. less than 300 μ m) giving rise to comparatively small responses hampered by noise; this may be explained by

considering that smaller granules seem to require a greater degree of compression in order to reduce their resistance to a specified value, hence these pockets of air are squeezed out, leading to significantly constrained polymer swelling. Also, the noisy signal can be attributed to electrical contact between adjacent granules being periodically ostracised by the airflow; lower flow rates appear to improve the performance of smaller granules, which may explain why the use of 152-300 μm granules in the old vapour sensor were successful. However, there is evidence that granules of size in the range of 300-1180 μm produce the best results, even in the old vapour sensor.²⁸ Another severe problem with smaller granules is that they tend to “cake” together, causing a dramatic increase in the resistance to vapour flow upon polymer swelling; this renders them practically useless in a multi-sensor array, since then the flow rates through all the other sensors will be affected. The data in **Table 1** was achieved with “low modulus silicone granules” (which have recently transpired to be “alpha 153” granules) with a likely loading ratio of 90 w/w %. The densities of bulk samples given in the table are theoretically determined values, making use of the equation in **Appendix D**, hence they will not contain any air bubbles. It can therefore be seen that about half (or more) of the volume occupied by uncompressed granules is air. The ideal scenario is that as much of this air is retained during compression to a specified resistance, and this seems to favour the larger granules. Large hollow granules would perhaps be the optimum form for vapour sensing.

Granule Size [microns]	Density of Uncompressed Granules [g/cm ³]
<75	1.6 \pm 1
75-152	2.2 \pm 1
152-300	2.6 \pm 1
300-500	2.8 \pm 1
500-1180	2.7 \pm 1
Bulk sample with 83 w/w % loading	3.1 \pm 1
Bulk sample with 90 w/w % loading	4.9 \pm 1

Table 1: Data showing how the density of granules in an uncompressed state increases with granule size, for alpha 153 granules with a likely loading ratio of 90 w/w %. Data given for bulk samples are theoretically determined values, thus do not incorporate any air bubbles

To confirm the validity of (23), (24) and (25), bubbler mass loss experiments were performed with acetone at various temperatures. 50 ml/min was set to flow through the bubblers for at least 15 hours, for each experiment, and the resulting mass loss in the two bubblers was measured; hence, there was a known quantity of solvent for a known volume of carrier gas, so with an appropriate conversion of units (i.e. mg/l), this can yield the solvent concentration in ppm. Substitution of the solvent temperature into (23), (24) and (25) (using atmospheric pressure in the bubblers) can also be used to find a value for ppm. The results are detailed in **Table 2**.

Solvent Temperature [degC]	Clausius-Clapeyron ppm			Actual ppm		
	Likeliest	Maximum	Minimum	Likeliest	Maximum	Minimum
-20±1	91	96	86	105	108	102
-10±1	153	161	145	147	151	144
0±1	248	260	237	288	299	279
10±1	388	405	371	436	452	424
15±1	479	499	459	597	633	572
20±1	587	611	564	742	796	710

Table 2: Data from bubbler mass loss experiments, showing how the predicted ppm from the Clausius-Clapeyron equation agrees quite well with values of actual ppm for temperatures up to 10 degC, although the values only agree to within error at –10 degC. The much higher actual ppm at temperatures above 10 degC than that predicted may be as a result of a breakdown of the ideal gas equation at the higher density of air associated with the higher solvent concentration

The table shows how predicted ppm from the Clausius-Clapeyron equation agrees quite well with values of actual ppm for temperatures up to 10 degC, although the values only agree to within error at –10 degC. The much higher actual ppm at temperatures above 10 degC than that predicted by the C-C equation may be as a result of a breakdown of the ideal gas equation at the higher density of air associated with the higher solvent concentration; if the van der Waals equation could be used, higher predicted values of ppm would be expected. Errors in the actual ppm were calculated by observation of the minimum and maximum values of volume flow rate on the mass flow controller and the mass flow meter throughout the course of the experiment. The effect of (24) is simply to add 1 ppm to the predicted concentration values above 1 degC, hence the air pressure in the bubbler can be deemed to have a negligible effect, except at extremely high pressures. However, the same experiments were repeated with acetone at 20 degC, but with a flow restriction placed after the bubblers, so that a pressure higher than atmospheric existed in the bubblers. At a pressure of 0.28 bar, the actual ppm was found to drop to 545 ppm, and at 0.33 bar, it dropped even further to 448 ppm. This gives credence to the idea that higher pressures in the liquid trap are exposing a weakness in it, allowing nitrogen to escape. Experiment confirms that the vast majority of mass loss occurs in the first bubbler, confirming almost-complete saturation; however, the precautionary measure of the second bubbler is justified by some mass loss.

Before the acquisition of frits, extensive work was done with sensors incorporating the nickel sponge. Some impressive, though understandably irreproducible, data has been collected. The granules were alpha 153 silicone rubber, low modulus silicone rubber (since been found to be alpha 153, though they appear to have been manufactured with a lower filler fraction than the named alpha 153 granules, since their responses were often noticeably different), Techsil polyurethane, Ucecoat DW5661 (an acrylic polyurethane hybrid), Ucecoat 018.B (an aqueous dispersion of polyurethane), and Krasol polybutadiene; all contained nickel 123 filler particles. All were available in a range of granule sizes, usually <75 µm, 75-152 µm, 152-300 µm and >300 µm, though it quickly became apparent that all granules below 300 µm performed poorly, hence most work was done on the granules above 300 µm. All these granules were exposed to a range of solvents, namely THF, hexane, ethanol, acetone and water, at a range of different ppm values calculated using the Clausius-

Clapeyron equation. The response to methane gas was also measured, though sadly it was found to be undetectable. The effect of different quantities of granules was examined by using masses of samples ranging from 10 to 40 mg (in contrast to the quantity of 3 g that was always used in the big vapour sensor), though initially there was a large electrostatic problem caused by the plastic pipette spout used to place the granules in the perspex cylinder, causing a generally unknown quantity to enter – this problem has since been solved by the use of a brass funnel that has been designed to place granules into the cylinder, where the use of PEEK has also improved the situation.

The solubility parameter of silicone rubber⁸ is from 14.9 to 15.59 (MPa)^{1/2}, and for polyurethane^{41,42} it is found to vary from 21 to 27 (MPa)^{1/2}. For acetone it is 20.25 (MPa)^{1/2}, ethanol it is 24.75 (MPa)^{1/2}, hexane it is 14.93 (MPa)^{1/2}, THF it is 18.61 (MPa)^{1/2}, and water it is 47.86 (MPa)^{1/2}.⁴³ The matching of the solubility parameters between solvent and polymer has been shown to have a considerable effect on the size of the response obtained. For instance, silicone rubber would be expected to respond especially well to hexane. **Fig.13** illustrates this eloquently with a fractional change in resistance of more than 7 orders of magnitude within one minute of exposure to hexane at 63% of SVP (saturated vapour pressure, at the standard temperature of 25 degC); such a response is unprecedented, and also shows impressive repeatability. There is, however, a problem with reproducibility, but this can only be expected with compression with nickel sponge.

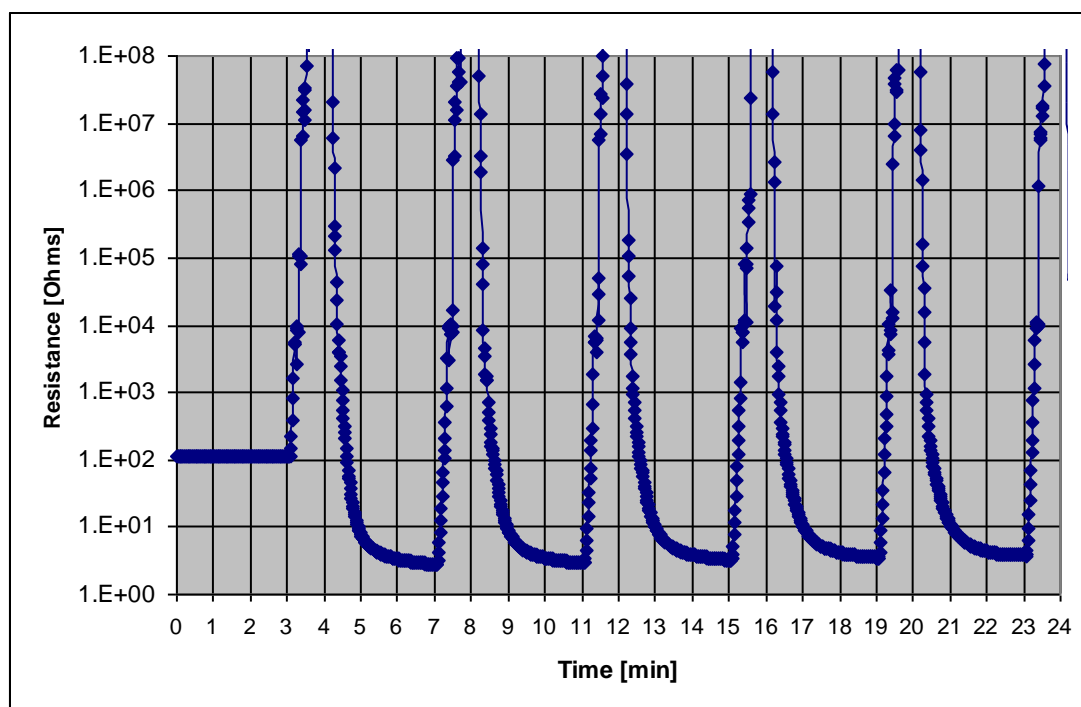


Fig.13: Response of approximately 20 mg of low modulus silicone rubber granules (> 300 microns) to 63% of SVP hexane flowed at 50 ml/min, in 1-minute exposures, and 50 ml/min nitrogen, in 3-minute purges, where there is always a purge at the beginning

There is also a problem with long-term repeatability that is not apparent in **Fig.13**, but is very obvious in **Fig.14**. This may be due to a chemical ageing effect such as chemisorption, or it may simply be that the nickel sponge is becoming increasingly compressed with each subsequent exposure, hence it compresses the granules to a

lesser extent each time. Comparison of experiments performed with and without frits gives some credence to this idea.

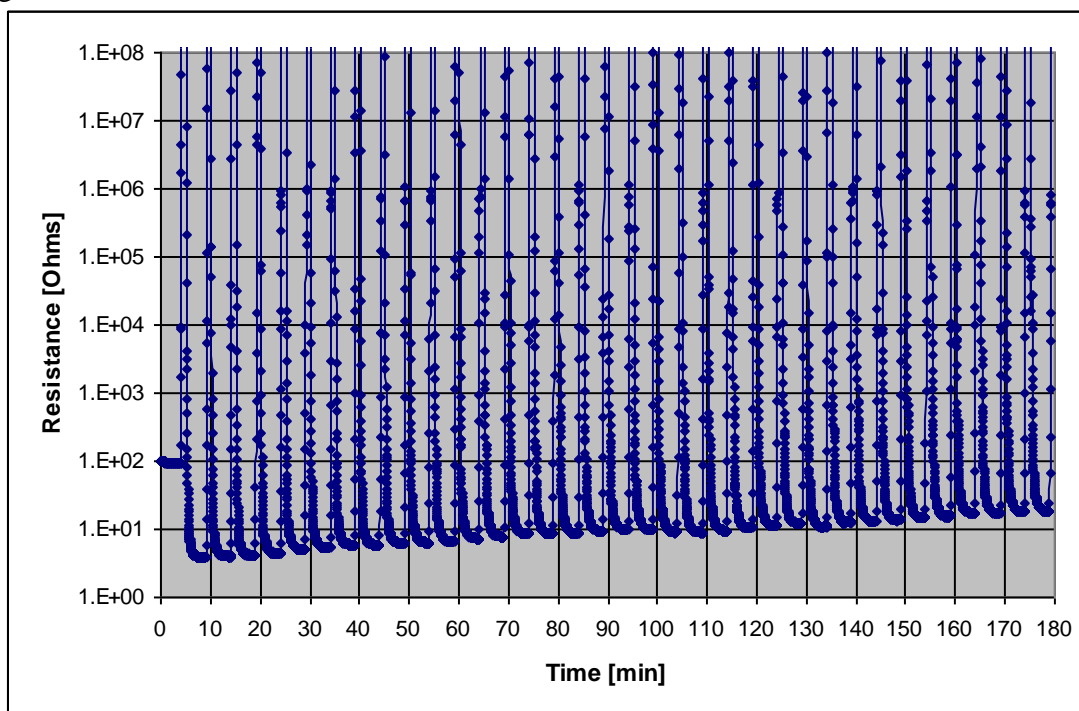


Fig.14: The experiment in Fig.13 was repeated, but this time for 3 hours, showing how the baseline resistance steadily rises upwards. This may be due to a chemical ageing effect such as chemisorption, or it may be that the nickel sponge is becoming increasingly compressed with each subsequent exposure, hence it compresses the granules to a lesser extent each time. Here, the purge has been extended to 4 minutes, to ensure that as much hexane as possible is flushed out

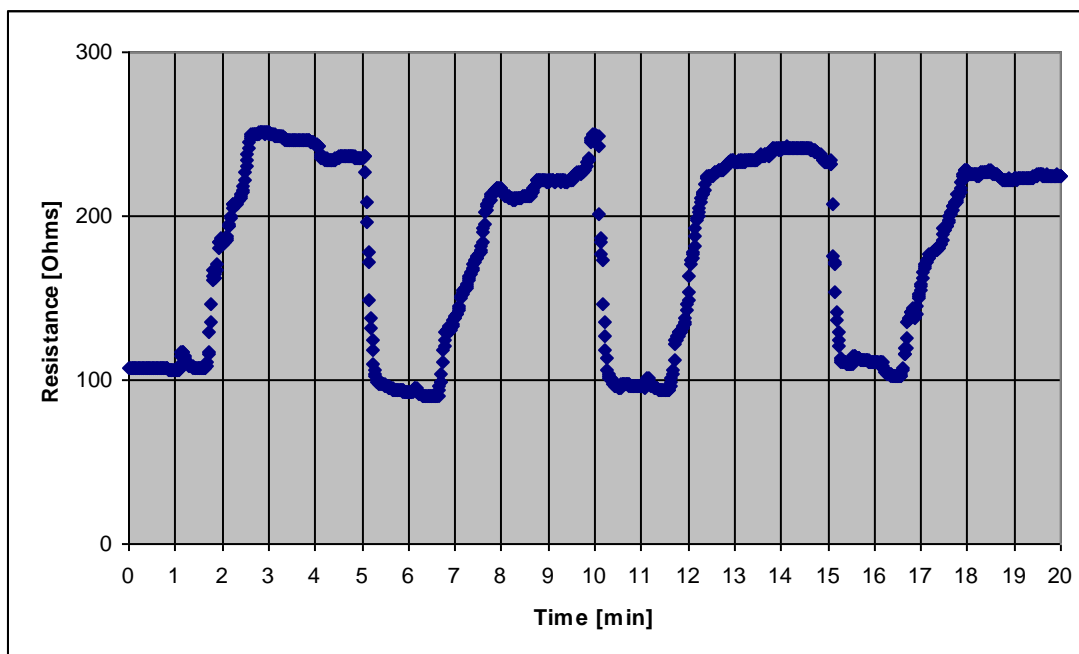


Fig.15: Response of approximately 20 mg of alpha 153 silicone rubber granules (> 300 microns) to hexane at -30 degC (5.5 % of SVP) at 2.8 ml/min, diluted with 47.2 ml/min nitrogen, to yield a concentration of 3 ppm. The purge is 1 minute long, and the exposure lasts 4 minutes. A fractional change in resistance of more than 2 can be seen, which is an excellent response for such a low concentration of solvent

It is ideal to be able to detect low concentrations, hence alpha 153 silicone rubber granules (>300 μm) were exposed to hexane at -30 degC (5.5 % of SVP) at 2.8

ml/min, diluted with 47.2 ml/min nitrogen, to yield a concentration of 3 ppm (error values are now meaningless, what with the finding that the Clausius-Clapeyron equation, in tandem with the ideal gas equation, does not predict accurate ppm values). This is shown in **Fig.15**, where a fractional change in resistance of more than 2 can be seen, which is an excellent response for such a low concentration of solvent.

Ethanol's solubility parameter can be seen to be very mismatched with silicone rubber's, but commensurate with polyurethane's, hence a small response to ethanol from silicone and a very large response from polyurethane may be expected; experiment confirms theory. None of the polymers respond well to water, but polyurethane (especially the aqueous dispersion) responds distinctly better than silicone, which would again be expected.

The porous metal frits allow for single granule experiments to be performed, but the results of a preliminary experiment indicate that a very small, unrepeatable response is attained. The effect of the quantity of granules used is still unclear; however, quantities below 10 mg (which would correspond with around a single layer of >300 μm granules) and above 40mg tend not to be very successful. However, more experiments are planned in this area.

The initial resistance of the granules has been shown to affect the maximum resistance reached quite considerably, though this will almost exclusively be due to the amount of compression the granules are under. The effects of chemical, mechanical and electrical history complicate the relationship between resistance of QTC and the amount of compression it is subjected to, hence simply by compressing the granules to the same starting resistance does not necessarily mean the same compression. This is the biggest obstacle to gaining reproducible data, hence much more work is planned on examining these effects in detail. It is anticipated that granules will have to be given some pre-exposure to a number of solvents, before completely repeatable data can be ascertained, in order to prevent effects such as chemisorption. However, experiments where granules were submerged in liquefied solvents for more than an hour show that irreparable degradation occurs, in that the sensitivity to solvent vapour is severely impaired. This casts some doubt over the workable lifetime of granules in the vapour-sensing application.

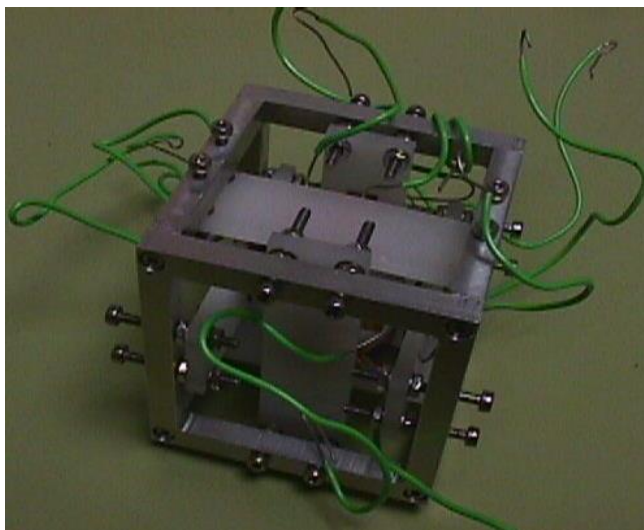
Some work has been done on stretched films in vapour sensing, though a slow and unrepeatable response was invariably obtained. It is still matter of debate as to whether stretching a QTC is superior to compression, when it comes to sensing vapours. The actual free volume may well remain constant in both compression and extension, but in compression, liberation of potential free volume might actually be facilitated, whereas it is likely to be marred under extension. There is a problem with cutting up films – any slight bur on the edge causes easy ripping of a sample under extension. The shiny finish of films, due to the fabrication process of rolling films between Teflon paper, is almost impermeable to solvents – removal with wire wool is therefore necessary, but this weakens a thin film, again giving rise to breakage under light extension. More work looking into ways of increasing the porosity of a film, to speed up saturation of a sample when exposed to vapour, should perhaps be carried out.

Mass uptake experiments, by measuring the change in mass of a sensor when exposed to a solvent vapour, have proven unsuccessful. It has been found to be almost impossible to weigh a sensor fitted with gas tubing without the measured mass being very sensitive to the orientation of the tubing. Hence, detecting a 20 to 30 mg change in mass is not feasible above a similar amount of noise. Thus, any future mass uptake experiments, to shed light on the diffusion kinetics occurring during polymer swelling, will have to be performed using the big sensor, where good results have already been obtained.

The advantages of QTC in vapour sensing are therefore obvious – an unprecedented size of response has been shown (which may allow detection of previously undetectable – with metal-polymer composites, at least - low concentrations of solvents), and a fast response is apparent. The main disadvantage is that only two polymers have hitherto been shown to wet the filler particles well, without breaking the spikes on the filler particles, and a wide variety of polymers is essential in creating a sensor array that can discriminate between a wide range of solvent vapours. However, this problem can be partially overcome by functionalising polydimethylsiloxane and polyurethane, so that the same backbone polymer can be made to have a substantially different solubility parameter. The requirement of some form of mechanical deformation in order to achieve a conductive state is not a problem in terms of restricting polymer expansion, since enormous responses have been demonstrated; the problem exists in the fact that extremely small changes in the initial deformation can give rise to a very large difference in the change in resistance upon exposure, so the response is a very sensitive function of the applied deformation, which is difficult to measure accurately – this is the main obstacle to reproducible results. Conventional composites require no mechanical deformation to create a conducting state, if they have been fabricated above the percolation threshold, so this issue does not complicate their response. In passing the solvent vapour *through* the samples, as opposed to *around*, as is the case in conventional metal-polymer composite vapour sensors, polymer swelling expansion may actually constrain the flow of vapour – this has been shown to occur for granules below 300 μm , but mercifully appears not to be a problem for the larger granules.

2.3 Orientation-measuring device utilising QTC

Fig.16: Prototype of an orientation-measuring device, where the cube has a length of 5 cm



The author has invented and designed a device using QTC that may be used to measure orientation, and a prototype has been fabricated; this is shown in **Fig.16**. The idea is to exploit QTC's sensitive pressure-sensing properties by essentially placing a QTC sample on the inside and centre of the 6 faces of a cube; placement of a sphere within this cube, such that the surface of the sphere is "just" in physical contact with the QTC samples (achieved in this prototype by means of adjustable non-conducting platforms) means that the sphere will exert a force on each sensor depending upon the structure's orientation with respect to the force of gravity. Each sample is self-adhered to a copper electrode on each of the platforms, and the other electrode is made from flexible and conductive "nickel paper", which is hinged to the platform so that it can rest over the QTC sample. At the point at which the sphere makes contact with this upper electrode, a PTFE disc (of diameter 2 mm and thickness 1mm) is glued to the nickel paper, in an effort to increase the pressure exerted on the QTC by the sphere.

Orientation-measuring devices form a critical part of aircraft – these sophisticated gadgets measure subtle changes in the motion of a gyroscope to enable the orientation of the craft to be measured to a fraction of a degree; such technology comes at a very high price. The remarkable inexpensiveness of QTC renders this new device idea a much cheaper alternative, with the requirement that the walls of the structure confine the sphere to such a precise dimension being the main obstacle and costliest element of fabrication. Another possible application of an orientation-measuring device would be in the entertainment industry – in the form of a virtual reality glove, for instance. Such a device would ideally be able to measure orientation to the nearest degree. The force exerted on the PTFE disc on the bottom platform in this invention will be equal to $mg \cos \theta$, where m is the mass of the sphere, g is the acceleration due to gravity, and θ is the angle between the platform and the horizontal, if the structure is rotated about a horizontal axis. Hence, to be able to measure to the nearest degree for all orientations, a force of $mg \cos 89^\circ$ must be sufficient to generate a large enough pressure to compress the QTC to a measurable resistance. Only compressing the sample to a resistance of the order of 10 to 100 M Ω would mean that the resistance of the QTC will be extremely sensitive to the exact size and shape of the PTFE disc, hence this "measurable" resistance must be defined as being at most 1 M Ω . Compression experiments on different thicknesses of sensitive QTC films then reveal that the mass of the sphere must be at least 3 kg, so that even with a material as dense as copper, a sphere of diameter of nearly 9 cm would be required – to make a compact device, a diameter of less than 1cm would be ideal. Hence, a means of increasing the pressure applied to the QTC is required – the requirement that the sphere is able to roll over the sensors prevents the use of a spiky sphere, and it would be impractical to reduce the diameter of the PTFE disc to much beyond 2 mm. What is desired is a QTC that is at least ten times as sensitive as current samples; even if this can be achieved, perhaps by the use of polymer with an extremely low bulk modulus, there are still the electrical history problems of particle charging and trap filling, and severe vibration susceptibility. To minimise the effects of polymer creep due to the viscoelastic nature of rubber, very thin samples may be used, though this may present problems regarding macroscopic homogeneity. If the structure is also subjected to translational motion, it may also function as an accelerometer, though this will also be prone to the same problems.

3. FUTURE WORK PLANNED

The failure of the Clausius-Clapeyron and ideal gas equations to accurately predict solvent ppm means that bubbler mass loss experiments will need to be performed for every solvent at different temperatures. It will be of use to prove the validity of (24) in our system by investigating whether bubbler air pressure affects ppm – if so, bubbler mass loss experiments may need to be performed at different temperatures and pressures for every solvent. It has been shown in our system that the ppm value for a solvent at a certain temperature is independent of volume flow rate of carrier gas through the bubblers,¹² with flow rates up to 50 ml/min – proof is required that this condition is maintained up to 100 ml/min, whilst keeping the air pressure in the bubblers constant by varying the flow restriction after.

Chemical history effects must be explored in more depth by sequentially exposing granules to a wide range of vapours, then testing reproducibility by re-exposing to the same vapours, so that a comparison of response between small and large chemical history can be made. The continuous expansion and relaxation of the granules during this process will also give rise to mechanical ageing. In an attempt to deconvolve the two effects, supplementary work on the effects of mechanical history should be carried out – this will be best performed at Peratech's HQ in Darlington, where there is a Lloyd testing machine specifically made for this task; reversible modification to this machine may need to be made in order to examine samples of small quantities, analogous to those that are used in the current vapour sensors (i.e. up to 30 mg). Chemical history effects may also be probed in tandem by subjecting granules that have varying degrees of chemical history to many compression/relaxation cycles. Electrical history effects are also a cause for concern, with a fresh, compliantly compressed sample giving rise to a continuously falling resistance value for several minutes; electrical inactivity of a sample for several hours leads to the same phenomenon being observed when measurements of resistance are resumed. If particle-charging effects are responsible for this phenomenon, a remedy may be found by the use of AC measurements; preliminary experiments indicate that this is not the case, but a thorough examination at low currents and a wide range of voltage frequency has yet to be carried out. It has been shown⁴⁴ that heat-treating a composite to temperatures of around 150 degC, prior to exposure to a solvent, can result in a substantial increase in maximum signal reached (albeit at the expense of a significantly larger baseline signal), for certain polymers; similarly, exposure to gamma radiation has been shown to strikingly improve reproducibility and stability. It may be of interest to attempt similar experiments with QTC granules.

Granule size has been shown to drastically affect measured responses to a solvent; the effect appears to be predominantly related to the degree of compression required to reduce a sample to a specified starting resistance. With regard to accelerating a sample's response to the presence of a solvent vapour, the use of small granules is desired; however, it has been shown that granules below a size of 300 microns are prone to producing a noisy signal, thought to be due to the flow of gas randomly ostracising electrical contact between particles. Currently, granules are only available in batches of very large granule size distribution (e.g. 300-500 and 500-1180 microns), due to the unavailability of appropriately sized sieves. Acquisition of such sieves would allow the effect of granule size to be studied in greater depth.

In order to compete with Cyrano's hand-held electronic nose, the QTC sensors must not give rise to a significant change in signal when in the presence of temperatures ranging from 0 to 40 degC. Across such a temperature range, there will be an appreciable change in dimension of the brass pistons (with steel frits) and the PEEK cylinder, in addition to the aluminium compression rig. This is even before the effects of heat-induced polymer swelling and temperature-enhanced solvent-mixing in the polymer (from (19)) are considered. Thus, temperature dependence is inevitable, but the effect must be quantified, by placing the sensor rig in a fridge/oven during sensing experiments.

It has recently been discovered that there are 4 different types of silicone rubber available (containing methyl-groups only, phenyl groups, vinyl groups, and fluorine-containing groups only) that can each give rise to a dramatically different volume change upon exposure to the same solvent, and each type responds very differently to different solvents.⁴⁵ Fabricating QTC granules using these polymers, and incorporating them into the sensor array, is expected to considerably enhance the discrimination ability of the present array.

Once the subtleties of the experimental set-up are fully understood, the sensor array will then be exposed sequentially to as many different organic solvents as possible, all at several different values of ppm, to test the qualitative and quantitative sensing properties of the array; principle component analysis may then be used to clearly visualise its resolving power. After which, the array may be exposed to several solvents *simultaneously*, to probe its discrimination ability still further.

Further work may be done on stretched QTC in the vapour-sensing application. Previous experiments have shown a slow and unrepeatable response from thin films, which are also prone to fracture when stretched to below 100 Ω . Better results may be achieved for stretched or bent porous, thin cylinders of QTC, which will be less susceptible to breakage.

It may be of interest to examine the Hall effect in QTC, at different degrees of stretching. In a conventional composite, the Hall voltage is found to have a similar dependence as the conductivity does in (1).⁴⁶ Since much of the electron motion in a stretched QTC film is likely to be oblique to the applied electric field, an orthogonally applied magnetic field may result in unusual phenomena, which may best be probed by measurements of the current in the direction of the applied field, and the Hall voltage in the direction that is perpendicular to both the electric and magnetic fields. These experiments may be complicated by the fact that QTC might flex quite considerably in the presence of a magnetic field, leading to a resistivity change simply by virtue of the induced mechanical deformation. The I-V characteristics of a stretched QTC appear to have no double peak on the first voltage sweep up and down,¹⁵ in contrast to what is observed for a compressed film – measuring I-V characteristics of QTC under different degrees of tension may shed more light on this.

It is of interest to perform SEM imaging of QTC that has been stretched into a conductive state; this work will be carried out in the near future.

QTC may contract into a conductive state when it is placed in low-temperature surroundings – to test this temperature dependence of conductivity, an undeformed

QTC film will be suspended above liquid nitrogen (and perhaps liquid helium) at different heights, whilst making measurements of resistance.

An attempt may be made to fabricate an ultra-thin polymer film, then place a nickel 123 particle on it, before applying a second coating of polymer. This would be with a view to measuring the I-V characteristics of a QTC with a single conductive particle.

There is much work still to be done on the computer simulation of QTC. Rather than simply calculate the electric field half way across the insulating gap, its value should be computed at several points, then averaged in some way; in order to remove the divergent electric field at the surface of a particle, consideration should then be given to the Schottky effect by using a more complex expression for the tunnelling probability. In fact, it would be ideal to use an entirely new tunnelling probability equation, which is derived by taking into account the non-uniform electric field across the insulating gap. If the minimum electric field across the gap is found to be higher than the dielectric strength of the polymer, a dielectric breakdown event should be reported, perhaps by counting the number of breakdown events per pass. It is inevitable that some dielectric breakdown will be occurring in QTC, albeit on a microscopic scale, so as not to leave a visible imprint. It is not reasonable to assume that the volume of a QTC remains constant when it is stretched and compressed, hence travelling microscope work will be used to deduce exactly how a real QTC deforms, then this can be incorporated into the simulation. The use of smooth, spherical particles in the model is still relevant to some conventional composites, so it was a useful starting point in demonstrating the transition between a conventional and quantum tunnelling composite. The percolation modelling of the program will be considerably improved if particles are not allowed to overlap when the composite is deformed, but rather they should slide around each other. Being pedantic, consideration may also be given to the *constriction resistance*² of the contact spot between two spheres. Consideration should be given to the fields generated by the 16 other particles that are adjacent to the tunnelling event, in order to allow for the “pinching off” of conducting pathways that must be occurring in real QTC; however, this calculation will be complicated by the partial screening of charge by the other particles. It is true to say that the surface charge on any particle will be influenced by the charge on all the other particles, but it would be almost impossible to consider this effect. The negative differential regime may be realised by allowing electrons to propagate backwards. Electrons should be allowed to propagate individually to different particles, rather than all simultaneously to one particle. Also, a neighbouring particle should be randomly selected, rather than have the present fixed selection regime, which gives a preferred direction for electron propagation, other than in the direction of the applied field. A more sophisticated model should be used to ascertain current/resistance/resistivity/conductivity values from the number of electrons emerging from the QTC in one sweep. Trap-filling effects may be included by assigning a probability to an electron being “captured” during a tunnelling event – this probability will depend upon the number of traps within a given volume of the QTC and the number that has been filled already within that volume, hence it will decrease with time. In order to stop this from resulting in a decreasing current with time, the number of net electrons within QTC can’t remain constant. Perhaps this could most realistically be achieved by placing a specified number of electrons on each particle in the first z-plane, at the start of every pass, regardless of how many electrons emerge from the QTC at the end of a pass. In the process of creating the QTC, if a cubic cell

is to be left empty, due to there being insufficient room for a particle within the stated diameter range, a smaller particle should be allowed to reside there; realistically, any metal-polymer composite will contain conductive particles that are smaller than the stated size distribution would allow. The main modification to be made to the simulation is to model the effects of spikes on the spherical particles. Immediately, there will be a larger number density of particles for the same filler fraction, when spiky spheres are considered. The average volume of a spiky sphere of a certain extent may be estimated by placing cones on a sphere of smaller extent, then summing the volumes of the individual elements. It is not presently clear how to calculate the electric field generated by these spiky spheres. Field enhancement factors may provide a simple solution, but it is hoped that a more sophisticated model can be created. The ultimate goal will be to produce a program that calculates current-voltage characteristics as a function of compression and extension, with the hope of being able to reproduce the observed negative differential resistance regime, peak shifting and current-limiting behaviour.

4. ACKNOWLEDGEMENTS

A plethora of sensational folk and awe-inspiring scientists have provided graciously received assistance to me in my toddle down QTC grove. Myriad thanks abound to my supervisors, Dr. Graham Cross, for his tolerance, good-naturedness and inspirational encouragement, and Prof. “DB” Bloor for his insightful hints and profound knowledge of “funny rubber”. A special mention must also go to my merry cohorts, Mr. Andy Smith and Mr. David Cassidy, who combine wit and sensitivity in equal measure. Luminaries of QTCs, soon-to-be-Dr. Phil Hands and Dr. Kennyward Donnelly, deserve immense gratitude for their much-needed guidance, and also for the vapour-sensor set-up that I inherited; I wish them both the finest of all things in their new positions. Dr. Paul Laughlin deserves plaudits aplenty for being a prolific provider of QTC samples, and a sage of composites. Virtuoso chemist, Dr. Marek Szablewski, and ingenious spectroscopist, Dr. Lars-Olof Pålsson, are owed a debt of gratitude, for their respective Polishness and Swedishness, not forgetting their plucky and effervescent demeanours. Magical machinist, George Teasdale, is owed a porous metal gold medal (diamond-encrusted) for his mastery in the mechanical workshop. The world’s greatest technicians, Duncan McCallum, Norman Thompson, John Dobson and Wayne Dobby, deserve Knighthoods for their outstanding, tireless help and diligence. Mottcorp of America are downright saintly for providing 55 of their wondrous porous metal frits, free of charge. Finally, I would like to give immeasurable thanks to EPSRC and Peratech for funding, and also to David Lussey for inventing this most peculiar of materials.

5. REFERENCES

- ¹ R. M. Scarisbrick, *Journal of Applied Physics* **6**, 2098-2109 (1973).
- ² R. Strumpler and J. Glatz-Reichenbach, *Journal of Electroceramics* **3**, 329-346 (1999).
- ³ R. Gangopadhyay and A. De, *Sensors and Actuators B* **77**, 326-329 (2001).
- ⁴ D. Stauffer, *Introduction to Percolation Theory* (Taylor and Francis, 1985).
- ⁵ X.-S. Yi, G. Wu, and Y. Pan, *Polymer International* **44**, 117-124 (1997).
- ⁶ I. Balberg, *Physical Review Letters* **59**, 1305-1308 (1987).

D. S. McLachlan, J. Physics C **20**, 865 (1987).

A. C. M. Kuo, *Poly(dimethylsiloxane) - Polymer Data Handbook* (Oxford University Press, Inc., 1999).

P. A. Tipler, *Physics for Scientists and Engineers*, Vol. 2, 3rd ed. (Worth, 1999).

C. Zwikker, *Physical Properties of Solid Materials*, 1st ed. (Pergamon Press, 1954).

P. J. W. Hands, First-Year Ph.D. Report Thesis, Durham University, 1999/2000.

P. J. W. Hands, Ph.D. Thesis, Durham University, 2003.

R. C. J. d. Vincent-Humphreys, M.Sci. Thesis, Durham University, 2002/2003.

P. J. W. Hands, M.Sci. Thesis, Durham University, 1998/1999.

R. Gordon, M.Sci. Thesis, Durham University, 1999/2000.

K. Donnelly, "Novel Metal-Polymer Composites Progress Report," (2000-2002).

M. Lenzlinger and E. H. Snow, Journal of Applied Physics **40**, 278-283 (1969).

M. Jang and J. Lee, ETRI Journal **24**, 455-461 (2002).

A. Modinos, Solid-State Electronics **45**, 809-816 (2001).

P. Sheng, Physical Review B **21**, 2180-2195 (1980).

P. Sheng and J. Klafter, Physical Review B **27**, 2583 (1983).

G. E. Pike and C. H. Seager, Journal of Applied Physics **48**, 5152-5169 (1977).

S. A. Nasar, *2000 Solved Problems in Electromagnetics* (McGraw-Hill, Inc., 1992).

O. B. Isayeva, M. V. Eliseev, A. G. Rozhnev, and N. M. Ryskin, Solid-State Electronics **45**, 871-877 (2001).

L. M. Raff, *Principles of Physical Chemistry*, 1st ed. (Prentice-Hall, Inc., 2001).

R. L. Rosen, *Fundamental Principles of Polymeric Materials*, 2nd ed. (John Wiley & Sons, 1993).

G. Rossi and K. A. Mazich, Physical Review E **48**, 1182-1189 (1993).

M. Noble, M.Sci. Thesis, Durham University, 2001/2002.

W. J. Moore, *Physical Chemistry*, 5th ed. (Prentice Hall, Inc., 1972).

E. J. Severin, B. J. Doleman, and N. S. Lewis, Anal. Chem **72**, 658-668 (2000).

M. C. Lonergan, E. J. Severin, B. J. Doleman, S. A. Beaber, R. H. Grubbs, and N. S. Lewis, Chem. Mater. **8**, 2298-2312 (1996).

T. Artursson and M. Holmberg, Sensors and Actuators B **87**, 379-391 (2002).

B. J. Doleman and N. S. Lewis, Sensors and Actuators B **72**, 41-50 (2001).

C. Distante, M. Leo, P. Siciliano, and K. C. Persaud, Sensors and Actuators B **87**, 274-288 (2002).

A. R. Hopkins and N. S. Lewis, Anal. Chem **73**, 884-892 (2001).

T. P. Vaid, M. C. Burl, and N. S. Lewis, Anal. Chem **73**, 321-331 (2001).

<http://cyranosciences.com>.

D. A. McQuarrie and J. D. Simon, *Molecular Thermodynamics*, 1st ed. (University Science Books, 1999).

P. W. Atkins, *Physical Chemistry* (W. H. Freeman and Co., 1994).

- 40 J. Chen and N. Tsubokawa, *Journal of Applied Polymer Science* **77**, 2437-
2447 (2000).
- 41 e. a. H. Nishimura, *Polymer Engineering and Science* **26**, 585 (1986).
- 42 Y. Camberlin and J. P. Pascaut, *Journal of Polymer Science, Polymer Physics*
Edition **22**, 545 (1984).
- 43 R. C. Weast, *Handbook of Chemistry and Physics*, 66th ed. (CRC Press,
1986).
- 44 J. Chen, H. Iwata, N. Tsubokawa, Y. Maekawa, and M. Yoshida, *Polymer* **43**,
2201-2206 (2002).
- 45 *Silastic Brand Silicone Rubber: Fluid Resistance Guide* (Dow Corning
Corporation, 2000/2001).
- 46 E. Duerling and D. J. Bergman, *Physica A* **157**, 125-129 (1989).

APPENDICES

APPENDIX A

```

PROGRAM QTCSIM
!
!By Ed Williams
!Purpose: To model the movement of charge through Peratech's QTC, modelling the conductive filler particles as spheres
!
IMPLICIT NONE
!
REAL,ALLOCATABLE::QTC(:,,:) !Matrix used to store particle centre coordinates in microns(columns 1-3), particle diameters
!in microns(column 4), no. of electrons on particle due to polarisation in applied field, with
!the same number of "lack of electrons" (positive charge) on the opposite hemisphere (column 5),
!and the net charge on a particle (column 6), with "-1" denoting the presence of one electron
REAL::X,Y,Z,A !Hold values of random numbers used in generating spherical particle coordinates and diameters
REAL::SFILL,LFILL !Used to store the stated smallest and largest filler particle diameters, in microns
REAL::FILCONC !Used to store the stated required filler concentration percentage, by mass
REAL::XCO,YCO,ZCO !Used to store random coordinates within a cubic cell that are provisional coordinates for the centre of
!a sphere within that cell, in microns
REAL::PSIZE !Used to store the randomly-assigned (between stated range) size of filler particle, in microns
REAL::CDIM !Used to store the dimension of a cubic cell, in microns
REAL::CVOL !Used to store the volume of a cubic cell, in cubic microns
REAL::QTCVOL !Used to store the volume of the QTC, in cubic microns
REAL::FILVOL !Used to store the volume occupied by the conductive filler particles, in cubic microns
REAL::SPVOL !Used to store the actual volume occupied by all the spheres in the QTC
REAL::DENNI !Used to store the density of silicone rubber
REAL::DENSr !Used to store the density of nickel
REAL::PSINC !Used to store the increment in particle size to be used in calculating the particle size distribution
REAL::XDIM,YDIM,ZDIM !Used to store the dimensions of the QTC, in mm
REAL::XDIF,YDIF,ZDIF !Used to store the cartesian coordinates of the position vector between the centres of two adjacent
!particles, in microns
REAL::DIF !Used to store the distance between the centres of two adjacent particles, in microns
REAL::MIDPOINTDIST !Used to store the shortest distance from the surface of a sphere to the midpoint between two
!neighbouring spheres, in microns
REAL::XDIFMID,YDIFMID,ZDIFMID !Used to store the cartesian coordinates of the position vector between the centre of a
!particle and the midpoint between the surface of that particle, and the surface of an
!adjacent particle, in microns
REAL::DIFMID !Used to store the distance between the centre of a particle and the point half way between the edge of
!that particle and the edge of an adjacent particle, in microns
REAL::PHI !Used to store the polar angle between centre of particle and centre of gap between adjacent particles, in degrees
REAL::THETA !Used to store the azimuthal angle between centre of particle and centre of gap between adjacent particles,
!in degrees
REAL::ALPHA !Used to store the angle about PHI and THETA at which point a line from the centre of the gap (midpoint)
!to the surface of the sphere is a tangent to the sphere, in degrees
REAL::INTPHI !Used to store the angle, in radians, about PHI over which to integrate the surface charge density over the
!surface area of a sphere, which has already been integrated between certain values of THETA
REAL::P !Used to store the random number which, if less than the tunnelling probability, T, allows an electron to tunnel
REAL::XPAT,YPAT,ZPAT !Used to store the cartesian coordinates of the centre of a patch on a sphere, over which the quantity
!of charge is calculated by integrating the surface charge density over the surface area, in order to
!calculate the electric field at the midpoint caused by the charge on the patch, in microns
REAL::DIFEF !Used to store the distance between the centre of the patch and the midpoint between the particles, in microns
REAL::TOTDIF !Used to store the sum of the shortest distances between the surface of a particle and the surface of all
!adjacent particles, without repetition, in microns
REAL::MAXDIF,MINDIF !Used to store, respectively, the maximum and minimum distances between the surfaces of adjacent
!particles, in microns
REAL::XMID,YMID,ZMID !Used to store the cartesian coordinates of the midpoint between the surfaces of two adjacent particles
!in microns
REAL::CHARGE !Used to store the charge, in Coulombs, on a particular patch on the surface of a sphere
REAL::XEFVECTOR,YEFVECTOR,ZEFVECTOR !Used to store the cartesian coordinates of the position vector from the centre of a
!patch on a sphere to the midpoint, which is in the same direction as the electric field
!from the patch at the midpoint, in microns
REAL::V !Used to store the voltage applied across the QTC in the negative z-direction, in volts
REAL::EF !Used to store the resulting applied electric field in the polymer in the negative z-direction, in volts/m
REAL::POLZDIM !Used to store the effective thickness of the polymer in the z-direction
REAL::DCP !Used to store the dielectric constant of the polymer (i.e. silicone rubber)
REAL::T !Used to store the tunnelling probability
REAL::B !Used to store the constant used in the numerator of the exponential used in the tunnelling probability equation
REAL::DEF !Used to store the existing percentage of deformation applied to the z-dimension of the QTC, where <100=compression
!and >100=extension
REAL::NDEF !Used to store the percentage of deformation to be applied to the z-dimension of the QTC, where <100=compression
!and >100=extension
REAL::ACTUALSCALAREF !Used to store the magnitude of the electric field vector in the direction of the line joining the
!centres of the two particles
REAL::TNOE !Used to store the running total number of electrons emerging from the QTC, then re-entering, per pass
REAL::TSNOE !Used to store the running total of the square of the no. of electrons emerging from the QTC per pass
INTEGER,ALLOCATABLE::PCOUNT(:) !Vector used to store particle size distribution (particle count)
INTEGER::I,J,K,L,C,D,E,F !DO loop variables
INTEGER::SI,SJ,SK !Substitutes for DO loop variables, used to temporarily store respective values within the DO loop
INTEGER::ZAP !Used to terminate the WHILE loop once a particle has been placed in an empty cubic cell
INTEGER::INPUT !Used to store number of option selected in main menu
INTEGER::ND !Used to indicate whether any QTC data has yet been created or retrieved ("1" for no data, "0" for data)
INTEGER::NOP !Used to store the number of overlapping particles
INTEGER::NOE !Used to store the number of electrons emerging from end of QTC in one pass
INTEGER::PASS !Used to store the number of "passes" to be made through QTC, where on pass is where all particles have

```

```

!been allowed to propagate one electron (in addition to surplus electrons) to all adjacent particles in
!the next and same z-planes, once, either by percolation, or by QM tunnelling
INTEGER::N !Used to store the provisional number of filler particles
INTEGER::NX,NY,NZ !Used to store the number of cells, respectively in the x, y, and z directions
INTEGER::LN !Used to store the number of while loops to perform in order to try to place particle in particular cell
INTEGER::EMPC !Used to store the number of empty cells
INTEGER::TOTALN !Used to store the actual number of cells
DOUBLE PRECISION::INTEGRAL !Function used to evaluate the integral over theta used in calculating the charge on a patch
!on a sphere
DOUBLE PRECISION::TOTALEF(3) !Vector storing the total electric field vector at the midpoint between the surfaces of two
!adjacent spheres
DOUBLE PRECISION::ACTUALEF(3) !Used to store the x-, y-, and z-components of the dot product between the total electric
!field vector and the unit vector in the direction of the line joining the centres of the
!two particles
CHARACTER(LEN=6)::FILENAME !Used to store the name of a text file to be written to, or read from
CHARACTER(LEN=1)::UNIFORM !Used to store whether or not an attempt should be made to create a uniform particle size
!distribution
CHARACTER(LEN=1)::QUANTUM !Used to store whether or not effects of quantum mechanical tunnelling should be considered in
!electron propagation
CHARACTER(LEN=1)::CV !Used to store whether or not a constant volume is to be used when compressing the QTC in the
!z-direction. If not, the x- and y-dimensions remain constant
!
ND=1
1 WRITE(*,*)'          MAIN MENU'
WRITE(*,*)
WRITE(*,*)'Select option:'
WRITE(*,*)
WRITE(*,*)'1 - Create QTC Data'
WRITE(*,*)'2 - Save QTC Data'
WRITE(*,*)'3 - Read Saved QTC Data'
WRITE(*,*)'4 - Compress QTC'
WRITE(*,*)'5 - Stretch QTC'
WRITE(*,*)'6 - Count Number of Overlapping Particles in QTC'
WRITE(*,*)'7 - Calculate Particle Size Distribution in QTC'
WRITE(*,*)'8 - Calculate Max., Min., and Average Distances Between Particles in QTC'
WRITE(*,*)'9 - Apply Electric Field across QTC'
WRITE(*,*)'10 - View QTC Parameters'
WRITE(*,*)'11 - End Program'
WRITE(*,*)
READ(*,*)INPUT
WHILE((ND>0.5).AND.(((INPUT>1.5).AND.(INPUT<2.5)).OR.((INPUT>3.5).AND.(INPUT<10.5))))DO
  WRITE(*,6,ADVANCE='NO')
6 FORMAT('Invalid! There is no QTC data yet! Re-enter option: ')
  READ(*,*)INPUT
END WHILE
WRITE(*,*)
SELECT CASE(INPUT)
CASE(1)
  WRITE(*,*)'The field is applied in the negative z-direction'
  WRITE(*,*)
  WRITE(*,10,ADVANCE='NO')
10 FORMAT('Enter x-dimension of sample (in mm): ')
  READ(*,*)XDIM
  WHILE((XDIM>1.0).OR.(XDIM<0.1))DO
    WRITE(*,15,ADVANCE='NO')
15 FORMAT('Invalid! Re-enter value between 0.1 and 1 mm: ')
    READ(*,*)XDIM
  END WHILE
  WRITE(*,20,ADVANCE='NO')
20 FORMAT('Enter y-dimension of sample (in mm): ')
  READ(*,*)YDIM
  WHILE((YDIM>1.0).OR.(YDIM<0.1))DO
    WRITE(*,25,ADVANCE='NO')
25 FORMAT('Invalid! Re-enter value between 0.1 and 1 mm: ')
    READ(*,*)YDIM
  END WHILE
  WRITE(*,30,ADVANCE='NO')
30 FORMAT('Enter z-dimension of sample (in mm): ')
  READ(*,*)ZDIM
  WHILE((ZDIM>1.0).OR.(ZDIM<0.1))DO
    WRITE(*,35,ADVANCE='NO')
35 FORMAT('Invalid! Re-enter value between 0.1 and 1 mm: ')
    READ(*,*)ZDIM
  END WHILE
  WRITE(*,*)
  WRITE(*,40,ADVANCE='NO')
40 FORMAT('Enter the smallest diameter of spherical filler particle (in microns): ')
  READ(*,*)SFILL
  WHILE((SFILL>50.0).OR.(SFILL<0.01))DO
    WRITE(*,45,ADVANCE='NO')
45 FORMAT('Invalid! Re-enter value between 0.01 and 50 microns: ')
    READ(*,*)SFILL
  END WHILE
  WRITE(*,50,ADVANCE='NO')
50 FORMAT('Enter the largest diameter of spherical filler particle (in microns): ')
  READ(*,*)LFILL

```

```

WHILE((LFILL>85.0).OR.(LFILL<=SFILL))DO
  WRITE(*,55,ADVANCE='NO')
55 FORMAT('Invalid! Re-enter value between the smallest diameter and 85 microns: ')
  READ(*,*)LFILL
END WHILE
WRITE(*,*)
WRITE(*,57,ADVANCE='NO')
57 FORMAT('Attempt to maintain a uniform particle size distribution ("Y" or "N")? ')
READ(*,*)UNIFORM
WHILE(((UNIFORM).NE.('Y')).AND.((UNIFORM).NE.('y')).AND.((UNIFORM).NE.('N')).AND.((UNIFORM).NE.('n'))))DO
  WRITE(*,58,ADVANCE='NO')
58 FORMAT('Invalid! Re-enter "Y" or "N": ')
  READ(*,*)UNIFORM
END WHILE
WRITE(*,*)
WRITE(*,60,ADVANCE='NO')
60 FORMAT('Enter the filler concentration (as w/w %): ')
READ(*,*)FILCONC
WHILE((FILCONC>=100.0).OR.(FILCONC<=0.0))DO
  WRITE(*,65,ADVANCE='NO')
65 FORMAT('Invalid! Re-enter value between 0 and 100%: ')
  READ(*,*)FILCONC
END WHILE
QTCVOL=XDIM*YDIM*ZDIM*1000000000
DENSr=0.97 !g/cm^3
DENNI=8.908 !g/cm^3
FILVOL=QTCVOL*(1-(1-FILCONC/100.0)/(1+FILCONC*(DENSr/DENNI-1.0)/100.0))
N=NINT(24*FILVOL*(LFILL-SFILL)/(3.141592654*(LFILL**4-SFILL**4))) !Calculation of number of spheres, with a uniform
!size distribution, required to fill FILVOL

CVOL=QTCVOL/N
CDIM=CVOL**(1.0/3.0)
NX=NINT(XDIM*1000.0/CDIM)
NY=NINT(YDIM*1000.0/CDIM)
NZ=NINT(ZDIM*1000.0/CDIM)
TOTALN=NX*NY*NZ
ALLOCATE(QTC(TOTALN,6)) !Create matrix with a row for every particle
QTC=0.0
EMPC=0
LN=0
CALL RANDOM_SEED
DO K=1,NZ,1
DO J=1,NY,1
DO I=1,NX,1
  ZAP=2
  IF(LN>99999)THEN !If true, cubic cell left empty
    EMPC=EMPC+1
  ENDIF
  LN=0
  WHILE((ZAP>1).AND.(LN<100000))DO !Loop to fill particular I,J,K cell with a particle, with 100,000 attempts
    CALL RANDOM_NUMBER(X)!Place random number in X
    CALL RANDOM_NUMBER(Y)!Place random number in Y
    CALL RANDOM_NUMBER(Z)!Place random number in Z
    XCO=X*CDIM !Random x-coordinate of centre of particle in cell
    YCO=Y*CDIM !Random y-coordinate of centre of particle in cell
    ZCO=Z*CDIM !Random z-coordinate of centre of particle in cell
    IF((UNIFORM=='Y').OR.(UNIFORM=='y'))THEN !If uniform particle size distribution is requested, the particle size
      !does not change between loops, otherwise a new random size is
      !generated with each loop, making smaller particles more likely
    ELSE
      IF(LN==0)THEN
        CALL RANDOM_NUMBER(A)!Place random number in A
        PSIZE=A*(LFILL-SFILL)+SFILL
      END IF
    ELSE
      CALL RANDOM_NUMBER(A)!Place random number in A
      PSIZE=A*(LFILL-SFILL)+SFILL
    END IF
    IF((I<2.0).AND.(J<2.0))THEN
      IF(K<2.0)THEN !First particle goes straight into QTC
        QTC(1,1)=XCO
        QTC(1,2)=YCO
        QTC(1,3)=ZCO
        QTC(1,4)=PSIZE
        ZAP=0
      ELSE
        XDIF=QTC((K-2)*NX*NY+1,1)-XCO !Checks to ensure there is no particle overlap are required elsewhere in QTC
        YDIF=QTC((K-2)*NX*NY+1,2)-YCO
        ZDIF=QTC((K-2)*NX*NY+1,3)-((K-1)*CDIM+ZCO)
        DIF=SQRT(XDIF**2+YDIF**2+ZDIF**2)
        IF(2*DIF>(PSIZE+QTC((K-2)*NX*NY+1,4)))THEN
          XDIF=QTC((K-2)*NX*NY+2,1)-XCO
          YDIF=QTC((K-2)*NX*NY+2,2)-YCO
          ZDIF=QTC((K-2)*NX*NY+2,3)-(ZCO+(K-1)*CDIM)
          DIF=SQRT(XDIF**2+YDIF**2+ZDIF**2)
          IF(2*DIF>(PSIZE+QTC((K-2)*NX*NY+2,4)))THEN
            XDIF=QTC((K-2)*NX*NY+NX+1,1)-XCO
            YDIF=QTC((K-2)*NX*NY+NX+1,2)-YCO

```



```

ZDIF=QTC((K-2)*NX*NY+NX+1,3)-(ZCO+(K-1)*CDIM)
DIF=SQRT(XDIF**2+YDIF**2+ZDIF**2)
IF(2*DIF>(PSIZE+QTC((K-2)*NX*NY+NX+1,4)))THEN
  XDIF=QTC((K-2)*NX*NY+NX+2,1)-XCO
  YDIF=QTC((K-2)*NX*NY+NX+2,2)-YCO
  ZDIF=QTC((K-2)*NX*NY+NX+2,3)-(ZCO+(K-1)*CDIM)
  DIF=SQRT(XDIF**2+YDIF**2+ZDIF**2)
  IF(2*DIF>(PSIZE+QTC((K-2)*NX*NY+NX+2,4)))THEN
    QTC((K-1)*NX*NY+1,1)=XCO
    QTC((K-1)*NX*NY+1,2)=YCO
    QTC((K-1)*NX*NY+1,3)=ZCO+(K-1)*CDIM
    QTC((K-1)*NX*NY+1,4)=PSIZE
    ZAP=0
  END IF
END IF
END IF
END IF
END IF
END IF
IF((I>1.0).AND.(J<2.0))THEN
  XDIF=QTC((K-1)*NX*NY+I-1,1)-(XCO+(I-1)*CDIM)
  YDIF=QTC((K-1)*NX*NY+I-1,2)-YCO
  ZDIF=QTC((K-1)*NX*NY+I-1,3)-(ZCO+(K-1)*CDIM)
  DIF=SQRT(XDIF**2+YDIF**2+ZDIF**2)
  IF(2*DIF>(PSIZE+QTC((K-1)*NX*NY+I-1,4)))THEN
    IF(K<2.0)THEN
      QTC(I,1)=XCO+(I-1)*CDIM
      QTC(I,2)=YCO
      QTC(I,3)=ZCO
      QTC(I,4)=PSIZE
      ZAP=0
    ELSE
      XDIF=QTC((K-2)*NX*NY+I-1,1)-(XCO+(I-1)*CDIM)
      YDIF=QTC((K-2)*NX*NY+I-1,2)-YCO
      ZDIF=QTC((K-2)*NX*NY+I-1,3)-(ZCO+(K-1)*CDIM)
      DIF=SQRT(XDIF**2+YDIF**2+ZDIF**2)
      IF(2*DIF>(PSIZE+QTC((K-2)*NX*NY+I-1,4)))THEN
        XDIF=QTC((K-2)*NX*NY+I,1)-(XCO+(I-1)*CDIM)
        YDIF=QTC((K-2)*NX*NY+I,2)-YCO
        ZDIF=QTC((K-2)*NX*NY+I,3)-(ZCO+(K-1)*CDIM)
        DIF=SQRT(XDIF**2+YDIF**2+ZDIF**2)
        IF(2*DIF>(PSIZE+QTC((K-2)*NX*NY+I,4)))THEN
          XDIF=QTC((K-2)*NX*NY+I+1,1)-(XCO+(I-1)*CDIM)
          YDIF=QTC((K-2)*NX*NY+I+1,2)-YCO
          ZDIF=QTC((K-2)*NX*NY+I+1,3)-(ZCO+(K-1)*CDIM)
          DIF=SQRT(XDIF**2+YDIF**2+ZDIF**2)
          IF(2*DIF>(PSIZE+QTC((K-2)*NX*NY+I+1,4)))THEN
            XDIF=QTC((K-2)*NX*NY+NX+I-1,1)-(XCO+(I-1)*CDIM)
            YDIF=QTC((K-2)*NX*NY+NX+I-1,2)-YCO
            ZDIF=QTC((K-2)*NX*NY+NX+I-1,3)-(ZCO+(K-1)*CDIM)
            DIF=SQRT(XDIF**2+YDIF**2+ZDIF**2)
            IF(2*DIF>(PSIZE+QTC((K-2)*NX*NY+NX+I-1,4)))THEN
              XDIF=QTC((K-2)*NX*NY+NX+I,1)-(XCO+(I-1)*CDIM)
              YDIF=QTC((K-2)*NX*NY+NX+I,2)-YCO
              ZDIF=QTC((K-2)*NX*NY+NX+I,3)-(ZCO+(K-1)*CDIM)
              DIF=SQRT(XDIF**2+YDIF**2+ZDIF**2)
              IF(2*DIF>(PSIZE+QTC((K-2)*NX*NY+NX+I,4)))THEN
                XDIF=QTC((K-2)*NX*NY+NX+I+1,1)-(XCO+(I-1)*CDIM)
                YDIF=QTC((K-2)*NX*NY+NX+I+1,2)-YCO
                ZDIF=QTC((K-2)*NX*NY+NX+I+1,3)-(ZCO+(K-1)*CDIM)
                DIF=SQRT(XDIF**2+YDIF**2+ZDIF**2)
                IF(2*DIF>(PSIZE+QTC((K-2)*NX*NY+NX+I+1,4)))THEN
                  QTC((K-1)*NX*NY+I,1)=XCO+(I-1)*CDIM
                  QTC((K-1)*NX*NY+I,2)=YCO
                  QTC((K-1)*NX*NY+I,3)=ZCO+(K-1)*CDIM
                  QTC((K-1)*NX*NY+I,4)=PSIZE
                  ZAP=0
                END IF
              END IF
            END IF
          END IF
        END IF
      END IF
    END IF
  END IF
END IF
IF((I<2.0).AND.(J>1.0))THEN
  XDIF=QTC((K-1)*NX*NY+(J-2)*NX+1,1)-XCO
  YDIF=QTC((K-1)*NX*NY+(J-2)*NX+1,2)-(YCO+(J-1)*CDIM)
  ZDIF=QTC((K-1)*NX*NY+(J-2)*NX+1,3)-(ZCO+(K-1)*CDIM)
  DIF=SQRT(XDIF**2+YDIF**2+ZDIF**2)
  IF(2*DIF>(PSIZE+QTC((K-1)*NX*NY+(J-2)*NX+1,4)))THEN
    XDIF=QTC((K-1)*NX*NY+(J-2)*NX+2,1)-XCO
    YDIF=QTC((K-1)*NX*NY+(J-2)*NX+2,2)-(YCO+(J-1)*CDIM)
    ZDIF=QTC((K-1)*NX*NY+(J-2)*NX+2,3)-(ZCO+(K-1)*CDIM)
    DIF=SQRT(XDIF**2+YDIF**2+ZDIF**2)
  END IF
END IF

```

```

IF(2*DIF>(PSIZE+QTC((K-1)*NX*NY+(J-2)*NX+2,4)))THEN
  IF(K<2.0)THEN
    QTC((J-1)*NX+1,1)=XCO
    QTC((J-1)*NX+1,2)=YCO+(J-1)*CDIM
    QTC((J-1)*NX+1,3)=ZCO+(K-1)*CDIM
    QTC((J-1)*NX+1,4)=PSIZE
    ZAP=0
  ELSE
    XDIF=QTC((K-2)*NX*NY+(J-2)*NX+1,1)-XCO
    YDIF=QTC((K-2)*NX*NY+(J-2)*NX+1,2)-(YCO+(J-1)*CDIM)
    ZDIF=QTC((K-2)*NX*NY+(J-2)*NX+1,3)-(ZCO+(K-1)*CDIM)
    DIF=SQRT(XDIF**2+YDIF**2+ZDIF**2)
    IF(2*DIF>(PSIZE+QTC((K-2)*NX*NY+(J-2)*NX+1,4)))THEN
      XDIF=QTC((K-2)*NX*NY+(J-2)*NX+2,1)-XCO
      YDIF=QTC((K-2)*NX*NY+(J-2)*NX+2,2)-(YCO+(J-1)*CDIM)
      ZDIF=QTC((K-2)*NX*NY+(J-2)*NX+2,3)-(ZCO+(K-1)*CDIM)
      DIF=SQRT(XDIF**2+YDIF**2+ZDIF**2)
      IF(2*DIF>(PSIZE+QTC((K-2)*NX*NY+(J-2)*NX+2,4)))THEN
        XDIF=QTC((K-2)*NX*NY+(J-1)*NX+1,1)-XCO
        YDIF=QTC((K-2)*NX*NY+(J-1)*NX+1,2)-(YCO+(J-1)*CDIM)
        ZDIF=QTC((K-2)*NX*NY+(J-1)*NX+1,3)-(ZCO+(K-1)*CDIM)
        DIF=SQRT(XDIF**2+YDIF**2+ZDIF**2)
        IF(2*DIF>(PSIZE+QTC((K-2)*NX*NY+(J-1)*NX+1,4)))THEN
          XDIF=QTC((K-2)*NX*NY+(J-1)*NX+2,1)-XCO
          YDIF=QTC((K-2)*NX*NY+(J-1)*NX+2,2)-(YCO+(J-1)*CDIM)
          ZDIF=QTC((K-2)*NX*NY+(J-1)*NX+2,3)-(ZCO+(K-1)*CDIM)
          DIF=SQRT(XDIF**2+YDIF**2+ZDIF**2)
          IF(2*DIF>(PSIZE+QTC((K-2)*NX*NY+(J-1)*NX+2,4)))THEN
            XDIF=QTC((K-2)*NX*NY+J*NX+1,1)-XCO
            YDIF=QTC((K-2)*NX*NY+J*NX+1,2)-(YCO+(J-1)*CDIM)
            ZDIF=QTC((K-2)*NX*NY+J*NX+1,3)-(ZCO+(K-1)*CDIM)
            DIF=SQRT(XDIF**2+YDIF**2+ZDIF**2)
            IF(2*DIF>(PSIZE+QTC((K-2)*NX*NY+J*NX+1,4)))THEN
              XDIF=QTC((K-2)*NX*NY+J*NX+2,1)-XCO
              YDIF=QTC((K-2)*NX*NY+J*NX+2,2)-(YCO+(J-1)*CDIM)
              ZDIF=QTC((K-2)*NX*NY+J*NX+2,3)-(ZCO+(K-1)*CDIM)
              DIF=SQRT(XDIF**2+YDIF**2+ZDIF**2)
              IF(2*DIF>(PSIZE+QTC((K-2)*NX*NY+J*NX+2,4)))THEN
                QTC((K-1)*NX*NY+(J-1)*NX+1,1)=XCO
                QTC((K-1)*NX*NY+(J-1)*NX+1,2)=YCO+(J-1)*CDIM
                QTC((K-1)*NX*NY+(J-1)*NX+1,3)=ZCO+(K-1)*CDIM
                QTC((K-1)*NX*NY+(J-1)*NX+1,4)=PSIZE
                ZAP=0
              END IF
            END IF
          END IF
        END IF
      END IF
    END IF
  END IF
END IF
IF((I>1.0).AND.(J>1.0))THEN
  XDIF=QTC((K-1)*NX*NY+(J-1)*NX+I-1,1)-(XCO+(I-1)*CDIM)
  YDIF=QTC((K-1)*NX*NY+(J-1)*NX+I-1,2)-(YCO+(J-1)*CDIM)
  ZDIF=QTC((K-1)*NX*NY+(J-1)*NX+I-1,3)-(ZCO+(K-1)*CDIM)
  DIF=SQRT(XDIF**2+YDIF**2+ZDIF**2)
  IF(2*DIF>(PSIZE+QTC((K-1)*NX*NY+(J-1)*NX+I-1,4)))THEN
    XDIF=QTC((K-1)*NX*NY+(J-2)*NX+I-1,1)-(XCO+(I-1)*CDIM)
    YDIF=QTC((K-1)*NX*NY+(J-2)*NX+I-1,2)-(YCO+(J-1)*CDIM)
    ZDIF=QTC((K-1)*NX*NY+(J-2)*NX+I-1,3)-(ZCO+(K-1)*CDIM)
    DIF=SQRT(XDIF**2+YDIF**2+ZDIF**2)
    IF(2*DIF>(PSIZE+QTC((K-1)*NX*NY+(J-2)*NX+I-1,4)))THEN
      XDIF=QTC((K-1)*NX*NY+(J-2)*NX+I,1)-(XCO+(I-1)*CDIM)
      YDIF=QTC((K-1)*NX*NY+(J-2)*NX+I,2)-(YCO+(J-1)*CDIM)
      ZDIF=QTC((K-1)*NX*NY+(J-2)*NX+I,3)-(ZCO+(K-1)*CDIM)
      DIF=SQRT(XDIF**2+YDIF**2+ZDIF**2)
      IF(2*DIF>(PSIZE+QTC((K-1)*NX*NY+(J-2)*NX+I,4)))THEN
        XDIF=QTC((K-1)*NX*NY+(J-2)*NX+I+1,1)-(XCO+(I-1)*CDIM)
        YDIF=QTC((K-1)*NX*NY+(J-2)*NX+I+1,2)-(YCO+(J-1)*CDIM)
        ZDIF=QTC((K-1)*NX*NY+(J-2)*NX+I+1,3)-(ZCO+(K-1)*CDIM)
        DIF=SQRT(XDIF**2+YDIF**2+ZDIF**2)
        IF(2*DIF>(PSIZE+QTC((K-1)*NX*NY+(J-2)*NX+I+1,4)))THEN
          IF(K<2.0)THEN
            QTC((J-1)*NX+I,1)=XCO+(I-1)*CDIM
            QTC((J-1)*NX+I,2)=YCO+(J-1)*CDIM
            QTC((J-1)*NX+I,3)=ZCO
            QTC((J-1)*NX+I,4)=PSIZE
            ZAP=0
          ELSE
            XDIF=QTC((K-2)*NX*NY+(J-2)*NX+I-1,1)-(XCO+(I-1)*CDIM)
            YDIF=QTC((K-2)*NX*NY+(J-2)*NX+I-1,2)-(YCO+(J-1)*CDIM)
            ZDIF=QTC((K-2)*NX*NY+(J-2)*NX+I-1,3)-(ZCO+(K-1)*CDIM)
            DIF=SQRT(XDIF**2+YDIF**2+ZDIF**2)
            IF(2*DIF>(PSIZE+QTC((K-2)*NX*NY+(J-2)*NX+I-1,4)))THEN

```



```

WRITE(*,*)'The loading ratio is:',FILCONC,'w/w %'
WRITE(*,*)'The size of the QTC in the z-direction is:',DEF,'% '
WRITE(*,*)'The QTC has x-dimension:',XDIM,'mm'
WRITE(*,*)'The QTC has y-dimension:',YDIM,'mm'
WRITE(*,*)'The QTC has z-dimension:',ZDIM,'mm'
READ(*,*)
DO I=1,30,1
  WRITE(*,*)
END DO
CASE(2)
  WRITE(*,70,ADVANCE='NO')
  70 FORMAT('Enter name of text file in which to save data (max. of 6 characters): ')
  READ(*,*)FILENAME
  OPEN(12,FILE=FILENAME//'.txt')
  WRITE(12,*)TOTALN
  WRITE(12,*)EMPC
  WRITE(12,*)NX
  WRITE(12,*)NY
  WRITE(12,*)NZ
  WRITE(12,*)CDIM
  WRITE(12,*)SFILL
  WRITE(12,*)LFILL
  WRITE(12,*)FILCONC
  WRITE(12,*)DEF
  DO I=1,TOTALN,1
    WRITE(12,80)QTC(I,1),QTC(I,2),QTC(I,3),QTC(I,4),QTC(I,5),QTC(I,6)
  END DO
  80 FORMAT(E15.10,5X,E15.10,5X,E15.10,5X,E15.10,5X,E15.4,5X,E15.4)
  CLOSE(12)
  DO I=1,30,1
    WRITE(*,*)
  END DO
CASE(3)
  WRITE(*,90,ADVANCE='NO')
  90 FORMAT('Enter name of text file from which to read data (max. of 6 characters): ')
  READ(*,*)FILENAME
  OPEN(13,FILE=FILENAME//'.txt')
  READ(13,*)TOTALN
  READ(13,*)EMPC
  READ(13,*)NX
  READ(13,*)NY
  READ(13,*)NZ
  READ(13,*)CDIM
  READ(13,*)SFILL
  READ(13,*)LFILL
  READ(13,*)FILCONC
  READ(13,*)DEF
  ALLOCATE(QTC(TOTALN,6))
  QTC=0.0
  DO I=1,TOTALN,1
    READ(13,100)QTC(I,1),QTC(I,2),QTC(I,3),QTC(I,4),QTC(I,5),QTC(I,6)
  END DO
  100 FORMAT(E15.10,5X,E15.10,5X,E15.10,5X,E15.10,5X,E15.4,5X,E15.4)
  IF(DEF<=100.0)THEN
    IF((CV=='Y').OR.(CV=='y'))THEN !If compression and constant volume, increase z-dimension by factor of DEF/100,
      DO I=1,TOTALN,1 !and decrease x- and y-dimensions by the same factor
        XDIM=NX*CDIM/(SQRT(DEF)*100.0)
        YDIM=NY*CDIM/(SQRT(DEF)*100.0)
        ZDIM=NZ*CDIM*DEF/100000.0
      END DO
    ELSE !If compression and not constant volume, increase z-dimension by factor of DEF/100
      XDIM=NX*CDIM/1000.0
      YDIM=NY*CDIM/1000.0
      ZDIM=NZ*CDIM*DEF/100000.0
    END IF
  ELSE !If extension, always constant volume, therefore increase z-dimension by factor of DEF/100, and decrease x-
    XDIM=NX*CDIM/(SQRT(DEF)*100.0) !and y-dimensions by the same factor
    YDIM=NY*CDIM/(SQRT(DEF)*100.0)
    ZDIM=NZ*CDIM*DEF/100000.0
  END IF
  WRITE(*,*)
  WRITE(*,*)'The number of cubic cells is:',TOTALN
  WRITE(*,*)'The number of empty cubic cells is:',EMPC
  WRITE(*,*)'Therefore, the number of filler particles is:',TOTALN-EMPC
  WRITE(*,*)'The number of cubic cells in the x-direction is:',NX
  WRITE(*,*)'The number of cubic cells in the y-direction is:',NY
  WRITE(*,*)'The number of cubic cells in the z-direction is:',NZ
  WRITE(*,*)'The original dimension of each cubic cell is:',CDIM,' microns'
  WRITE(*,*)'The smallest particle diameter is:',SFILL,' microns'
  WRITE(*,*)'The largest particle diameter is:',LFILL,' microns'
  WRITE(*,*)'The loading ratio is:',FILCONC,'w/w %'
  WRITE(*,*)'The size of the QTC in the z-direction is:',DEF,'% '
  WRITE(*,*)'The QTC has x-dimension:',XDIM,'mm'
  WRITE(*,*)'The QTC has y-dimension:',YDIM,'mm'
  WRITE(*,*)'The QTC has z-dimension:',ZDIM,'mm'
  READ(*,*)

```

```

CLOSE(13)
ND=0
DO I=1,30,1
  WRITE(*,*)
END DO
CASE(4)
IF(DEF<=50.0)THEN
  WRITE(*,*)QTC cannot be compressed any further!
  READ(*,*)
ELSE
  WRITE(*,110,ADVANCE='NO')
110 FORMAT('Enter compression in z-direction (i.e. what % of original z-dim. is QTC): ')
  READ(*,*)NDEF
  DEF=DEF*NDEF/100.0
  WHILE((NDEF>100.0).OR.(DEF<50.0))DO
    DEF=DEF*100.0/NDEF
    WRITE(*,*)'Invalid! Re-enter value between',5000.0/DEF,'and 100%:'
    READ(*,*)NDEF
    DEF=DEF*NDEF/100.0
  END WHILE
  WRITE(*,111,ADVANCE='NO')
111 FORMAT('Maintain constant volume ("Y" or "N")? ')
  READ(*,*)CV
  WHILE(((CV).NE.('Y')).AND.((CV).NE.('y')).AND.((CV).NE.('N')).AND.((CV).NE.('n'))))DO
    WRITE(*,112,ADVANCE='NO')
112 FORMAT('Invalid! Re-enter "Y" or "N": ')
    READ(*,*)CV
  END WHILE
  IF((CV=='Y').OR.(CV=='y'))THEN !If constant volume, increase z-coordinates of centres of particles by factor of
    DO I=1,TOTALN,1 !DEF/100, and decrease x- and y-coordinates of centres of particles by same factor
      QTC(I,1)=QTC(I,1)*SQRT(100.0/DEF)
      QTC(I,2)=QTC(I,2)*SQRT(100.0/DEF)
      QTC(I,3)=QTC(I,3)*DEF/100.0
    END DO
  ELSE !If not constant volume, only increase z-coordinates of centres of particles by factor of DEF/100
    DO I=1,TOTALN,1
      QTC(I,3)=QTC(I,3)*DEF/100.0
    END DO
  END IF
END IF
DO I=1,30,1
  WRITE(*,*)
END DO
CASE(5)
IF(DEF>=200.0)THEN
  WRITE(*,*)QTC cannot be stretched any further!
  READ(*,*)
ELSE
  WRITE(*,120,ADVANCE='NO')
120 FORMAT('Enter extension in z-direction (i.e. what % of original z-dim. is QTC): ')
  READ(*,*)NDEF
  DEF=DEF*NDEF/100.0
  WHILE((NDEF<100.0).OR.(DEF>200.0))DO
    DEF=DEF*100.0/NDEF
    WRITE(*,*)'Invalid! Re-enter value between 100 and',20000.0/DEF,'%:'
    READ(*,*)NDEF
    DEF=DEF*NDEF/100.0
  END WHILE
  DO I=1,TOTALN,1 !Increase z-coordinates of centres of particles by factor of DEF/100, and decrease x- and
    QTC(I,2)=QTC(I,2)*SQRT(100.0/DEF) !y-coordinates of centres of particles by samefactor
    QTC(I,1)=QTC(I,1)*SQRT(100.0/DEF)
    QTC(I,3)=QTC(I,3)*DEF/100.0
  END DO
END IF
DO I=1,30,1
  WRITE(*,*)
END DO
CASE(6)
NOP=0
DO K=1,NZ,1
  DO J=1,NY,1
    DO I=1,NX,1
      IF(QTC((K-1)*NX*NY+(J-1)*NX+I,4)>=SFILL)THEN !Check to see if particular cell has particle in it
        IF(I<NX)THEN
          XDIF=QTC((K-1)*NX*NY+(J-1)*NX+I,1)-QTC((K-1)*NX*NY+(J-1)*NX+I+1,1)
          YDIF=QTC((K-1)*NX*NY+(J-1)*NX+I,2)-QTC((K-1)*NX*NY+(J-1)*NX+I+1,2)
          ZDIF=QTC((K-1)*NX*NY+(J-1)*NX+I,3)-QTC((K-1)*NX*NY+(J-1)*NX+I+1,3)
          DIF=SQRT(XDIF**2+YDIF**2+ZDIF**2)
          IF(NINT(2000.0*DIF)/1000.0<=NINT((1000*(QTC((K-1)*NX*NY+(J-1)*NX+I,4)+QTC((K-1)*NX*NY+(J-1)*&
            &NX+I+1,4)))/1000.0)THEN
            NOP=NOP+1
          END IF
        END IF
      END IF
    END IF
  END IF
  IF(J<NY)THEN
    XDIF=QTC((K-1)*NX*NY+(J-1)*NX+I,1)-QTC((K-1)*NX*NY+J*NX+I,1)
    YDIF=QTC((K-1)*NX*NY+(J-1)*NX+I,2)-QTC((K-1)*NX*NY+J*NX+I,2)

```

```

ZDIF=QTC((K-1)*NX*NY+(J-1)*NX+I,3)-QTC((K-1)*NX*NY+J*NX+I,3)
DIF=SQRT(XDIF**2+YDIF**2+ZDIF**2)
IF(NINT(2000.0*DIF)/1000.0<=NINT((1000*(QTC((K-1)*NX*NY+(J-1)*NX+I,4)+QTC((K-1)*NX*NY+J*&
&NX+I,4)))/1000.0)THEN
  NOP=NOP+1
END IF
IF(I>1)THEN
  XDIF=QTC((K-1)*NX*NY+(J-1)*NX+I,1)-QTC((K-1)*NX*NY+J*NX+I-1,1)
  YDIF=QTC((K-1)*NX*NY+(J-1)*NX+I,2)-QTC((K-1)*NX*NY+J*NX+I-1,2)
  ZDIF=QTC((K-1)*NX*NY+(J-1)*NX+I,3)-QTC((K-1)*NX*NY+J*NX+I-1,3)
  DIF=SQRT(XDIF**2+YDIF**2+ZDIF**2)
  IF(NINT(2000.0*DIF)/1000.0<=NINT((1000*(QTC((K-1)*NX*NY+(J-1)*NX+I,4)+QTC((K-1)*NX*NY+J*&
&NX+I-1,4)))/1000.0)THEN
    NOP=NOP+1
  END IF
END IF
IF(I<NX)THEN
  XDIF=QTC((K-1)*NX*NY+(J-1)*NX+I,1)-QTC((K-1)*NX*NY+J*NX+I+1,1)
  YDIF=QTC((K-1)*NX*NY+(J-1)*NX+I,2)-QTC((K-1)*NX*NY+J*NX+I+1,2)
  ZDIF=QTC((K-1)*NX*NY+(J-1)*NX+I,3)-QTC((K-1)*NX*NY+J*NX+I+1,3)
  DIF=SQRT(XDIF**2+YDIF**2+ZDIF**2)
  IF(NINT(2000.0*DIF)/1000.0<=NINT((1000*(QTC((K-1)*NX*NY+(J-1)*NX+I,4)+QTC((K-1)*NX*NY+J*&
&NX+I+1,4)))/1000.0)THEN
    NOP=NOP+1
  END IF
END IF
END IF
IF(K<NZ)THEN
  XDIF=QTC((K-1)*NX*NY+(J-1)*NX+I,1)-QTC(K*NX*NY+(J-1)*NX+I,1)
  YDIF=QTC((K-1)*NX*NY+(J-1)*NX+I,2)-QTC(K*NX*NY+(J-1)*NX+I,2)
  ZDIF=QTC((K-1)*NX*NY+(J-1)*NX+I,3)-QTC(K*NX*NY+(J-1)*NX+I,3)
  DIF=SQRT(XDIF**2+YDIF**2+ZDIF**2)
  IF(NINT(2000.0*DIF)/1000.0<=NINT((1000*(QTC((K-1)*NX*NY+(J-1)*NX+I,4)+QTC(K*NX*NY+(J-1)*&
&NX+I,4)))/1000.0)THEN
    NOP=NOP+1
  END IF
END IF
IF(I>1)THEN
  XDIF=QTC((K-1)*NX*NY+(J-1)*NX+I,1)-QTC(K*NX*NY+(J-1)*NX+I-1,1)
  YDIF=QTC((K-1)*NX*NY+(J-1)*NX+I,2)-QTC(K*NX*NY+(J-1)*NX+I-1,2)
  ZDIF=QTC((K-1)*NX*NY+(J-1)*NX+I,3)-QTC(K*NX*NY+(J-1)*NX+I-1,3)
  DIF=SQRT(XDIF**2+YDIF**2+ZDIF**2)
  IF(NINT(2000.0*DIF)/1000.0<=NINT((1000*(QTC((K-1)*NX*NY+(J-1)*NX+I,4)+QTC(K*NX*NY+(J-1)*&
&NX+I-1,4)))/1000.0)THEN
    NOP=NOP+1
  END IF
END IF
IF(I<NX)THEN
  XDIF=QTC((K-1)*NX*NY+(J-1)*NX+I,1)-QTC(K*NX*NY+(J-1)*NX+I+1,1)
  YDIF=QTC((K-1)*NX*NY+(J-1)*NX+I,2)-QTC(K*NX*NY+(J-1)*NX+I+1,2)
  ZDIF=QTC((K-1)*NX*NY+(J-1)*NX+I,3)-QTC(K*NX*NY+(J-1)*NX+I+1,3)
  DIF=SQRT(XDIF**2+YDIF**2+ZDIF**2)
  IF(NINT(2000.0*DIF)/1000.0<=NINT((1000*(QTC((K-1)*NX*NY+(J-1)*NX+I,4)+QTC(K*NX*NY+(J-1)*&
&NX+I+1,4)))/1000.0)THEN
    NOP=NOP+1
  END IF
END IF
END IF
IF(J<NY)THEN
  XDIF=QTC((K-1)*NX*NY+(J-1)*NX+I,1)-QTC(K*NX*NY+J*NX+I,1)
  YDIF=QTC((K-1)*NX*NY+(J-1)*NX+I,2)-QTC(K*NX*NY+J*NX+I,2)
  ZDIF=QTC((K-1)*NX*NY+(J-1)*NX+I,3)-QTC(K*NX*NY+J*NX+I,3)
  DIF=SQRT(XDIF**2+YDIF**2+ZDIF**2)
  IF(NINT(2000.0*DIF)/1000.0<=NINT((1000*(QTC((K-1)*NX*NY+(J-1)*NX+I,4)+QTC(K*NX*NY+J*&
&NX+I,4)))/1000.0)THEN
    NOP=NOP+1
  END IF
END IF
IF(I>1)THEN
  XDIF=QTC((K-1)*NX*NY+(J-1)*NX+I,1)-QTC(K*NX*NY+J*NX+I-1,1)
  YDIF=QTC((K-1)*NX*NY+(J-1)*NX+I,2)-QTC(K*NX*NY+J*NX+I-1,2)
  ZDIF=QTC((K-1)*NX*NY+(J-1)*NX+I,3)-QTC(K*NX*NY+J*NX+I-1,3)
  DIF=SQRT(XDIF**2+YDIF**2+ZDIF**2)
  IF(NINT(2000.0*DIF)/1000.0<=NINT((1000*(QTC((K-1)*NX*NY+(J-1)*NX+I,4)+QTC(K*NX*NY+J*&
&NX+I-1,4)))/1000.0)THEN
    NOP=NOP+1
  END IF
END IF
IF(I<NX)THEN
  XDIF=QTC((K-1)*NX*NY+(J-1)*NX+I,1)-QTC(K*NX*NY+J*NX+I+1,1)
  YDIF=QTC((K-1)*NX*NY+(J-1)*NX+I,2)-QTC(K*NX*NY+J*NX+I+1,2)
  ZDIF=QTC((K-1)*NX*NY+(J-1)*NX+I,3)-QTC(K*NX*NY+J*NX+I+1,3)
  DIF=SQRT(XDIF**2+YDIF**2+ZDIF**2)
  IF(NINT(2000.0*DIF)/1000.0<=NINT((1000*(QTC((K-1)*NX*NY+(J-1)*NX+I,4)+QTC(K*NX*NY+J*&
&NX+I+1,4)))/1000.0)THEN
    NOP=NOP+1
  END IF
END IF
END IF
END IF

```

```

        END IF
    END IF
END DO
END DO
END DO
WRITE(*,*)'The number of overlapping particles is:',NOP
READ(*,*)
DO I=1,30,1
    WRITE(*,*)
END DO
CASE(7)
IF(NINT(2*(LFILL-SFILL))==0)THEN
    WRITE(*,*)'There is no particle size distribution!'
ELSE
    ALLOCATE(PCOUNT(NINT(2*(LFILL-SFILL)))) !Set vector with number of rows to allow a count to be stored of the number
    PCOUNT=0 !of particles of a particular size, within the range, with 0.5 micron
    PSINC=(LFILL-SFILL)/REAL(NINT(2*(LFILL-SFILL))) !increments
    DO I=1,TOTALN,1
        IF(QTC(I,4)>=SFILL)THEN !Check to see if particular cell has particle in it
            DO J=1,NINT(2*(LFILL-SFILL)),1
                K=0
                IF(QTC(I,4)<(SFILL+J*PSINC)).AND.(QTC(I,4)>=(SFILL+(J-1)*PSINC))THEN !Check to see if particular sphere
                    PCOUNT(J)=PCOUNT(J)+1 !lies within particular range
                    GOTO 7
                END IF
                IF(J==NINT(2*(LFILL-SFILL)).AND.(QTC(I,4)>=LFILL))THEN !If particle size is exactly the maximum allowed
                    PCOUNT(J)=PCOUNT(J)+1 !it won't be counted in above check, hence
                END IF !the requirement for this further check
            END DO
        END IF
    END DO
7 END DO
    WRITE(*,*)'The number of particles of size:'
    WRITE(*,*)
    DO J=1,NINT(2*(LFILL-SFILL)),1
        WRITE(*,*)SFILL+(J-1)*PSINC,'to',SFILL+J*PSINC,'microns is',PCOUNT(J)
    END DO
END IF
READ(*,*)
DO I=1,30,1
    WRITE(*,*)
END DO
CASE(8)
MAXDIF=0.0
MINDIF=1000.0
TOTDIF=0.0
NOP=0
DO K=1,NZ,1
    DO J=1,NY,1
        DO I=1,NX,1
            IF(QTC((K-1)*NX*NY+(J-1)*NX+I,4)>=SFILL)THEN !Check to see if particular cell has particle in it
                IF(I<NX)THEN
                    IF(QTC((K-1)*NX*NY+(J-1)*NX+I+1,4)>=SFILL)THEN !Check to see if particular cell has particle in it
                        XDIF=QTC((K-1)*NX*NY+(J-1)*NX+I,1)-QTC((K-1)*NX*NY+(J-1)*NX+I+1,1)
                        YDIF=QTC((K-1)*NX*NY+(J-1)*NX+I,2)-QTC((K-1)*NX*NY+(J-1)*NX+I+1,2)
                        ZDIF=QTC((K-1)*NX*NY+(J-1)*NX+I,3)-QTC((K-1)*NX*NY+(J-1)*NX+I+1,3)
                        DIF=SQRT(XDIF**2+YDIF**2+ZDIF**2)
                        TOTDIF=TOTDIF+DIF-(QTC((K-1)*NX*NY+(J-1)*NX+I,4)+QTC((K-1)*NX*NY+(J-1)*NX+I+1,4))/2.0
                        NOP=NOP+1 !Here, NOP is the number of particle distances considered in TOTDIF
                        IF(DIF-(QTC((K-1)*NX*NY+(J-1)*NX+I,4)+QTC((K-1)*NX*NY+(J-1)*NX+I+1,4))/2.0>MAXDIF)THEN
                            MAXDIF=DIF-(QTC((K-1)*NX*NY+(J-1)*NX+I,4)+QTC((K-1)*NX*NY+(J-1)*NX+I+1,4))/2.0
                        END IF
                        IF(DIF-(QTC((K-1)*NX*NY+(J-1)*NX+I,4)+QTC((K-1)*NX*NY+(J-1)*NX+I+1,4))/2.0<MINDIF)THEN
                            MINDIF=DIF-(QTC((K-1)*NX*NY+(J-1)*NX+I,4)+QTC((K-1)*NX*NY+(J-1)*NX+I+1,4))/2.0
                        END IF
                    END IF
                END IF
            END IF
            IF(J<NY)THEN
                IF(QTC((K-1)*NX*NY+J*NX+I,4)>=SFILL)THEN
                    XDIF=QTC((K-1)*NX*NY+(J-1)*NX+I,1)-QTC((K-1)*NX*NY+J*NX+I,1)
                    YDIF=QTC((K-1)*NX*NY+(J-1)*NX+I,2)-QTC((K-1)*NX*NY+J*NX+I,2)
                    ZDIF=QTC((K-1)*NX*NY+(J-1)*NX+I,3)-QTC((K-1)*NX*NY+J*NX+I,3)
                    DIF=SQRT(XDIF**2+YDIF**2+ZDIF**2)
                    TOTDIF=TOTDIF+DIF-(QTC((K-1)*NX*NY+(J-1)*NX+I,4)+QTC((K-1)*NX*NY+J*NX+I,4))/2.0
                    NOP=NOP+1
                    IF(DIF-(QTC((K-1)*NX*NY+(J-1)*NX+I,4)+QTC((K-1)*NX*NY+J*NX+I,4))/2.0>MAXDIF)THEN
                        MAXDIF=DIF-(QTC((K-1)*NX*NY+(J-1)*NX+I,4)+QTC((K-1)*NX*NY+J*NX+I,4))/2.0
                    END IF
                    IF(DIF-(QTC((K-1)*NX*NY+(J-1)*NX+I,4)+QTC((K-1)*NX*NY+J*NX+I,4))/2.0<MINDIF)THEN
                        MINDIF=DIF-(QTC((K-1)*NX*NY+(J-1)*NX+I,4)+QTC((K-1)*NX*NY+J*NX+I,4))/2.0
                    END IF
                END IF
            END IF
            IF(I>1)THEN
                IF(QTC((K-1)*NX*NY+J*NX+I-1,4)>=SFILL)THEN
                    XDIF=QTC((K-1)*NX*NY+(J-1)*NX+I-1,1)-QTC((K-1)*NX*NY+J*NX+I-1,1)
                    YDIF=QTC((K-1)*NX*NY+(J-1)*NX+I-1,2)-QTC((K-1)*NX*NY+J*NX+I-1,2)
                    ZDIF=QTC((K-1)*NX*NY+(J-1)*NX+I-1,3)-QTC((K-1)*NX*NY+J*NX+I-1,3)
                END IF
            END IF
        END DO
    END DO
END DO

```

```

DIF=SQRT(XDIF**2+YDIF**2+ZDIF**2)
TOTDIF=TOTDIF+DIF-(QTC((K-1)*NX*NY+(J-1)*NX+I,4)+QTC((K-1)*NX*NY+J*NX+I-1,4))/2.0
NOP=NOP+1
IF(DIF-(QTC((K-1)*NX*NY+(J-1)*NX+I,4)+QTC((K-1)*NX*NY+J*NX+I-1,4))/2.0>MAXDIF)THEN
  MAXDIF=DIF-(QTC((K-1)*NX*NY+(J-1)*NX+I,4)+QTC((K-1)*NX*NY+J*NX+I-1,4))/2.0
END IF
IF(DIF-(QTC((K-1)*NX*NY+(J-1)*NX+I,4)+QTC((K-1)*NX*NY+J*NX+I-1,4))/2.0<MINDIF)THEN
  MINDIF=DIF-(QTC((K-1)*NX*NY+(J-1)*NX+I,4)+QTC((K-1)*NX*NY+J*NX+I-1,4))/2.0
END IF
END IF
END IF
END IF
IF(I<NX)THEN
  IF(QTC((K-1)*NX*NY+J*NX+I+1,4)>=SFILL)THEN
    XDIF=QTC((K-1)*NX*NY+(J-1)*NX+I,1)-QTC((K-1)*NX*NY+J*NX+I+1,1)
    YDIF=QTC((K-1)*NX*NY+(J-1)*NX+I,2)-QTC((K-1)*NX*NY+J*NX+I+1,2)
    ZDIF=QTC((K-1)*NX*NY+(J-1)*NX+I,3)-QTC((K-1)*NX*NY+J*NX+I+1,3)
    DIF=SQRT(XDIF**2+YDIF**2+ZDIF**2)
    TOTDIF=TOTDIF+DIF-(QTC((K-1)*NX*NY+(J-1)*NX+I,4)+QTC((K-1)*NX*NY+J*NX+I+1,4))/2.0
    NOP=NOP+1
    IF(DIF-(QTC((K-1)*NX*NY+(J-1)*NX+I,4)+QTC((K-1)*NX*NY+J*NX+I+1,4))/2.0>MAXDIF)THEN
      MAXDIF=DIF-(QTC((K-1)*NX*NY+(J-1)*NX+I,4)+QTC((K-1)*NX*NY+J*NX+I+1,4))/2.0
    END IF
    IF(DIF-(QTC((K-1)*NX*NY+(J-1)*NX+I,4)+QTC((K-1)*NX*NY+J*NX+I+1,4))/2.0<MINDIF)THEN
      MINDIF=DIF-(QTC((K-1)*NX*NY+(J-1)*NX+I,4)+QTC((K-1)*NX*NY+J*NX+I+1,4))/2.0
    END IF
  END IF
END IF
END IF
IF(K<NZ)THEN
  IF(QTC(K*NX*NY+(J-1)*NX+I,4)>=SFILL)THEN
    XDIF=QTC((K-1)*NX*NY+(J-1)*NX+I,1)-QTC(K*NX*NY+(J-1)*NX+I,1)
    YDIF=QTC((K-1)*NX*NY+(J-1)*NX+I,2)-QTC(K*NX*NY+(J-1)*NX+I,2)
    ZDIF=QTC((K-1)*NX*NY+(J-1)*NX+I,3)-QTC(K*NX*NY+(J-1)*NX+I,3)
    DIF=SQRT(XDIF**2+YDIF**2+ZDIF**2)
    TOTDIF=TOTDIF+DIF-(QTC((K-1)*NX*NY+(J-1)*NX+I,4)+QTC(K*NX*NY+(J-1)*NX+I,4))/2.0
    NOP=NOP+1
    IF(DIF-(QTC((K-1)*NX*NY+(J-1)*NX+I,4)+QTC(K*NX*NY+(J-1)*NX+I,4))/2.0>MAXDIF)THEN
      MAXDIF=DIF-(QTC((K-1)*NX*NY+(J-1)*NX+I,4)+QTC(K*NX*NY+(J-1)*NX+I,4))/2.0
    END IF
    IF(DIF-(QTC((K-1)*NX*NY+(J-1)*NX+I,4)+QTC(K*NX*NY+(J-1)*NX+I,4))/2.0<MINDIF)THEN
      MINDIF=DIF-(QTC((K-1)*NX*NY+(J-1)*NX+I,4)+QTC(K*NX*NY+(J-1)*NX+I,4))/2.0
    END IF
  END IF
END IF
IF(I>1)THEN
  IF(QTC(K*NX*NY+(J-1)*NX+I-1,4)>=SFILL)THEN
    XDIF=QTC((K-1)*NX*NY+(J-1)*NX+I,1)-QTC(K*NX*NY+(J-1)*NX+I-1,1)
    YDIF=QTC((K-1)*NX*NY+(J-1)*NX+I,2)-QTC(K*NX*NY+(J-1)*NX+I-1,2)
    ZDIF=QTC((K-1)*NX*NY+(J-1)*NX+I,3)-QTC(K*NX*NY+(J-1)*NX+I-1,3)
    DIF=SQRT(XDIF**2+YDIF**2+ZDIF**2)
    TOTDIF=TOTDIF+DIF-(QTC((K-1)*NX*NY+(J-1)*NX+I,4)+QTC(K*NX*NY+(J-1)*NX+I-1,4))/2.0
    NOP=NOP+1
    IF(DIF-(QTC((K-1)*NX*NY+(J-1)*NX+I,4)+QTC(K*NX*NY+(J-1)*NX+I-1,4))/2.0>MAXDIF)THEN
      MAXDIF=DIF-(QTC((K-1)*NX*NY+(J-1)*NX+I,4)+QTC(K*NX*NY+(J-1)*NX+I-1,4))/2.0
    END IF
    IF(DIF-(QTC((K-1)*NX*NY+(J-1)*NX+I,4)+QTC(K*NX*NY+(J-1)*NX+I-1,4))/2.0<MINDIF)THEN
      MINDIF=DIF-(QTC((K-1)*NX*NY+(J-1)*NX+I,4)+QTC(K*NX*NY+(J-1)*NX+I-1,4))/2.0
    END IF
  END IF
END IF
END IF
IF(I<NX)THEN
  IF(QTC(K*NX*NY+(J-1)*NX+I+1,4)>=SFILL)THEN
    XDIF=QTC((K-1)*NX*NY+(J-1)*NX+I,1)-QTC(K*NX*NY+(J-1)*NX+I+1,1)
    YDIF=QTC((K-1)*NX*NY+(J-1)*NX+I,2)-QTC(K*NX*NY+(J-1)*NX+I+1,2)
    ZDIF=QTC((K-1)*NX*NY+(J-1)*NX+I,3)-QTC(K*NX*NY+(J-1)*NX+I+1,3)
    DIF=SQRT(XDIF**2+YDIF**2+ZDIF**2)
    TOTDIF=TOTDIF+DIF-(QTC((K-1)*NX*NY+(J-1)*NX+I,4)+QTC(K*NX*NY+(J-1)*NX+I+1,4))/2.0
    NOP=NOP+1
    IF(DIF-(QTC((K-1)*NX*NY+(J-1)*NX+I,4)+QTC(K*NX*NY+(J-1)*NX+I+1,4))/2.0>MAXDIF)THEN
      MAXDIF=DIF-(QTC((K-1)*NX*NY+(J-1)*NX+I,4)+QTC(K*NX*NY+(J-1)*NX+I+1,4))/2.0
    END IF
    IF(DIF-(QTC((K-1)*NX*NY+(J-1)*NX+I,4)+QTC(K*NX*NY+(J-1)*NX+I+1,4))/2.0<MINDIF)THEN
      MINDIF=DIF-(QTC((K-1)*NX*NY+(J-1)*NX+I,4)+QTC(K*NX*NY+(J-1)*NX+I+1,4))/2.0
    END IF
  END IF
END IF
END IF
IF(J<NY)THEN
  IF(QTC(K*NX*NY+J*NX+I,4)>=SFILL)THEN
    XDIF=QTC((K-1)*NX*NY+(J-1)*NX+I,1)-QTC(K*NX*NY+J*NX+I,1)
    YDIF=QTC((K-1)*NX*NY+(J-1)*NX+I,2)-QTC(K*NX*NY+J*NX+I,2)
    ZDIF=QTC((K-1)*NX*NY+(J-1)*NX+I,3)-QTC(K*NX*NY+J*NX+I,3)
    DIF=SQRT(XDIF**2+YDIF**2+ZDIF**2)
    TOTDIF=TOTDIF+DIF-(QTC((K-1)*NX*NY+(J-1)*NX+I,4)+QTC(K*NX*NY+J*NX+I,4))/2.0
    NOP=NOP+1
    IF(DIF-(QTC((K-1)*NX*NY+(J-1)*NX+I,4)+QTC(K*NX*NY+J*NX+I,4))/2.0>MAXDIF)THEN
      MAXDIF=DIF-(QTC((K-1)*NX*NY+(J-1)*NX+I,4)+QTC(K*NX*NY+J*NX+I,4))/2.0
    END IF
  END IF
END IF

```



```

&NX+I-1,4))))/1000.0)THEN
  IF((QTC((K-1)*NX*NY+(J-1)*NX+I,6)<=QTC(K*NX*NY+(J-2)*NX+I-1,6)).AND.&
    &(QTC((K-1)*NX*NY+(J-1)*NX+I,6)<0.0))THEN
    IF(K<NZ-1)THEN
      QTC(K*NX*NY+(J-2)*NX+I-1,6)=QTC(K*NX*NY+(J-2)*NX+I-1,6)+QTC((K-1)*NX*NY+(J-1)*NX+I,6)
    ELSE
      QTC((J-2)*NX+I-1,6)=QTC((J-2)*NX+I-1,6)+QTC((K-1)*NX*NY+(J-1)*NX+I,6)
      NOE=NOE-QTC((K-1)*NX*NY+(J-1)*NX+I,6)
    END IF
    QTC((K-1)*NX*NY+(J-1)*NX+I,6)=0.0
    GOTO 3
  END IF
END IF
END IF
END IF
IF(I<NX)THEN
  XDIF=QTC(K*NX*NY+(J-2)*NX+I+1,1)-QTC((K-1)*NX*NY+(J-1)*NX+I,1)
  YDIF=QTC(K*NX*NY+(J-2)*NX+I+1,2)-QTC((K-1)*NX*NY+(J-1)*NX+I,2)
  ZDIF=QTC(K*NX*NY+(J-2)*NX+I+1,3)-QTC((K-1)*NX*NY+(J-1)*NX+I,3)
  DIF=SQRT(XDIF**2+YDIF**2+ZDIF**2)
  IF(NINT(2000.0*DIF)/1000.0<=NINT((1000*(QTC((K-1)*NX*NY+(J-1)*NX+I,4)+QTC(K*NX*NY+(J-2)*&
    &NX+I+1,4))))/1000.0)THEN
    IF((QTC((K-1)*NX*NY+(J-1)*NX+I,6)<=QTC(K*NX*NY+(J-2)*NX+I+1,6)).AND.&
      &(QTC((K-1)*NX*NY+(J-1)*NX+I,6)<0.0))THEN
      IF(K<NZ-1)THEN
        QTC(K*NX*NY+(J-2)*NX+I+1,6)=QTC(K*NX*NY+(J-2)*NX+I+1,6)+QTC((K-1)*NX*NY+(J-1)*NX+I,6)
      ELSE
        QTC((J-2)*NX+I+1,6)=QTC((J-2)*NX+I+1,6)+QTC((K-1)*NX*NY+(J-1)*NX+I,6)
        NOE=NOE-QTC((K-1)*NX*NY+(J-1)*NX+I,6)
      END IF
      QTC((K-1)*NX*NY+(J-1)*NX+I,6)=0.0
      GOTO 3
    END IF
  END IF
END IF
END IF
IF(J<NY)THEN
  XDIF=QTC(K*NX*NY+J*NX+I,1)-QTC((K-1)*NX*NY+(J-1)*NX+I,1)
  YDIF=QTC(K*NX*NY+J*NX+I,2)-QTC((K-1)*NX*NY+(J-1)*NX+I,2)
  ZDIF=QTC(K*NX*NY+J*NX+I,3)-QTC((K-1)*NX*NY+(J-1)*NX+I,3)
  DIF=SQRT(XDIF**2+YDIF**2+ZDIF**2)
  IF(NINT(2000.0*DIF)/1000.0<=NINT((1000*(QTC((K-1)*NX*NY+(J-1)*NX+I,4)+QTC(K*NX*NY+J*&
    &NX+I,4))))/1000.0)THEN
    IF((QTC((K-1)*NX*NY+(J-1)*NX+I,6)<=QTC(K*NX*NY+J*NX+I,6)).AND.&
      &(QTC((K-1)*NX*NY+(J-1)*NX+I,6)<0.0))THEN
      IF(K<NZ-1)THEN
        QTC(K*NX*NY+J*NX+I,6)=QTC(K*NX*NY+J*NX+I,6)+QTC((K-1)*NX*NY+(J-1)*NX+I,6)
      ELSE
        QTC(J*NX+I,6)=QTC(J*NX+I,6)+QTC((K-1)*NX*NY+(J-1)*NX+I,6)
        NOE=NOE-QTC((K-1)*NX*NY+(J-1)*NX+I,6)
      END IF
      QTC((K-1)*NX*NY+(J-1)*NX+I,6)=0.0
      GOTO 3
    END IF
  END IF
END IF
IF(I>1)THEN
  XDIF=QTC(K*NX*NY+J*NX+I-1,1)-QTC((K-1)*NX*NY+(J-1)*NX+I,1)
  YDIF=QTC(K*NX*NY+J*NX+I-1,2)-QTC((K-1)*NX*NY+(J-1)*NX+I,2)
  ZDIF=QTC(K*NX*NY+J*NX+I-1,3)-QTC((K-1)*NX*NY+(J-1)*NX+I,3)
  DIF=SQRT(XDIF**2+YDIF**2+ZDIF**2)
  IF(NINT(2000.0*DIF)/1000.0<=NINT((1000*(QTC((K-1)*NX*NY+(J-1)*NX+I,4)+QTC(K*NX*NY+J*&
    &NX+I-1,4))))/1000.0)THEN
    IF((QTC((K-1)*NX*NY+(J-1)*NX+I,6)<=QTC(K*NX*NY+J*NX+I-1,6)).AND.&
      &(QTC((K-1)*NX*NY+(J-1)*NX+I,6)<0.0))THEN
      IF(K<NZ-1)THEN
        QTC(K*NX*NY+J*NX+I-1,6)=QTC(K*NX*NY+J*NX+I-1,6)+QTC((K-1)*NX*NY+(J-1)*NX+I,6)
      ELSE
        QTC(J*NX+I-1,6)=QTC(J*NX+I-1,6)+QTC((K-1)*NX*NY+(J-1)*NX+I,6)
        NOE=NOE-QTC((K-1)*NX*NY+(J-1)*NX+I,6)
      END IF
      QTC((K-1)*NX*NY+(J-1)*NX+I,6)=0.0
      GOTO 3
    END IF
  END IF
END IF
END IF
IF(I<NX)THEN
  XDIF=QTC(K*NX*NY+J*NX+I+1,1)-QTC((K-1)*NX*NY+(J-1)*NX+I,1)
  YDIF=QTC(K*NX*NY+J*NX+I+1,2)-QTC((K-1)*NX*NY+(J-1)*NX+I,2)
  ZDIF=QTC(K*NX*NY+J*NX+I+1,3)-QTC((K-1)*NX*NY+(J-1)*NX+I,3)
  DIF=SQRT(XDIF**2+YDIF**2+ZDIF**2)
  IF(NINT(2000.0*DIF)/1000.0<=NINT((1000*(QTC((K-1)*NX*NY+(J-1)*NX+I,4)+QTC(K*NX*NY+J*&
    &NX+I+1,4))))/1000.0)THEN
    IF((QTC((K-1)*NX*NY+(J-1)*NX+I,6)<=QTC(K*NX*NY+J*NX+I+1,6)).AND.&
      &(QTC((K-1)*NX*NY+(J-1)*NX+I,6)<0.0))THEN
      IF(K<NZ-1)THEN
        QTC(K*NX*NY+J*NX+I+1,6)=QTC(K*NX*NY+J*NX+I+1,6)+QTC((K-1)*NX*NY+(J-1)*NX+I,6)

```

```

ELSE
  QTC(J*NX+I+1,6)=QTC(J*NX+I+1,6)+QTC((K-1)*NX*NY+(J-1)*NX+I,6)
  NOE=NOE-QTC((K-1)*NX*NY+(J-1)*NX+I,6)
END IF
QTC((K-1)*NX*NY+(J-1)*NX+I,6)=0.0
GOTO 3
END IF
END IF
END IF
END IF
IF((QUANTUM=='Y').OR.(QUANTUM=='y'))THEN !Quantum tunnelling to next z-plane is allowed, if percolation
DO E=1,9,1 !has not been successful
IF(E==1)THEN
  SI=I
  SJ=J
  SK=K+1
END IF
IF(E==2)THEN
  IF(I>1)THEN
    SI=I-1
    SJ=J
    SK=K+1
  ELSE
    GOTO 4
  END IF
END IF
IF(E==3)THEN
  IF(I<NX)THEN
    SI=I+1
    SJ=J
    SK=K+1
  ELSE
    GOTO 4
  END IF
END IF
IF(E==4)THEN
  IF(J>1)THEN
    SI=I
    SJ=J-1
    SK=K+1
  ELSE
    GOTO 4
  END IF
END IF
IF(E==5)THEN
  IF((J>1).AND.(I>1))THEN
    SI=I-1
    SJ=J-1
    SK=K+1
  ELSE
    GOTO 4
  END IF
END IF
IF(E==6)THEN
  IF((J>1).AND.(I<NX))THEN
    SI=I+1
    SJ=J-1
    SK=K+1
  ELSE
    GOTO 4
  END IF
END IF
IF(E==7)THEN
  IF(J<NY)THEN
    SI=I
    SJ=J+1
    SK=K+1
  ELSE
    GOTO 4
  END IF
END IF
IF(E==8)THEN
  IF((J<NY).AND.(I>1))THEN
    SI=I-1
    SJ=J+1
    SK=K+1
  ELSE
    GOTO 4
  END IF
END IF
IF(E==9)THEN
  IF((J<NY).AND.(I<NX))THEN
    SI=I+1
    SJ=J+1
    SK=K+1
  ELSE

```

```

      GOTO 4
    END IF
  END IF
  XDIF=QTC((SK-1)*NX*NY+(SJ-1)*NX+SI,1)-QTC((K-1)*NX*NY+(J-1)*NX+I,1)
  YDIF=QTC((SK-1)*NX*NY+(SJ-1)*NX+SI,2)-QTC((K-1)*NX*NY+(J-1)*NX+I,2)
  ZDIF=QTC((SK-1)*NX*NY+(SJ-1)*NX+SI,3)-QTC((K-1)*NX*NY+(J-1)*NX+I,3)
  DIF=SQRT(XDIF**2+YDIF**2+ZDIF**2)
  IF(NINT(2000.0*DIF)/1000.0<=NINT((1000.0*(QTC((K-1)*NX*NY+(J-1)*NX+I,4)+QTC((SK-1)*NX*NY+(SJ-1)*NX+SI,4)))/1000.0)THEN
    GOTO 4 !No tunnelling if particles overlap
  END IF
  MIDPOINTDIST=(DIF-(QTC((SK-1)*NX*NY+(SJ-1)*NX+SI,4)+QTC((K-1)*NX*NY+(J-1)*NX+I,4))/2.0)/2.0
  XMID=QTC((K-1)*NX*NY+(J-1)*NX+I,1)+(QTC((K-1)*NX*NY+(J-1)*NX+I,4)/2.0+MIDPOINTDIST)*XDIF/DIF
  YMID=QTC((K-1)*NX*NY+(J-1)*NX+I,2)+(QTC((K-1)*NX*NY+(J-1)*NX+I,4)/2.0+MIDPOINTDIST)*YDIF/DIF
  ZMID=QTC((K-1)*NX*NY+(J-1)*NX+I,3)+(QTC((K-1)*NX*NY+(J-1)*NX+I,4)/2.0+MIDPOINTDIST)*ZDIF/DIF
  TOTALEF=0.0
  TOTALEF(3)=-EF !Set initial electric field vector to be the applied field in the minus z-direction
  DO F=1,2,1
    IF(F==1)THEN
      SI=I
      SJ=J
      SK=K
    ELSE
      IF(E==1)THEN
        SI=I
        SJ=J
        SK=K+1
      END IF
      IF(E==2)THEN
        SI=I-1
        SJ=J
        SK=K+1
      END IF
      IF(E==3)THEN
        SI=I+1
        SJ=J
        SK=K+1
      END IF
      IF(E==4)THEN
        SI=I
        SJ=J-1
        SK=K+1
      END IF
      IF(E==5)THEN
        SI=I-1
        SJ=J-1
        SK=K+1
      END IF
      IF(E==6)THEN
        SI=I+1
        SJ=J-1
        SK=K+1
      END IF
      IF(E==7)THEN
        SI=I
        SJ=J+1
        SK=K+1
      END IF
      IF(E==8)THEN
        SI=I-1
        SJ=J+1
        SK=K+1
      END IF
      IF(E==9)THEN
        SI=I+1
        SJ=J+1
        SK=K+1
      END IF
    END IF
    XDIFMID=XMID-QTC((SK-1)*NX*NY+(SJ-1)*NX+SI,1)
    YDIFMID=YMID-QTC((SK-1)*NX*NY+(SJ-1)*NX+SI,2)
    ZDIFMID=ZMID-QTC((SK-1)*NX*NY+(SJ-1)*NX+SI,3)
    DIFMID=SQRT(XDIFMID**2+YDIFMID**2+ZDIFMID**2)
    IF((ZDIFMID>0.0).OR.(ZDIFMID<0.0))THEN
      THETA=ATAN(SQRT(XDIFMID**2+YDIFMID**2)/ZDIFMID)*180/3.141592654
      IF(THETA<0.0)THEN
        THETA=-THETA
      END IF
    ELSE
      THETA=90.0
    END IF
    IF((XMID-QTC((SK-1)*NX*NY+(SJ-1)*NX+SI,1)>0.0).OR.(XMID-QTC((SK-1)*NX*NY+(SJ-1)*NX+SI,1)<0.0))THEN
      PHI=ATAN((YMID-QTC((SK-1)*NX*NY+(SJ-1)*NX+SI,2))/(XMID-QTC((SK-1)*NX*NY+(SJ-1)*NX+SI,1)))*180/3.141592654
    ELSE

```

```

    PHI=90.0
END IF
IF(XDIFMID<0.0)THEN
    PHI=PHI+180.0
END IF
ALPHA=ACOS(QTC((SK-1)*NX*NY+(SJ-1)*NX+SI,4)/(2.0*DIFMID))*180.0/3.141592654
DO C=1,5,1 !Integrate charge over the polar angle across the surface. Midpoint only exposed
    CHARGE=0.0 !to charge from THETA +/- ALPHA. This total angle is split up into 5 patches
    IF(THETA-ALPHA+2.0*(C-1)*ALPHA/5.0<0.0)THEN
        IF(THETA-ALPHA+2.0*C*ALPHA/5.0<0.0)THEN
            CHARGE=8.85E-12*DCP*EF*(QTC((SK-1)*NX*NY+(SJ-1)*NX+SI,4)/2000000.0)**2*&
                &INTEGRAL(-(THETA-ALPHA+2.0D0*(C-1)*ALPHA/5.0),-(THETA-ALPHA+2.0D0*C*&
                    &ALPHA/5.0))
            IF(ZDIFMID>0.0)THEN
                CHARGE=-CHARGE
            END IF
            CHARGE=CHARGE+QTC((SK-1)*NX*NY+(SJ-1)*NX+SI,6)*1.6E-19*ABS(COS(3.141592654*&
                &(THETA-ALPHA+2.0*(C-1)*ALPHA/(5.0*180.0)))-COS(3.141592654*(THETA-ALPHA+2.0*&
                &C*ALPHA/(5.0*180.0))))/(4.0*3.141592654) !The charge caused by net electrons
                !or unit positive charges, forming a uniform charge distribution over the
                !sphere is added to the total charge on the patch
            CHARGE=CHARGE*3.141592654/4.0 !Charge distribution over PHI is constant, hence
                !integral over PHI is simply a matter of mutiplying the charge on a patch
                !by a quarter of the total PHI angle the the midpoint is exposed to (i.e.
                !4 patches are considered over PHI, meaning the total area the midpoint is
                !exposed to is divided up into 20 patches
        END IF
        DO D=1,4,1
            XPAT=(QTC((SK-1)*NX*NY+(SJ-1)*NX+SI,4)/2.0*COS((PHI+90*(-1.25+D/2.0))*&
                &3.141592654/180.0)*SIN(THETA-ALPHA+(2.0*C-1)*ALPHA/5.0))
            YPAT=(QTC((SK-1)*NX*NY+(SJ-1)*NX+SI,4)/2.0*SIN((PHI+90*(-1.25+D/2.0))*&
                &3.141592654/180.0)*SIN(THETA-ALPHA+(2.0*C-1)*ALPHA/5.0))
            IF(ZDIFMID>0.0)THEN
                ZPAT=QTC((SK-1)*NX*NY+(SJ-1)*NX+SI,4)/2.0*COS((THETA-ALPHA+(2.0*C-1)*&
                    &ALPHA/5.0)*3.141592654/180.0)
            ELSE
                ZPAT=-(QTC((SK-1)*NX*NY+(SJ-1)*NX+SI,4)/2.0*COS(THETA-ALPHA+(2.0*C-1)*&
                    &ALPHA/5.0)*3.141592654/180.0)
            END IF
            XEFVECTOR=XDIFMID-XPAT
            YEFVECTOR=YDIFMID-YPAT
            ZEFVECTOR=ZDIFMID-ZPAT
            DIFEF=SQRT(XEFVECTOR**2+YEFVECTOR**2+ZEFVECTOR**2)
            TOTALEF(1)=TOTALEF(1)+1D12*CHARGE*XEFVECTOR/(4.0*3.141592654*8.85D-12*DCP*DIFEF**3)
                !Here, the magnitude of the electric field vector in the x-direction
                !is multiplied by the x-component of the unit vector in the direction
                !of the electric field
            TOTALEF(2)=TOTALEF(2)+1D12*CHARGE*YEFVECTOR/(4.0*3.141592654*8.85D-12*DCP*DIFEF**3)
            TOTALEF(3)=TOTALEF(3)+1D12*CHARGE*ZEFVECTOR/(4.0*3.141592654*8.85D-12*DCP*DIFEF**3)
        END DO
    ELSE
        CHARGE=8.85E-12*DCP*EF*(QTC((SK-1)*NX*NY+(SJ-1)*NX+SI,4)/2000000.0)**2*&
            &(INTEGRAL(-(THETA-ALPHA+2.0D0*(C-1)*ALPHA/5.0D0),0.0D0)+&
            &INTEGRAL(0.0D0,THETA-ALPHA+2.0D0*C*ALPHA/5.0))
        IF(ZDIFMID>0.0)THEN
            CHARGE=-CHARGE
        END IF
        CHARGE=CHARGE+QTC((SK-1)*NX*NY+(SJ-1)*NX+SI,6)*1.6E-19*(COS(3.141592654*&
            &(THETA-ALPHA+2.0*(C-1)*ALPHA/(5.0*180.0)))+COS(3.141592654*(THETA-ALPHA+2.0*&
            &C*ALPHA/(5.0*180.0))))/(4.0*3.141592654)
        CHARGE=CHARGE*3.141592654/4.0
        DO D=1,4,1
            XPAT=QTC((SK-1)*NX*NY+(SJ-1)*NX+SI,4)/2.0*COS((PHI+90*(-1.25+D/2.0))*&
                &3.141592654/180.0)*SIN(THETA-ALPHA+(2.0*C-1)*ALPHA/5.0)
            YPAT=QTC((SK-1)*NX*NY+(SJ-1)*NX+SI,4)/2.0*SIN((PHI+90*(-1.25+D/2.0))*&
                &3.141592654/180.0)*SIN(THETA-ALPHA+(2.0*C-1)*ALPHA/5.0)
            IF(ZDIFMID>0.0)THEN
                ZPAT=QTC((SK-1)*NX*NY+(SJ-1)*NX+SI,4)/2.0*COS((THETA-ALPHA+(2.0*C-1)*&
                    &ALPHA/5.0)*3.141592654/180.0)
            ELSE
                ZPAT=-(QTC((SK-1)*NX*NY+(SJ-1)*NX+SI,4)/2.0*COS(THETA-ALPHA+(2.0*C-1)*&
                    &ALPHA/5.0)*3.141592654/180.0)
            END IF
            XEFVECTOR=XDIFMID-XPAT
            YEFVECTOR=YDIFMID-YPAT
            ZEFVECTOR=ZDIFMID-ZPAT
            DIFEF=SQRT(XEFVECTOR**2+YEFVECTOR**2+ZEFVECTOR**2)
            TOTALEF(1)=TOTALEF(1)+1D12*CHARGE*XEFVECTOR/(4.0*3.141592654*8.85D-12*DCP*DIFEF**3)
            TOTALEF(2)=TOTALEF(2)+1D12*CHARGE*YEFVECTOR/(4.0*3.141592654*8.85D-12*DCP*DIFEF**3)
            TOTALEF(3)=TOTALEF(3)+1D12*CHARGE*ZEFVECTOR/(4.0*3.141592654*8.85D-12*DCP*DIFEF**3)
        END DO
    END IF
ELSE
    IF(THETA-ALPHA+2.0*(C-1)*ALPHA/5.0<90.0)THEN
        IF(THETA-ALPHA+2.0*C*ALPHA/5.0<90.0)THEN
            CHARGE=8.85E-12*DCP*EF*(QTC((SK-1)*NX*NY+(SJ-1)*NX+SI,4)/2000000.0)**2*&
                &INTEGRAL(THETA-ALPHA+2.0D0*(C-1)*ALPHA/5.0,THETA-ALPHA+2.0D0*C*ALPHA/5.0)
        END IF
    END IF

```

```

IF(ZDIFMID>0.0)THEN
  CHARGE=-CHARGE
END IF
CHARGE=CHARGE+QTC((SK-1)*NX*NY+(SJ-1)*NX+SI,6)*1.6E-19*ABS(COS(3.141592654*&
  &(THETA-ALPHA+2.0*(C-1)*ALPHA/(5.0*180.0)))-COS(3.141592654*&
  &(THETA-ALPHA+2.0*C*ALPHA/(5.0*180.0)))/(4.0*3.141592654)
INTPHI=ACOS(COS(ALPHA*3.141592654/180.0)/COS((ALPHA-(2*C-1)*ALPHA/5.0)*&
  &3.141592654/180.0))
CHARGE=CHARGE*2*INTPHI/4.0
DO D=1,4,1
  XPAT=QTC((SK-1)*NX*NY+(SJ-1)*NX+SI,4)/2.0*COS(PHI*3.141592654/180.0+INTPHI*&
    &(-1.25+D/2.0))*SIN(THETA-ALPHA+(2.0*C-1)*ALPHA/5.0)
  YPAT=QTC((SK-1)*NX*NY+(SJ-1)*NX+SI,4)/2.0*SIN(PHI*3.141592654/180.0+INTPHI*&
    &(-1.25+D/2.0))*SIN(THETA-ALPHA+(2.0*C-1)*ALPHA/5.0)
  IF(ZDIFMID>0.0)THEN
    ZPAT=QTC((SK-1)*NX*NY+(SJ-1)*NX+SI,4)/2.0*COS((THETA-ALPHA+(2.0*C-1)*&
      &ALPHA/5.0)*3.141592654/180.0)
  ELSE
    ZPAT=-QTC((SK-1)*NX*NY+(SJ-1)*NX+SI,4)/2.0*COS((THETA-ALPHA+(2.0*C-1)*&
      &ALPHA/5.0)*3.141592654/180.0)
  END IF
  XEFVECTOR=XDIFMID-XPAT
  YEFVECTOR=YDIFMID-YPAT
  ZEFVECTOR=ZDIFMID-ZPAT
  DIFE=SQRT(XEFVECTOR**2+YEFVECTOR**2+ZEFVECTOR**2)
  TOTALEF(1)=TOTALEF(1)+1D12*CHARGE*XEFVECTOR/(4.0*3.141592654*8.85D-12*DCP*&
    &DIFE**3)
  TOTALEF(2)=TOTALEF(2)+1D12*CHARGE*YEFVECTOR/(4.0*3.141592654*8.85D-12*DCP*&
    &DIFE**3)
  TOTALEF(3)=TOTALEF(3)+1D12*CHARGE*ZEFVECTOR/(4.0*3.141592654*8.85D-12*DCP*&
    &DIFE**3)
END DO
ELSE
  CHARGE=8.85E-12*DCP*EF*(QTC((SK-1)*NX*NY+(SJ-1)*NX+SI,4)/2000000.0)**2*&
    &(INTEGRAL(THETA-ALPHA+2.0D0*(C-1)*ALPHA/5.0,89.99999999999999D0)-&
    &INTEGRAL(179.99999999999999D0-(THETA-ALPHA+2.0D0*C*ALPHA/5.0),&
    &89.99999999999999D0))
  IF(ZDIFMID>0.0)THEN
    CHARGE=-CHARGE
  END IF
  CHARGE=CHARGE+QTC((SK-1)*NX*NY+(SJ-1)*NX+SI,6)*1.6E-19*ABS(COS(3.141592654*&
    &(THETA-ALPHA+2.0*(C-1)*ALPHA/(5.0*180.0)))+COS(3.141592654*&
    &(1.0-THETA-ALPHA+2.0*C*ALPHA/(5.0*180.0)))/(4.0*3.141592654)
  INTPHI=ACOS(COS(ALPHA*3.141592654/180.0)/COS((ALPHA-(2*C-1)*ALPHA/5.0)*&
    &3.141592654/180.0))
  CHARGE=CHARGE*2*INTPHI/4.0
  DO D=1,4,1
    XPAT=QTC((SK-1)*NX*NY+(SJ-1)*NX+SI,4)/2.0*COS(PHI*3.141592654/180.0+INTPHI*&
      &(-1.25+D/2.0))*SIN(THETA-ALPHA+(2.0*C-1)*ALPHA/5.0)
    YPAT=QTC((SK-1)*NX*NY+(SJ-1)*NX+SI,4)/2.0*SIN(PHI*3.141592654/180.0+INTPHI*&
      &(-1.25+D/2.0))*SIN(THETA-ALPHA+(2.0*C-1)*ALPHA/5.0)
    IF(ZDIFMID>0.0)THEN
      ZPAT=QTC((SK-1)*NX*NY+(SJ-1)*NX+SI,4)/2.0*COS((THETA-ALPHA+(2.0*C-1)*&
        &ALPHA/5.0)*3.141592654/180.0)
    ELSE
      ZPAT=-QTC((SK-1)*NX*NY+(SJ-1)*NX+SI,4)/2.0*COS((THETA-ALPHA+(2.0*C-1)*&
        &ALPHA/5.0)*3.141592654/180.0)
    END IF
    XEFVECTOR=XDIFMID-XPAT
    YEFVECTOR=YDIFMID-YPAT
    ZEFVECTOR=ZDIFMID-ZPAT
    DIFE=SQRT(XEFVECTOR**2+YEFVECTOR**2+ZEFVECTOR**2)
    TOTALEF(1)=TOTALEF(1)+1D12*CHARGE*XEFVECTOR/(4.0*3.141592654*8.85D-12*DCP*&
      &DIFE**3)
    TOTALEF(2)=TOTALEF(2)+1D12*CHARGE*YEFVECTOR/(4.0*3.141592654*8.85D-12*DCP*&
      &DIFE**3)
    TOTALEF(3)=TOTALEF(3)+1D12*CHARGE*ZEFVECTOR/(4.0*3.141592654*8.85D-12*DCP*&
      &DIFE**3)
  END DO
END IF
ELSE
  CHARGE=-8.85E-12*DCP*EF*(QTC((SK-1)*NX*NY+(SJ-1)*NX+SI,4)/2000000.0)**2*INTEGRAL(&
    &179.99999999999999D0-(THETA-ALPHA+2.0D0*C*ALPHA/5.0),179.99999999999999D0-&
    &(THETA-ALPHA+2.0D0*(C-1)*ALPHA/5.0))
  IF(ZDIFMID>0.0)THEN
    CHARGE=-CHARGE
  END IF
  CHARGE=CHARGE+QTC((SK-1)*NX*NY+(SJ-1)*NX+SI,6)*1.6E-19*ABS(COS(3.141592654*&
    &(1.0-THETA-ALPHA+2.0*(C-1)*ALPHA/(5.0*180.0)))-COS(3.141592654*&
    &(1.0-THETA-ALPHA+2.0*C*ALPHA/(5.0*180.0)))/(4.0*3.141592654)
  INTPHI=ACOS(COS(ALPHA*3.141592654/180.0)/COS((ALPHA-(2*C-1)*ALPHA/5.0)*&
    &3.141592654/180.0))
  CHARGE=CHARGE*2*INTPHI/4.0
  DO D=1,4,1
    XPAT=QTC((SK-1)*NX*NY+(SJ-1)*NX+SI,4)/2.0*COS(PHI*3.141592654/180.0+INTPHI*&
      &(-1.25+D/2.0))*SIN(THETA-ALPHA+(2.0*C-1)*ALPHA/5.0)

```

```

YPAT=QTC((SK-1)*NX*NY+(SJ-1)*NX+SI,4)/2.0*SIN(PHI*3.141592654/180.0+INTPHI*&
&(-1.25+D/2.0))*SIN(THETA-ALPHA+(2.0*C-1)*ALPHA/5.0)
IF(ZDIFMID>0.0)THEN
  ZPAT=QTC((SK-1)*NX*NY+(SJ-1)*NX+SI,4)/2.0*COS((THETA-ALPHA+(2.0*C-1)*&
&ALPHA/5.0)*3.141592654/180.0)
ELSE
  ZPAT=-QTC((SK-1)*NX*NY+(SJ-1)*NX+SI,4)/2.0*COS((THETA-ALPHA+(2.0*C-1)*&
&ALPHA/5.0)*3.141592654/180.0)
END IF
XEFVECTOR=XMID-XPAT
YEFVECTOR=YMID-YPAT
ZEFVECTOR=ZMID-ZPAT
DIFEFSQRT(XEFVECTOR**2+YEFVECTOR**2+ZEFVECTOR**2)
TOTALEF(1)=TOTALEF(1)+ID12*CHARGE*XEFVECTOR/(4.0*3.141592654*8.85D-12*DCP*DIFEFSQRT)
TOTALEF(2)=TOTALEF(2)+ID12*CHARGE*YEFVECTOR/(4.0*3.141592654*8.85D-12*DCP*DIFEFSQRT)
TOTALEF(3)=TOTALEF(3)+ID12*CHARGE*ZEFVECTOR/(4.0*3.141592654*8.85D-12*DCP*DIFEFSQRT)
END DO
END IF
END IF
END DO
END DO
ACTUALEF(1)=TOTALEF(1)*XDIFMID/DIFMID
ACTUALEF(2)=TOTALEF(2)*YDIFMID/DIFMID
ACTUALEF(3)=TOTALEF(3)*ZDIFMID/DIFMID
ACTUALSCALAREF=ACTUALEF(1)+ACTUALEF(2)+ACTUALEF(3) !Find dot product of total electric field
IF(ACTUALSCALAREF>0.0)THEN !vector with unit vector pointing from midpoint
  B=7.973253226E10 !to the centre of the particle propagating from
  T=EXP(-B/ACTUALSCALAREF)
ELSE
  T=0.0
END IF
CALL RANDOM_NUMBER(P)!Place random number in P
IF((P<=T).AND.(T>0.0))THEN
  IF((QTC((K-1)*NX*NY+(J-1)*NX+I,6)<=QTC((SK-1)*NX*NY+(SJ-1)*NX+SI,6)).AND.&
&(QTC((K-1)*NX*NY+(J-1)*NX+I,6)<0.0))THEN !All electrons propagate if particle
!propagating from is negatively charged and particle propagating to is less negatively
!charged
  IF(K<NZ-1)THEN
    QTC((SK-1)*NX*NY+(SJ-1)*NX+SI,6)=QTC((SK-1)*NX*NY+(SJ-1)*NX+SI,6)+&
&QTC((K-1)*NX*NY+(J-1)*NX+I,6)
  ELSE
    QTC((SJ-1)*NX+SI,6)=QTC((SJ-1)*NX+SI,6)+QTC((K-1)*NX*NY+(J-1)*NX+I,6)
    NOE=NOE-QTC((K-1)*NX*NY+(J-1)*NX+I,6)
  END IF
  QTC((K-1)*NX*NY+(J-1)*NX+I,6)=0.0
  GOTO 3
END IF
END IF
END IF
4 END DO
END IF
END IF
IF(I>1)THEN
  XDIF=QTC((K-1)*NX*NY+(J-1)*NX+I-1,1)-QTC((K-1)*NX*NY+(J-1)*NX+I,1) !Now consider percolating pathways
  YDIF=QTC((K-1)*NX*NY+(J-1)*NX+I-1,2)-QTC((K-1)*NX*NY+(J-1)*NX+I,2) !in the same z-plane
  ZDIF=QTC((K-1)*NX*NY+(J-1)*NX+I-1,3)-QTC((K-1)*NX*NY+(J-1)*NX+I,3)
  DIF=SQRT(XDIF**2+YDIF**2+ZDIF**2)
  IF(NINT(2000.0*DIF)/1000.0<=NINT((1000*(QTC((K-1)*NX*NY+(J-1)*NX+I,4)+QTC((K-1)*NX*NY+(J-1)*&
&NX+I-1,4)))/1000.0)THEN
    IF((QTC((K-1)*NX*NY+(J-1)*NX+I,6)<=QTC((K-1)*NX*NY+(J-1)*NX+I-1,6)).AND.&
&(QTC((K-1)*NX*NY+(J-1)*NX+I,6)<0.0))THEN
      QTC((K-1)*NX*NY+(J-1)*NX+I-1,6)=QTC((K-1)*NX*NY+(J-1)*NX+I-1,6)+&
&QTC((K-1)*NX*NY+(J-1)*NX+I,6)
      QTC((K-1)*NX*NY+(J-1)*NX+I,6)=0.0
      GOTO 3
    END IF
  END IF
END IF
END IF
IF(I<NX)THEN
  XDIF=QTC((K-1)*NX*NY+(J-1)*NX+I+1,1)-QTC((K-1)*NX*NY+(J-1)*NX+I,1)
  YDIF=QTC((K-1)*NX*NY+(J-1)*NX+I+1,2)-QTC((K-1)*NX*NY+(J-1)*NX+I,2)
  ZDIF=QTC((K-1)*NX*NY+(J-1)*NX+I+1,3)-QTC((K-1)*NX*NY+(J-1)*NX+I,3)
  DIF=SQRT(XDIF**2+YDIF**2+ZDIF**2)
  IF(NINT(2000.0*DIF)/1000.0<=NINT((1000*(QTC((K-1)*NX*NY+(J-1)*NX+I,4)+QTC((K-1)*NX*NY+(J-1)*&
&NX+I+1,4)))/1000.0)THEN
    IF((QTC((K-1)*NX*NY+(J-1)*NX+I,6)<=QTC((K-1)*NX*NY+(J-1)*NX+I+1,6)).AND.&
&(QTC((K-1)*NX*NY+(J-1)*NX+I,6)<0.0))THEN
      QTC((K-1)*NX*NY+(J-1)*NX+I+1,6)=QTC((K-1)*NX*NY+(J-1)*NX+I+1,6)+&
&QTC((K-1)*NX*NY+(J-1)*NX+I,6)
      QTC((K-1)*NX*NY+(J-1)*NX+I,6)=0.0
      GOTO 3
    END IF
  END IF
END IF
END IF
IF(J>1)THEN
  XDIF=QTC((K-1)*NX*NY+(J-2)*NX+I,1)-QTC((K-1)*NX*NY+(J-1)*NX+I,1)
  YDIF=QTC((K-1)*NX*NY+(J-2)*NX+I,2)-QTC((K-1)*NX*NY+(J-1)*NX+I,2)
  ZDIF=QTC((K-1)*NX*NY+(J-2)*NX+I,3)-QTC((K-1)*NX*NY+(J-1)*NX+I,3)

```



```

DIF=SQRT(XDIF**2+YDIF**2+ZDIF**2)
IF(NINT(2000.0*DIF)/1000.0<=NINT((1000*(QTC((K-1)*NX*NY+(J-1)*NX+I,4)+QTC((K-1)*NX*NY+(J-2)*&
&NX+I,4)))/1000.0)THEN
  IF((QTC((K-1)*NX*NY+(J-1)*NX+I,6)<=QTC((K-1)*NX*NY+(J-2)*NX+I,6)).AND.&
    &(QTC((K-1)*NX*NY+(J-1)*NX+I,6)<0.0))THEN
    QTC((K-1)*NX*NY+(J-2)*NX+I,6)=QTC((K-1)*NX*NY+(J-2)*NX+I,6)+QTC((K-1)*NX*NY+(J-1)*NX+I,6)
    QTC((K-1)*NX*NY+(J-1)*NX+I,6)=0.0
    GOTO 3
  END IF
  IF(I>1)THEN
    XDIF=QTC((K-1)*NX*NY+(J-2)*NX+I-1,1)-QTC((K-1)*NX*NY+(J-1)*NX+I,1)
    YDIF=QTC((K-1)*NX*NY+(J-2)*NX+I-1,2)-QTC((K-1)*NX*NY+(J-1)*NX+I,2)
    ZDIF=QTC((K-1)*NX*NY+(J-2)*NX+I-1,3)-QTC((K-1)*NX*NY+(J-1)*NX+I,3)
    DIF=SQRT(XDIF**2+YDIF**2+ZDIF**2)
    IF(NINT(2000.0*DIF)/1000.0<=NINT((1000*(QTC((K-1)*NX*NY+(J-1)*NX+I,4)+QTC((K-1)*NX*NY+(J-2)*&
    &NX+I-1,4)))/1000.0)THEN
      IF((QTC((K-1)*NX*NY+(J-1)*NX+I,6)<=QTC((K-1)*NX*NY+(J-2)*NX+I-1,6)).AND.&
        &(QTC((K-1)*NX*NY+(J-1)*NX+I,6)<0.0))THEN
        QTC((K-1)*NX*NY+(J-2)*NX+I-1,6)=QTC((K-1)*NX*NY+(J-2)*NX+I-1,6)+&
          &QTC((K-1)*NX*NY+(J-1)*NX+I,6)
        QTC((K-1)*NX*NY+(J-1)*NX+I,6)=0.0
        GOTO 3
      END IF
    END IF
  END IF
END IF
IF(I<NX)THEN
  XDIF=QTC((K-1)*NX*NY+(J-2)*NX+I+1,1)-QTC((K-1)*NX*NY+(J-1)*NX+I,1)
  YDIF=QTC((K-1)*NX*NY+(J-2)*NX+I+1,2)-QTC((K-1)*NX*NY+(J-1)*NX+I,2)
  ZDIF=QTC((K-1)*NX*NY+(J-2)*NX+I+1,3)-QTC((K-1)*NX*NY+(J-1)*NX+I,3)
  DIF=SQRT(XDIF**2+YDIF**2+ZDIF**2)
  IF(NINT(2000.0*DIF)/1000.0<=NINT((1000*(QTC((K-1)*NX*NY+(J-1)*NX+I,4)+QTC((K-1)*NX*NY+(J-2)*&
  &NX+I+1,4)))/1000.0)THEN
    IF((QTC((K-1)*NX*NY+(J-1)*NX+I,6)<=QTC((K-1)*NX*NY+(J-2)*NX+I+1,6)).AND.&
      &(QTC((K-1)*NX*NY+(J-1)*NX+I,6)<0.0))THEN
      QTC((K-1)*NX*NY+(J-2)*NX+I+1,6)=QTC((K-1)*NX*NY+(J-2)*NX+I+1,6)+&
        &QTC((K-1)*NX*NY+(J-1)*NX+I,6)
      QTC((K-1)*NX*NY+(J-1)*NX+I,6)=0.0
      GOTO 3
    END IF
  END IF
END IF
IF(J<NY)THEN
  XDIF=QTC((K-1)*NX*NY+J*NX+I,1)-QTC((K-1)*NX*NY+(J-1)*NX+I,1)
  YDIF=QTC((K-1)*NX*NY+J*NX+I,2)-QTC((K-1)*NX*NY+(J-1)*NX+I,2)
  ZDIF=QTC((K-1)*NX*NY+J*NX+I,3)-QTC((K-1)*NX*NY+(J-1)*NX+I,3)
  DIF=SQRT(XDIF**2+YDIF**2+ZDIF**2)
  IF(NINT(2000.0*DIF)/1000.0<=NINT((1000*(QTC((K-1)*NX*NY+(J-1)*NX+I,4)+QTC((K-1)*NX*NY+J*&
  &NX+I,4)))/1000.0)THEN
    IF((QTC((K-1)*NX*NY+(J-1)*NX+I,6)<=QTC((K-1)*NX*NY+J*NX+I,6)).AND.&
      &(QTC((K-1)*NX*NY+(J-1)*NX+I,6)<0.0))THEN
      QTC((K-1)*NX*NY+J*NX+I,6)=QTC((K-1)*NX*NY+J*NX+I,6)+QTC((K-1)*NX*NY+(J-1)*NX+I,6)
      QTC((K-1)*NX*NY+(J-1)*NX+I,6)=0.0
      GOTO 3
    END IF
  END IF
END IF
XDIF=QTC((K-1)*NX*NY+J*NX+I+1,1)-QTC((K-1)*NX*NY+(J-1)*NX+I,1)
YDIF=QTC((K-1)*NX*NY+J*NX+I+1,2)-QTC((K-1)*NX*NY+(J-1)*NX+I,2)
ZDIF=QTC((K-1)*NX*NY+J*NX+I+1,3)-QTC((K-1)*NX*NY+(J-1)*NX+I,3)
DIF=SQRT(XDIF**2+YDIF**2+ZDIF**2)
IF(NINT(2000.0*DIF)/1000.0<=NINT((1000*(QTC((K-1)*NX*NY+(J-1)*NX+I,4)+QTC((K-1)*NX*NY+J*&
&NX+I+1,4)))/1000.0)THEN
  IF((QTC((K-1)*NX*NY+(J-1)*NX+I,6)<=QTC((K-1)*NX*NY+J*NX+I+1,6)).AND.&
    &(QTC((K-1)*NX*NY+(J-1)*NX+I,6)<0.0))THEN
    QTC((K-1)*NX*NY+J*NX+I+1,6)=QTC((K-1)*NX*NY+J*NX+I+1,6)+QTC((K-1)*NX*NY+(J-1)*NX+I,6)
    QTC((K-1)*NX*NY+(J-1)*NX+I,6)=0.0
    GOTO 3
  END IF
END IF
END IF
IF(I<NX)THEN
  XDIF=QTC((K-1)*NX*NY+J*NX+I+1,1)-QTC((K-1)*NX*NY+(J-1)*NX+I,1)
  YDIF=QTC((K-1)*NX*NY+J*NX+I+1,2)-QTC((K-1)*NX*NY+(J-1)*NX+I,2)
  ZDIF=QTC((K-1)*NX*NY+J*NX+I+1,3)-QTC((K-1)*NX*NY+(J-1)*NX+I,3)
  DIF=SQRT(XDIF**2+YDIF**2+ZDIF**2)
  IF(NINT(2000.0*DIF)/1000.0<=NINT((1000*(QTC((K-1)*NX*NY+(J-1)*NX+I,4)+QTC((K-1)*NX*NY+J*&
  &NX+I+1,4)))/1000.0)THEN
    IF((QTC((K-1)*NX*NY+(J-1)*NX+I,6)<=QTC((K-1)*NX*NY+J*NX+I+1,6)).AND.&
      &(QTC((K-1)*NX*NY+(J-1)*NX+I,6)<0.0))THEN
      QTC((K-1)*NX*NY+J*NX+I+1,6)=QTC((K-1)*NX*NY+J*NX+I+1,6)+QTC((K-1)*NX*NY+(J-1)*NX+I,6)
      QTC((K-1)*NX*NY+(J-1)*NX+I,6)=0.0
      GOTO 3
    END IF
  END IF
END IF
END IF

```

```

IF((QUANTUM=='Y').OR.(QUANTUM=='y'))THEN !Quantum tunnelling to same z-plane is allowed, if percolation
DO E=1,8,1 !in same z-plane is not successful
  IF(E==1)THEN
    IF(I>1)THEN
      SI=I-1
      SJ=J
      SK=K
    ELSE
      GOTO 5
    END IF
  END IF
  IF(E==2)THEN
    IF(I<NX)THEN
      SI=I+1
      SJ=J
      SK=K
    ELSE
      GOTO 5
    END IF
  END IF
  IF(E==3)THEN
    IF(J>1)THEN
      SI=I
      SJ=J-1
      SK=K
    ELSE
      GOTO 5
    END IF
  END IF
  IF(E==4)THEN
    IF((J>1).AND.(I>1))THEN
      SI=I-1
      SJ=J-1
      SK=K
    ELSE
      GOTO 5
    END IF
  END IF
  IF(E==5)THEN
    IF((J>1).AND.(I<NX))THEN
      SI=I+1
      SJ=J-1
      SK=K
    ELSE
      GOTO 5
    END IF
  END IF
  IF(E==6)THEN
    IF(J<NY)THEN
      SI=I
      SJ=J+1
      SK=K
    ELSE
      GOTO 5
    END IF
  END IF
  IF(E==7)THEN
    IF((J<NY).AND.(I>1))THEN
      SI=I-1
      SJ=J+1
      SK=K
    ELSE
      GOTO 5
    END IF
  END IF
  IF(E==8)THEN
    IF((J<NY).AND.(I<NX))THEN
      SI=I+1
      SJ=J+1
      SK=K
    ELSE
      GOTO 5
    END IF
  END IF
  XDIF=QTC((SK-1)*NX*NY+(SJ-1)*NX+SI,1)-QTC((K-1)*NX*NY+(J-1)*NX+I,1)
  YDIF=QTC((SK-1)*NX*NY+(SJ-1)*NX+SI,2)-QTC((K-1)*NX*NY+(J-1)*NX+I,2)
  ZDIF=QTC((SK-1)*NX*NY+(SJ-1)*NX+SI,3)-QTC((K-1)*NX*NY+(J-1)*NX+I,3)
  DIF=SQR(XDIF**2+YDIF**2+ZDIF**2)
  IF(NINT(2000.0*DIF)/1000.0<=NINT((1000.0*(QTC((K-1)*NX*NY+(J-1)*NX+I,4)+QTC((SK-1)*NX*NY+(SJ-1)*
    &NX+SI,4)))/1000.0)THEN
    GOTO 5
  END IF
  MIDPOINTDIST=(DIF-(QTC((SK-1)*NX*NY+(SJ-1)*NX+SI,4)+QTC((K-1)*NX*NY+(J-1)*NX+I,4))/2.0)/2.0
  XMID=QTC((K-1)*NX*NY+(J-1)*NX+I,1)+(QTC((K-1)*NX*NY+(J-1)*NX+I,4)/2.0+MIDPOINTDIST)*XDIF/DIF
  YMID=QTC((K-1)*NX*NY+(J-1)*NX+I,2)+(QTC((K-1)*NX*NY+(J-1)*NX+I,4)/2.0+MIDPOINTDIST)*YDIF/DIF
  ZMID=QTC((K-1)*NX*NY+(J-1)*NX+I,3)+(QTC((K-1)*NX*NY+(J-1)*NX+I,4)/2.0+MIDPOINTDIST)*ZDIF/DIF

```

```

TOTALEF=0.0
TOTALEF(3)=-EF
DO F=1,2,1
  IF(F==1)THEN
    SI=I
    SJ=J
    SK=K
  ELSE
    IF(E==1)THEN
      SI=I-1
      SJ=J
      SK=K
    END IF
    IF(E==2)THEN
      SI=I+1
      SJ=J
      SK=K
    END IF
    IF(E==3)THEN
      SI=I
      SJ=J-1
      SK=K
    END IF
    IF(E==4)THEN
      SI=I-1
      SJ=J-1
      SK=K
    END IF
    IF(E==5)THEN
      SI=I+1
      SJ=J-1
      SK=K
    END IF
    IF(E==6)THEN
      SI=I
      SJ=J+1
      SK=K
    END IF
    IF(E==7)THEN
      SI=I-1
      SJ=J+1
      SK=K
    END IF
    IF(E==8)THEN
      SI=I+1
      SJ=J+1
      SK=K
    END IF
  END IF
  XDIFMID=XMID-QTC((SK-1)*NX*NY+(SJ-1)*NX+SI,1)
  YDIFMID=YMID-QTC((SK-1)*NX*NY+(SJ-1)*NX+SI,2)
  ZDIFMID=ZMID-QTC((SK-1)*NX*NY+(SJ-1)*NX+SI,3)
  DIFMID=SQRT(XDIFMID**2+YDIFMID**2+ZDIFMID**2)
  IF((ZDIFMID>0.0).OR.(ZDIFMID<0.0))THEN
    THETA=ATAN(SQRT(XDIFMID**2+YDIFMID**2)/ZDIFMID)*180/3.141592654
    IF(THETA<0.0)THEN
      THETA=-THETA
    END IF
  ELSE
    THETA=90.0
  END IF
  IF((XMID-QTC((SK-1)*NX*NY+(SJ-1)*NX+SI,1)>0.0).OR.(XMID-QTC((SK-1)*NX*NY+(SJ-1)*NX+SI,1)<0.0))THEN
    PHI=ATAN((YMID-QTC((SK-1)*NX*NY+(SJ-1)*NX+SI,2))/(XMID-QTC((SK-1)*NX*NY+(SJ-1)*NX+SI,1)))*180/3.141592654
  ELSE
    PHI=90.0
  END IF
  IF(XDIFMID<0.0)THEN
    PHI=PHI+180.0
  END IF
  ALPHA=ACOS(QTC((SK-1)*NX*NY+(SJ-1)*NX+SI,4)/(2.0*DIFMID))*180.0/3.141592654
  DO C=1,5,1
    CHARGE=0.0
    IF(THETA-ALPHA+2.0*(C-1)*ALPHA/5.0<0.0)THEN
      IF(THETA-ALPHA+2.0*C*ALPHA/5.0<0.0)THEN
        CHARGE=8.85E-12*DCP*EF*(QTC((SK-1)*NX*NY+(SJ-1)*NX+SI,4)/2000000.0)**2*&
          &INTEGRAL(-(THETA-ALPHA+2.0D0*(C-1)*ALPHA/5.0),-(THETA-ALPHA+2.0D0*C*&
            &ALPHA/5.0))
        IF(ZDIFMID>0.0)THEN
          CHARGE=-CHARGE
        END IF
        CHARGE=CHARGE+QTC((SK-1)*NX*NY+(SJ-1)*NX+SI,6)*1.6E-19*ABS(COS(3.141592654*&
          &(THETA-ALPHA+2.0*(C-1)*ALPHA/(5.0*180.0)))-COS(3.141592654*(THETA-ALPHA+2.0*&
            &C*ALPHA/(5.0*180.0))))/(4.0*3.141592654)
        CHARGE=CHARGE*3.141592654/4.0
      END IF
    END IF
  END DO

```

```

DO D=1,4,1
  XPAT=(QTC((SK-1)*NX*NY+(SJ-1)*NX+SI,4)/2.0*COS((PHI+90*(-1.25+D/2.0)))*&
    &3.141592654/180.0)*SIN(THETA-ALPHA+(2.0*C-1)*ALPHA/5.0))
  YPAT=(QTC((SK-1)*NX*NY+(SJ-1)*NX+SI,4)/2.0*SIN((PHI+90*(-1.25+D/2.0)))*&
    &3.141592654/180.0)*SIN(THETA-ALPHA+(2.0*C-1)*ALPHA/5.0))
  IF(ZDIFMID>0.0)THEN
    ZPAT=QTC((SK-1)*NX*NY+(SJ-1)*NX+SI,4)/2.0*COS((THETA-ALPHA+(2.0*C-1)*&
      &ALPHA/5.0)*3.141592654/180.0)
  ELSE
    ZPAT=-(QTC((SK-1)*NX*NY+(SJ-1)*NX+SI,4)/2.0*COS(THETA-ALPHA+(2.0*C-1)*&
      &ALPHA/5.0)*3.141592654/180.0)
  END IF
  XEFVECTOR=XDIFMID-XPAT
  YEFVECTOR=YDIFMID-YPAT
  ZEFVECTOR=ZDIFMID-ZPAT
  DIFEF=SQRT(XEFVECTOR**2+YEFVECTOR**2+ZEFVECTOR**2)
  TOTALEF(1)=TOTALEF(1)+1D12*CHARGE*1E12*XEFVECTOR/(4.0*3.141592654*8.85D-12*DCP*&
    &DIFEF**3)
  TOTALEF(2)=TOTALEF(2)+1D12*CHARGE*1E12*YEFVECTOR/(4.0*3.141592654*8.85D-12*DCP*&
    &DIFEF**3)
  TOTALEF(3)=TOTALEF(3)+1D12*CHARGE*1E12*ZEFVECTOR/(4.0*3.141592654*8.85D-12*DCP*&
    &DIFEF**3)
END DO
ELSE
  CHARGE=8.85E-12*DCP*EF*(QTC((SK-1)*NX*NY+(SJ-1)*NX+SI,4)/2000000.0)**2*&
    &(INTEGRAL(-(THETA-ALPHA+2.0D0*(C-1)*ALPHA/5.0D0),0.0D0)+&
    &INTEGRAL(0.0D0,THETA-ALPHA+2.0D0*C*ALPHA/5.0))
  IF(ZDIFMID>0.0)THEN
    CHARGE=-CHARGE
  END IF
  CHARGE=CHARGE+QTC((SK-1)*NX*NY+(SJ-1)*NX+SI,6)*1.6E-19*(COS(3.141592654*&
    &(THETA-ALPHA+2.0*(C-1)*ALPHA/(5.0*180.0)))+COS(3.141592654*(THETA-ALPHA+2.0*&
    &C*ALPHA/(5.0*180.0)))/(4.0*3.141592654)
  CHARGE=CHARGE*3.141592654/4.0
  DO D=1,4,1
    XPAT=QTC((SK-1)*NX*NY+(SJ-1)*NX+SI,4)/2.0*COS((PHI+90*(-1.25+D/2.0)))*&
      &3.141592654/180.0)*SIN(THETA-ALPHA+(2.0*C-1)*ALPHA/5.0)
    YPAT=QTC((SK-1)*NX*NY+(SJ-1)*NX+SI,4)/2.0*SIN((PHI+90*(-1.25+D/2.0)))*&
      &3.141592654/180.0)*SIN(THETA-ALPHA+(2.0*C-1)*ALPHA/5.0)
    IF(ZDIFMID>0.0)THEN
      ZPAT=QTC((SK-1)*NX*NY+(SJ-1)*NX+SI,4)/2.0*COS((THETA-ALPHA+(2.0*C-1)*&
        &ALPHA/5.0)*3.141592654/180.0)
    ELSE
      ZPAT=-(QTC((SK-1)*NX*NY+(SJ-1)*NX+SI,4)/2.0*COS(THETA-ALPHA+(2.0*C-1)*&
        &ALPHA/5.0)*3.141592654/180.0)
    END IF
    XEFVECTOR=XDIFMID-XPAT
    YEFVECTOR=YDIFMID-YPAT
    ZEFVECTOR=ZDIFMID-ZPAT
    DIFEF=SQRT(XEFVECTOR**2+YEFVECTOR**2+ZEFVECTOR**2)
    TOTALEF(1)=TOTALEF(1)+1D12*CHARGE*XEFVECTOR/(4.0*3.141592654*8.85D-12*DCP*DIFEF**3)
    TOTALEF(2)=TOTALEF(2)+1D12*CHARGE*YEFVECTOR/(4.0*3.141592654*8.85D-12*DCP*DIFEF**3)
    TOTALEF(3)=TOTALEF(3)+1D12*CHARGE*ZEFVECTOR/(4.0*3.141592654*8.85D-12*DCP*DIFEF**3)
  END DO
END IF
ELSE
  IF(THETA-ALPHA+2.0*(C-1)*ALPHA/5.0<90.0)THEN
    IF(THETA-ALPHA+2.0*C*ALPHA/5.0<90.0)THEN
      CHARGE=8.85E-12*DCP*EF*(QTC((SK-1)*NX*NY+(SJ-1)*NX+SI,4)/2000000.0)**2*&
        &INTEGRAL(THETA-ALPHA+2.0D0*(C-1)*ALPHA/5.0,THETA-ALPHA+2.0D0*C*ALPHA/5.0)
      IF(ZDIFMID>0.0)THEN
        CHARGE=-CHARGE
      END IF
      CHARGE=CHARGE+QTC((SK-1)*NX*NY+(SJ-1)*NX+SI,6)*1.6E-19*ABS(COS(3.141592654*&
        &(THETA-ALPHA+2.0*(C-1)*ALPHA/(5.0*180.0)))-COS(3.141592654*&
        &(THETA-ALPHA+2.0*C*ALPHA/(5.0*180.0)))/(4.0*3.141592654)
      INTPHI=ACOS(COS(ALPHA*3.141592654/180.0)/COS((ALPHA-(2*C-1)*ALPHA/5.0)*&
        &3.141592654/180.0))
      CHARGE=CHARGE*2*INTPHI/4.0
    DO D=1,4,1
      XPAT=QTC((SK-1)*NX*NY+(SJ-1)*NX+SI,4)/2.0*COS(PHI*3.141592654/180.0+INTPHI*&
        &(-1.25+D/2.0))*SIN(THETA-ALPHA+(2.0*C-1)*ALPHA/5.0)
      YPAT=QTC((SK-1)*NX*NY+(SJ-1)*NX+SI,4)/2.0*SIN(PHI*3.141592654/180.0+INTPHI*&
        &(-1.25+D/2.0))*SIN(THETA-ALPHA+(2.0*C-1)*ALPHA/5.0)
      IF(ZDIFMID>0.0)THEN
        ZPAT=QTC((SK-1)*NX*NY+(SJ-1)*NX+SI,4)/2.0*COS((THETA-ALPHA+(2.0*C-1)*&
          &ALPHA/5.0)*3.141592654/180.0)
      ELSE
        ZPAT=-(QTC((SK-1)*NX*NY+(SJ-1)*NX+SI,4)/2.0*COS((THETA-ALPHA+(2.0*C-1)*&
          &ALPHA/5.0)*3.141592654/180.0)
      END IF
      XEFVECTOR=XMID-XPAT
      YEFVECTOR=YMID-YPAT
      ZEFVECTOR=ZMID-ZPAT
      DIFEF=SQRT(XEFVECTOR**2+YEFVECTOR**2+ZEFVECTOR**2)
      TOTALEF(1)=TOTALEF(1)+1D12*CHARGE*XEFVECTOR/(4.0*3.141592654*8.85D-12*DCP*&

```

```

        &DIFEFF**3)
TOTALF(2)=TOTALF(2)+1D12*CHARGE*YEFVECTOR/(4.0*3.141592654*8.85D-12*DCP*&
        &DIFEFF**3)
TOTALF(3)=TOTALF(3)+1D12*CHARGE*ZEFVECTOR/(4.0*3.141592654*8.85D-12*DCP*&
        &DIFEFF**3)
END DO
ELSE
CHARGE=8.85E-12*DCP*EF*(QTC((SK-1)*NX*NY+(SJ-1)*NX+SI,4)/2000000.0)**2*&
        &(INTEGRAL(THETA-ALPHA+2.0D0*(C-1)*ALPHA/5.0,89.99999999999999D0)-&
        &INTEGRAL(179.99999999999999D0-(THETA-ALPHA+2.0D0*C*ALPHA/5.0),&
        &89.99999999999999D0))
IF(ZDIFMID>0.0)THEN
    CHARGE=-CHARGE
END IF
CHARGE=CHARGE+QTC((SK-1)*NX*NY+(SJ-1)*NX+SI,6)*1.6E-19*ABS(COS(3.141592654*&
        &(THETA-ALPHA+2.0*(C-1)*ALPHA/(5.0*180.0)))+COS(3.141592654*&
        &(1.0-THETA-ALPHA+2.0*C*ALPHA/(5.0*180.0)))/(4.0*3.141592654)
INTPHI=ACOS(COS(ALPHA*3.141592654/180.0)/COS((ALPHA-(2*C-1)*ALPHA/5.0)*&
        &3.141592654/180.0))
CHARGE=CHARGE*2*INTPHI/4.0
DO D=1,4,1
    XPAT=QTC((SK-1)*NX*NY+(SJ-1)*NX+SI,4)/2.0*COS(PHI*3.141592654/180.0+INTPHI*&
        &(-1.25+D/2.0))*SIN(THETA-ALPHA+(2.0*C-1)*ALPHA/5.0)
    YPAT=QTC((SK-1)*NX*NY+(SJ-1)*NX+SI,4)/2.0*SIN(PHI*3.141592654/180.0+INTPHI*&
        &(-1.25+D/2.0))*SIN(THETA-ALPHA+(2.0*C-1)*ALPHA/5.0)
    IF(ZDIFMID>0.0)THEN
        ZPAT=QTC((SK-1)*NX*NY+(SJ-1)*NX+SI,4)/2.0*COS((THETA-ALPHA+(2.0*C-1)*&
            &ALPHA/5.0)*3.141592654/180.0)
    ELSE
        ZPAT=-QTC((SK-1)*NX*NY+(SJ-1)*NX+SI,4)/2.0*COS((THETA-ALPHA+(2.0*C-1)*&
            &ALPHA/5.0)*3.141592654/180.0)
    END IF
    XEFVECTOR=XDIFMID-XPAT
    YEFVECTOR=YDIFMID-YPAT
    ZEFVECTOR=ZDIFMID-ZPAT
    DIFEFF=SQRT(XEFVECTOR**2+YEFVECTOR**2+ZEFVECTOR**2)
    TOTALF(1)=TOTALF(1)+1D12*CHARGE*XEFVECTOR/(4.0*3.141592654*8.85D-12*DCP*&
        &DIFEFF**3)
    TOTALF(2)=TOTALF(2)+1D12*CHARGE*YEFVECTOR/(4.0*3.141592654*8.85D-12*DCP*&
        &DIFEFF**3)
    TOTALF(3)=TOTALF(3)+1D12*CHARGE*ZEFVECTOR/(4.0*3.141592654*8.85D-12*DCP*&
        &DIFEFF**3)
END DO
END IF
ELSE
CHARGE=-8.85E-12*DCP*EF*(QTC((SK-1)*NX*NY+(SJ-1)*NX+SI,4)/2000000.0)**2*INTEGRAL(&
        &179.99999999999999D0-(THETA-ALPHA+2.0D0*C*ALPHA/5.0),179.99999999999999D0-&
        &(THETA-ALPHA+2.0D0*(C-1)*ALPHA/5.0))
IF(ZDIFMID>0.0)THEN
    CHARGE=-CHARGE
END IF
CHARGE=CHARGE+QTC((SK-1)*NX*NY+(SJ-1)*NX+SI,6)*1.6E-19*ABS(COS(3.141592654*&
        &(1.0-THETA-ALPHA+2.0*(C-1)*ALPHA/(5.0*180.0)))-COS(3.141592654*&
        &(1.0-THETA-ALPHA+2.0*C*ALPHA/(5.0*180.0)))/(4.0*3.141592654)
INTPHI=ACOS(COS(ALPHA*3.141592654/180.0)/COS((ALPHA-(2*C-1)*ALPHA/5.0)*&
        &3.141592654/180.0))
CHARGE=CHARGE*2*INTPHI/4.0
DO D=1,4,1
    XPAT=QTC((SK-1)*NX*NY+(SJ-1)*NX+SI,4)/2.0*COS(PHI*3.141592654/180.0+INTPHI*&
        &(-1.25+D/2.0))*SIN(THETA-ALPHA+(2.0*C-1)*ALPHA/5.0)
    YPAT=QTC((SK-1)*NX*NY+(SJ-1)*NX+SI,4)/2.0*SIN(PHI*3.141592654/180.0+INTPHI*&
        &(-1.25+D/2.0))*SIN(THETA-ALPHA+(2.0*C-1)*ALPHA/5.0)
    IF(ZDIFMID>0.0)THEN
        ZPAT=QTC((SK-1)*NX*NY+(SJ-1)*NX+SI,4)/2.0*COS((THETA-ALPHA+(2.0*C-1)*&
            &ALPHA/5.0)*3.141592654/180.0)
    ELSE
        ZPAT=-QTC((SK-1)*NX*NY+(SJ-1)*NX+SI,4)/2.0*COS((THETA-ALPHA+(2.0*C-1)*&
            &ALPHA/5.0)*3.141592654/180.0)
    END IF
    XEFVECTOR=XDIFMID-XPAT
    YEFVECTOR=YDIFMID-YPAT
    ZEFVECTOR=ZDIFMID-ZPAT
    DIFEFF=SQRT(XEFVECTOR**2+YEFVECTOR**2+ZEFVECTOR**2)
    TOTALF(1)=TOTALF(1)+1D12*CHARGE*XEFVECTOR/(4.0*3.141592654*8.85D-12*DCP*DIFEFF**3)
    TOTALF(2)=TOTALF(2)+1D12*CHARGE*YEFVECTOR/(4.0*3.141592654*8.85D-12*DCP*DIFEFF**3)
    TOTALF(3)=TOTALF(3)+1D12*CHARGE*ZEFVECTOR/(4.0*3.141592654*8.85D-12*DCP*DIFEFF**3)
END DO
END IF
END IF
END DO
END DO
ACTUALEF(1)=TOTALF(1)*XDIFMID/DIFMID
ACTUALEF(2)=TOTALF(2)*YDIFMID/DIFMID
ACTUALEF(3)=TOTALF(3)*ZDIFMID/DIFMID
ACTUALSCALAREF=ACTUALEF(1)+ACTUALEF(2)+ACTUALEF(3)
IF(ACTUALSCALAREF>0.0)THEN

```

```

        B=7.973253226E10
        T=EXP(-B/ACTUALSCALAREF)
    ELSE
        T=0.0
    END IF
    CALL RANDOM_NUMBER(P)!Place random number in P
    IF((P<=T).AND.(T>0.0))THEN
        IF((QTC((K-1)*NX*NY+(J-1)*NX+I,6)<=QTC((SK-1)*NX*NY+(SJ-1)*NX+SI,6)).AND.&
            &(QTC((K-1)*NX*NY+(J-1)*NX+I,6)<0.0))THEN
            QTC((SK-1)*NX*NY+(SJ-1)*NX+SI,6)=QTC((SK-1)*NX*NY+(SJ-1)*NX+SI,6)+&
                &QTC((K-1)*NX*NY+(J-1)*NX+I,6)
            QTC((K-1)*NX*NY+(J-1)*NX+I,6)=0.0
            GOTO 3
        END IF
    END IF
    5 END DO
END IF
END IF
3 END DO
END DO
END DO
WRITE(*,*)'The number of electrons emerging from QTC in one pass is:',NOE
TSNOE=TSNOE+REAL(NOE)
TSNOE=TSNOE+REAL(NOE)**2
END DO
WRITE(*,*)
IF(PASS>1)THEN
    WRITE(*,*)'The mean number of electrons emerging in',PASS,' passes is:',TNOE/REAL(PASS)
    WRITE(*,*)'The standard error on the mean is:',SQRT(TSNOE/REAL(PASS)/REAL(PASS-1)-TNOE**2/REAL(PASS)**2/&
        &REAL(PASS-1))
END IF
WRITE(*,*)
IF((INT(TNOE)==0))THEN
    WRITE(*,*)'The current is zero!'
    WRITE(*,*)'This corresponds to an infinite resistance'
    WRITE(*,*)'The resistivity of the QTC is therefore infinite'
    WRITE(*,*)'The conductivity of the QTC is therefore zero'
ELSE
    WRITE(*,*)'A rough estimate of the current is: ',TNOE/REAL(PASS)*14.6*V*CDIM/(NZ*(NZ-1)*(DEF/100.0)**2*&
        &DCP),' Amps'
    WRITE(*,*)'This corresponds to a resistance of: ',V/(TNOE/REAL(PASS)*14.6*V*CDIM/(NZ*(NZ-1)*&
        &(DEF/100.0)**2*DCP)),' Ohms'
    WRITE(*,*)'The resistivity of the QTC is therefore: ',DCP*NX*NY*(NZ-1)/(TNOE/REAL(PASS)*146.0E5),' Ohm m'
    WRITE(*,*)'The conductivity of the QTC is therefore: ',TNOE/REAL(PASS)*146.0E5/(DCP*REAL(NX)*REAL(NY)*&
        &REAL(NZ-1)),' Siemens'
END IF
READ(*,*)
DO I=1,30,1
    WRITE(*,*)
END DO
CASE(10)
IF(DEF<=100.0)THEN
    IF((CV=='Y').OR.(CV=='y'))THEN
        DO I=1,TOTALN,1
            XDIM=NX*CDIM/(SQRT(DEF)*100.0)
            YDIM=NY*CDIM/(SQRT(DEF)*100.0)
            ZDIM=NZ*CDIM*DEF/100000.0
        END DO
    ELSE
        XDIM=NX*CDIM/1000.0
        YDIM=NY*CDIM/1000.0
        ZDIM=NZ*CDIM*DEF/100000.0
    END IF
END IF
WRITE(*,*)
WRITE(*,*)'The number of cubic cells is:',TOTALN
WRITE(*,*)'The number of empty cubic cells is:',EMPC
WRITE(*,*)'Therefore, the number of filler particles is:',TOTALN-EMPC
WRITE(*,*)'The number of cubic cells in the x-direction is:',NX
WRITE(*,*)'The number of cubic cells in the y-direction is:',NY
WRITE(*,*)'The number of cubic cells in the z-direction is:',NZ
WRITE(*,*)'The original dimension of each cubic cell is:',CDIM,' microns'
WRITE(*,*)'The smallest particle diameter is:',SFILL,' microns'
WRITE(*,*)'The largest particle diameter is:',LFILL,' microns'
WRITE(*,*)'The loading ratio is:',FILCONC,'w/w %'
WRITE(*,*)'The size of the QTC in the z-direction is:',DEF,'% '
WRITE(*,*)'The QTC has x-dimension:',XDIM,'mm'
WRITE(*,*)'The QTC has y-dimension:',YDIM,'mm'
WRITE(*,*)'The QTC has z-dimension:',ZDIM,'mm'
READ(*,*)
CLOSE(13)
ND=0
DO I=1,30,1
    WRITE(*,*)
END DO
CASE(11)

```

```

      GOTO 2
CASE DEFAULT
      GOTO 1
ENDSELECT
GOTO 1
2 END PROGRAM QTCSIM
!
FUNCTION INTEGRAL(X,Y)
!
!Purpose: To compute the integral used in the calculation of the number of electrons on the surface of a nickel sphere
!
IMPLICIT NONE
!
DOUBLE PRECISION,INTENT(IN)::X,Y
DOUBLE PRECISION::A,B
DOUBLE PRECISION::INTEGRAL
!
A=DLOG(1.0D0/DCOS(X*DASIN(1.0D0)/90.0D0))/DLOG(2.718281828D0)
B=DLOG(1.0D0/DCOS(Y*DASIN(1.0D0)/90.0D0))/DLOG(2.718281828D0)
INTEGRAL=ABS(B-A)
!
END FUNCTION INTEGRAL

```

APPENDIX B

Explanation of how the current, resistance and resistivity of QTC are derived from the number of electrons, N , emerging in one pass, by attributing a time-step to one pass by comparison with the conductivity of pure nickel.

$$J = \sigma E = \frac{I}{A} = \frac{Q}{A\Delta t} = \frac{\sigma V}{d\epsilon_r}$$

$$\Rightarrow \Delta t = \frac{Qd\epsilon_r}{\sigma VA} = \frac{NX * NY * (NZ - 1) * e * NZ * DEF * \epsilon_r * CDIM}{\sigma * V * \frac{NX * NY}{DEF} * CDIM^2}$$

$$\therefore \Delta t = \frac{e * NZ * (NZ - 1) * DEF^2 * \epsilon_r}{\sigma * V * CDIM}$$

$$I = \frac{Q}{\Delta t} = \frac{N * e}{\Delta t} = \frac{N * \sigma * V * CDIM}{NZ * (NZ - 1) * DEF^2 * \epsilon_r}$$

$$\Rightarrow R = \frac{NZ * DEF^2 * \epsilon_r * (NZ - 1)}{N * \sigma * CDIM}$$

$$\Rightarrow \rho = \frac{RA}{d} = \frac{R * \frac{NX * NY}{DEF} * CDIM^2}{NZ * CDIM * DEF} = \frac{\frac{NZ * DEF^2 * \epsilon_r * (NZ - 1)}{N * \sigma * CDIM} * \frac{NX * NY}{DEF} * CDIM^2}{NZ * CDIM * DEF}$$

$$\therefore \rho = \frac{(NZ - 1) * \epsilon_r * NX * NY}{N * \sigma}$$

$$\sigma = 14.6 * 10^6 \Omega^{-1} m^{-1}$$

APPENDIX C

If there is a net charge on a sphere, a constant surface charge density will result from it. The charge, Q , due to N unit charges around the sphere, from azimuthal angle θ_1 to θ_2 , and from polar angle ϕ_1 to ϕ_2 , is calculated as follows:

$$\sigma = \frac{Ne}{A} = \frac{Ne}{4\pi r^2} = \frac{dq}{dA}$$

$$dA = r^2 \sin \theta d\theta d\phi$$

$$dq = \frac{Ne}{4\pi} \sin \theta d\theta d\phi$$

$$\Rightarrow Q = \int_0^Q dq = \frac{Ne}{4\pi} \int_{\theta_1}^{\theta_2} \sin \theta d\theta \int_{\phi_1}^{\phi_2} d\phi$$

$$\therefore Q = \frac{Ne}{4\pi} [\cos \theta_1 - \cos \theta_2] (\phi_2 - \phi_1)$$

APPENDIX D

If the loading ratio, L , of a metal-polymer composite is expressed as a w/w fraction, the volume within the composite occupied by the metal, V_m , can be calculated as follows, where V is the volume of the composite, and V_p is the volume occupied by the polymer:

$$L = \frac{m_m}{m_m + m_p} \Rightarrow \frac{m_m}{m_p} = \frac{L}{1-L}$$

$$V = V_p + V_m$$

$$= \frac{m_p}{\rho_p} + \frac{m_m}{\rho_m}$$

$$= \frac{m_p}{\rho_p} + \frac{m_p L}{\rho_m (1-L)}$$

$$= m_p \left(\frac{1}{\rho_p} + \frac{L}{\rho_m (1-L)} \right)$$

$$= m_p \left(\frac{\rho_m - \rho_m L + \rho_p L}{\rho_p \rho_m (1-L)} \right)$$

$$\Rightarrow m_p = \frac{V \rho_p \rho_m (1-L)}{\rho_m + L(\rho_p - \rho_m)} = \rho_p V_p$$

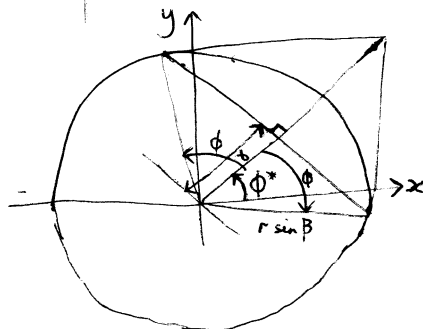
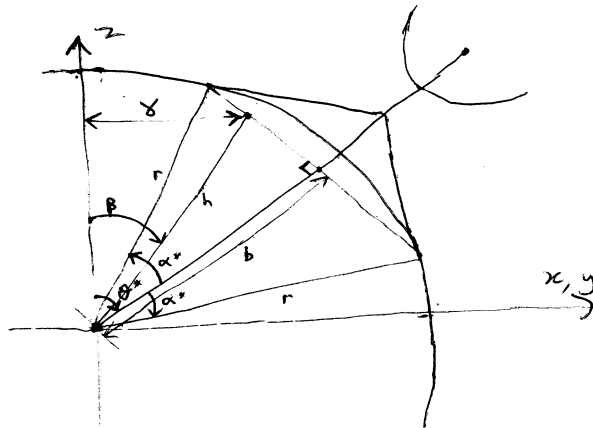
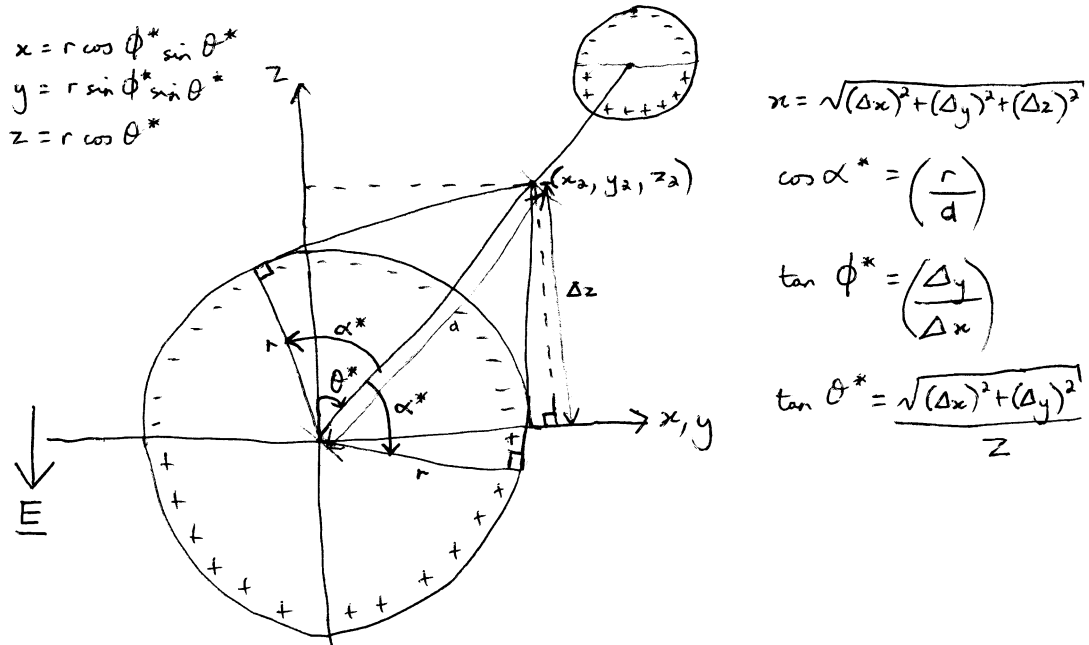
$$\Rightarrow V_p = \frac{V \rho_m (1-L)}{\rho_m + L(\rho_p - \rho_m)} = \frac{V(1-L)}{1 + L \left(\frac{\rho_p}{\rho_m} - 1 \right)}$$

$$\Rightarrow V_m = V - \frac{V(1-L)}{1 + L \left(\frac{\rho_p}{\rho_m} - 1 \right)}$$

$$\therefore V_m = V \left(1 - \frac{(1-L)}{1 + L \left(\frac{\rho_p}{\rho_m} - 1 \right)} \right)$$

APPENDIX E

The midpoint between two spherical particles can only "see" a certain area upon each surface. The surface charge density must be integrated over this area, using the correct values of the polar and azimuthal angles. The following treatment was used in ascertaining these values for the computer simulation.



$$\phi = \pm \cos^{-1} \left(\frac{\cos \alpha^*}{\cos(\theta^* - \beta)} \right) \quad \begin{cases} \text{for } \beta > 0^\circ \\ \phi = \pm 90^\circ \\ \text{for } \beta < 0^\circ \end{cases}$$